

RR 91 / 199

**THE OPTIMIZATION OF COMPACTION
SPECIFICATIONS FOR DIFFERENT
PAVEMENT LAYERS**

Prepared on behalf of the SOUTH AFRICAN ROADS BOARD

TITEL/TITLE: THE OPTIMIZATION OF COMPACTION SPECIFICATIONS FOR DIFFERENT PAVEMENTS			
VERSLAG NR: REPORT NO: RR 91/199	ISBN: 1-86844-159-8	DATUM: DATE: March 1994	VERSLAGSTATUS: REPORT STATUS: Final
NAVORSINGSNR / RESEARCH NO: 91/199			
GEDOEN DEUR: CARRIED OUT BY: Division of Roads and Transport Technology, CSIR P O Box 395 Pretoria 0001		OPDRAGGEWER: COMMISSIONED BY: Director General: Transport Private Bag X193 PRETORIA 0001	
OUTEUR(S): AUTHOR(S): C J Semmelink M Groenewald E G du Plessis		NAVRAE: ENQUIRIES: Department of Transport Directorate : Transport Economic Analysis Private Bag X193 PRETORIA 0001	
SINOPSIS: Die verslag handel oor die terreinondersoeke na verdigtingstandaarde, d.w.s werklike in situ droë digthede wat bereik is in vergelyking tot spesifikasievereistes, vir padlaagwerk vir die periodes 91/92, 92/93 en 93/94. Die redes vir die ondersoek word kortliks bespreek. Daarna word 'n kort uiteensetting van die terrein-ondersoekmetodiek gegee waarna die resultate van die verskillende laagwerke in die onderskeie periodes bespreek word. Dit word gevolg deur gevolgtrekkings en aanbevelings.		SYNOPSIS: The report deals with the site investigations in connection with the compaction standards, that is a comparison between actual in situ dry densities achieved compared to specification requirements, for road layer work for the periods 91/92, 92/93 and 93/94. The reasons for the investigation are outlined briefly. This is followed by a brief outline of the site investigation methodology, whereafter the results of different layer works in the different time periods are discussed. This is followed by conclusions and recommendations.	
TREFWOORDE: KEYWORDS: Compactability, compaction, dry density, moisture content, grading, roller			
KOPIEREG: COPYRIGHT: Departement van Vervoer, behalwe vir verwysingsdoeleindes Department of Transport, except for reference purposes			VERSLAGKOSTE: REPORT COST: R35.00

DISCLAIMER

The views and opinions in this report are those of the authors and do not represent Department of Transport policy.

ACKNOWLEDGEMENT

The authors of the report would gratefully like to acknowledge the permission granted by the Department of Transport to monitor the construction process on Site 1 in the period 92/93 and the permission granted by the Transvaal Provincial Roads Department to monitor the construction on Site 2 during the periods 92/93 and 93/94.

The authors of the report would also like to acknowledge their gratitude to the people involved in the construction of these roads, namely:

Site personnel of Basil Read (Pty) Ltd

Site and laboratory staff of BKS Inc (Consulting Engineers)

Regional Engineer in charge of the Middelburg Construction Unit of the TPA Roads Department

Site personnel of Middelburg Construction Unit of the TPA Roads Department.

THIS REPORT WAS REVIEWED BY THREE INDEPENDENT REFEREES, TWO OF WHICH ARE:

MR J P NOTHNAGEL

MR H C THOMSON

LIST OF CONTENTS

	<u>PAGE</u>
1. INTRODUCTION	1-1
2. ACTUAL SITE WORK	2-1
2.1 INTRODUCTION	2-1
2.2 SITE 1 (THE PRETORIA END OF THE PRETORIA-RUSTENBURG TOLL ROAD) ...	2-1
2.3 THE METHOD OF COMPACTION AND CONTROL PROCEDURE FOLLOWED	2-2
2.4 THE DENSITY RESULTS MEASURED	2-3
2.4.1 Fill	2-3
2.4.2 Selected subgrade	2-5
2.4.3 Lower cement stabilized subbase (125 mm thick)	2-7
2.4.4 Upper cement stabilized subbase (125 mm thick)	2-12
2.4.5 Crushed stone base course (150 mm thick)	2-20
2.5 SITE 2 (THE RECONSTRUCTION OF THE BRONKHORSTSPRUIT-BAPSFONTEIN PROVINCIAL ROAD)	2-31
2.6 THE DENSITY RESULTS MEASURED	2-32
2.6.1 Second selected subgrade (upper)	2-32
2.6.2 First stabilised subbase (lower)	2-36
2.6.3 Second stabilised subbase (upper)	2-42
2.6.4 Crushed stone base course (G1)	2-46
2.7 THE WORK AT THE BRONKHORSTSPRUIT CONSTRUCTION SITE IN 1993/94 ...	2-51
2.8 THE DENSITY RESULTS MEASURED	2-53
2.8.1 Fill	2-53
2.8.2 Lower selected subgrade	2-57
2.8.3 Upper selected subgrade	2-64
2.8.4 Lower stabilized subbase	2-70
2.8.5 Upper stabilized subbase	2-77
2.8.6 Crushed stone base	2-83
2.9 RESULTS OF THE VIBRATORY COMPACTION TABLE	2-89

LIST OF CONTENTS (Continued)

	<u>PAGE</u>
3. CONCLUSIONS	3-1
3.1 THE EFFECT OF THE MOISTURE CONTENT	3-1
3.2 THE COMPACTIVE EFFORT APPLIED	3-2
3.3 THE LEVELLING OF THE LAYER	3-3
3.4 THE DRY DENSITIES THAT CAN BE ACHIEVED	3-3
3.5 PREDICTION OF REQUIRED MOISTURE CONTENT BY MEANS OF COMPACTABILITY SOFTWARE PACKAGE	3-5
3.6 POSSIBLE RAPID METHODS FOR THE DETERMINATION OF THE OMC	3-5
4. RECOMMENDATIONS	4-1
5. REFERENCES	5-1
APPENDIX A: ORIGINAL PROPOSED TECHNIQUE FOR THE CONSTRUCTION OF THE TEST STRIP FOR THE OPTIMIZATION OF DENSITY STANDARDS AND COMPACTION TECHNIQUES AND ADDITIONAL RECOMMENDATIONS FOR DUAL-AMPLITUDE VIBRATORY ROLLERS	A-1
APPENDIX B: PREDICTION RESULTS OF COMPACTABILITY SOFTWARE PACKAGE AND DRY DENSITY - MOISTURE CONTENT CURVES OF VIBRATORY COMPACTION	B-1

LIST OF TABLES

PAGE

Table 1.1: Comparison of the measured and predicted densities of materials in different layers on some HVS sites	1-2
Table 2.1: Predicted and measured Maximum Dry Density and Optimum Moisture Content values using the Compactability Software Package and the vibratory compaction table	2-90
Table 2.2: Predicted and measured Maximum Dry Density, Optimum Moisture Content and Zero Air Voids Moisture Content values using the Compactability Software Package and the vibratory compaction table	2-91

LIST OF FIGURES

	<u>PAGE</u>
Figure 1.1: The relation between MDD(mod.AASHTO)(laboratory)(%SD) and MDD(vibratory compaction table)(%SD)	1-1
Figure 2.1: Measured dry densities against measured moisture contents on fill compacted with a vibratory tamping-foot roller (6 passes)	2-4
Figure 2.2: Measured dry densities against measured moisture contents on fill compacted with a five-sided impact roller (20 passes) (250 mm layer)	2-4
Figure 2.3: Average measured dry densities for different layer thicknesses of fill as well as method of compaction	2-5
Figure 2.4: Measured dry densities against measured moisture contents for compacted selected subgrade materials using two CPN nuclear gauges	2-6
Figure 2.5: The compaction growth curve of the selected subgrade layer	2-7
Figure 2.6: Measured dry densities against measured moisture contents for the lower cement stabilized subbase after two passes with grid roller	2-8
Figure 2.7: Measured dry densities against measured moisture contents for the lower cement stabilized subbase after grading the grid-rolled section	2-8
Figure 2.8: Measured dry densities against measured moisture contents for the lower cement stabilized subbase after two extra grid roller passes on graded section	2-9
Figure 2.9: Measured dry densities against measured moisture contents for the lower cement stabilized subbase after a second grading and one full pass with vibratory roller (G2 + V1)	2-9
Figure 2.10: Measured dry densities against measured moisture contents for the lower cement stabilized subbase after one pass with pneumatic-tyred roller (PTR) on the vibratory compacted section	2-10

LIST OF FIGURES (Continued)

	<u>PAGE</u>
Figure 2.11: The compaction growth curve of the lower cement stabilized subbase of Section 2 showing the average dry densities (measured) against the activity prior to taking the density measurements (average moisture content value is printed below data point)	2-10
Figure 2.12: The compaction growth curve of Section 3 showing the average dry densities (measured) against the activity prior to taking the density measurements (average moisture content value is printed below data point)	2-11
Figure 2.13: The compaction growth curve of Section 6 showing the average dry densities (measured) against the activity prior to taking the density measurements (average moisture content value is predicted below data point)	2-12
Figure 2.14: Measured dry densities against measured moisture contents for upper cement stabilized subbase after one and a half passes with pneumatic-tyred roller	2-13
Figure 2.15: Measured dry densities against measured moisture contents for upper cement stabilized subbase after grading the pneumatic-tyred rolled section	2-13
Figure 2.16: Measured dry densities against measured moisture contents for upper cement stabilized subbase after half a pass with the vibratory roller (high amplitude/low frequency) on the graded section	2-14
Figure 2.17: Measured dry densities against measured moisture contents for upper cement stabilized subbase after another half a pass with the vibratory roller (low amplitude/high frequency)	2-14
Figure 2.18: Measured dry densities against measured moisture contents for upper cement stabilized subbase after half a pass with pneumatic-tyred roller on the vibratory-rolled section	2-15
Figure 2.19: Measured dry densities against measured moisture contents for upper cement stabilized subbase after one full pass with the pneumatic-tyred roller	2-15

LIST OF FIGURES (Continued)

	<u>PAGE</u>	
Figure 2.20:	The compaction growth curve of the upper cement stabilized subbase of Section 6 showing the average measured dry density against the activity prior to taking the moisture/density measurements (average measured moisture content value is printed below data point)	2-16
Figure 2.21:	The compaction growth curve of the upper cement stabilized subbase of Sections 1 and 2 showing the average measured dry density against the activity prior to taking the moisture/density measurements (average measured moisture content value is printed below data point)	2-17
Figure 2.22:	The compaction growth curve of the upper cement stabilized subbase of Section 3 showing the average measured dry density against the activity prior to taking the moisture/density measurements (average measured moisture content value is printed below data point)	2-17
Figure 2.23:	The compaction growth curve of the upper cement stabilized subbase of Section 5 showing the average measured dry density against the activity prior to taking the moisture/density measurements (average measured content value is printed below data point)	2-18
Figure 2.24:	The compaction growth curve of the upper cement stabilized subbase of Section 7 showing the average measured dry density against the activity prior to taking the moisture/density measurements (average measured content value is printed below data point)	2-18
Figure 2.25:	Measured dry densities against measured moisture contents of upper cement stabilized subbase after half a pass with the pneumatic-tyred roller on the vibratory-rolled section	2-19
Figure 2.26:	The compaction growth of the upper cement stabilized subbase of Section 7 showing the average measured dry density against the activity prior to the moisture/density measurements (minus the readings in the edge lane for 0.5 PTR) (average measured moisture content value is printed below data point)	2-20

LIST OF FIGURES (Continued)

	<u>PAGE</u>
Figure 2.27: Measured dry densities against measured moisture contents for base course layer of Sections 1 and 2 after initial grading with grader	2-21
Figure 2.28: Measured dry densities against measured moisture contents for base course layer of Sections 1 and 2 after initial two passes with grid roller and one pass with pneumatic tyred roller	2-22
Figure 2.29: Measured dry densities against measured moisture contents for base course layer of Sections 1 and 2 after final grading with grader	2-22
Figure 2.30: Measured dry densities against measured moisture contents for base course layer of Sections 1 and 2 after half a pass with vibratory roller (high amplitude/low frequency)	2-23
Figure 2.31: Measured dry densities against measured moisture contents for base course layer of Sections 1 and 2 after half a pass with vibratory roller (low amplitude/high frequency)	2-23
Figure 2.32: Measured dry densities against measured moisture contents for base course layer of Sections 1 and 2 after one full pass with vibratory roller (low amplitude/high frequency)	2-24
Figure 2.33: Measured dry densities against measured moisture contents for base course layer of Sections 1 and 2 after one and a half passes with vibratory roller (low amplitude/high frequency)	2-24
Figure 2.34: Measured dry densities against measured moisture contents for base course layer of Sections 1 and 2 after half a pass with pneumatic-tyred roller on vibratory-rolled layer	2-25
Figure 2.35: Measured dry densities against measured moisture contents for base course layer of Sections 1 and 2 after one full pass with pneumatic-tyred roller	2-25
Figure 2.36: Measured dry densities against measured moisture for base course layer of Sections 1 and 2 after one and a half passes with pneumatic-tyred roller	2-26

LIST OF FIGURES (Continued)

	<u>PAGE</u>
Figure 2.37: Measured dry densities against measured moisture contents for base course layer of Sections 1 and 2 after two full passes of pneumatic-tyred roller	2-26
Figure 2.38: Compaction growth curve of the base course layer of Sections 1 and 2 showing the average measured dry density against the activity prior to taking the moisture/density measurements (average measured moisture content value printed below data point)	2-27
Figure 2.39: Compaction growth curve of the base course layer of Section 3 showing the average measured dry density against the activity prior to taking the moisture/density measurements (average measured moisture content value printed below data point)	2-28
Figure 2.40: Compaction growth curve of the reconstructed base course layer of Section 3 showing the average measured dry density against the activity prior to taking the moisture/density measurements (average measured moisture content value printed below data point)	2-28
Figure 2.41: Compaction growth curve of the base course layer of Section 7 showing the average measured dry density against the activity prior to taking the moisture/density measurement (average measured moisture content value printed below data point)	2-29
Figure 2.42: Average measured dry densities for different depths including back-scatter (zero depth) as well as back-calculated average zone dry densities against depth of measurement	2-31
Figure 2.43: Measured dry densities against measured moisture contents on second selected subgrade layer after one pass with the grid roller following initial mixing and levelling	2-33
Figure 2.44: Measured dry densities against measured moisture contents on second selected subgrade after half a pass with grid roller on finally graded layer	2-33

LIST OF FIGURES (Continued)

	<u>PAGE</u>
Figure 2.45: Measured dry densities against moisture contents on second selected subgrade layer after one pass with grid roller on finally graded layer	2-34
Figure 2.46: Measured dry densities against measured moisture contents of second selected subgrade after half a pass with pneumatic-tyred roller on grid-rolled layer	2-34
Figure 2.47: Measured dry densities against moisture contents of second selected subgrade after one pass with vibratory roller on pneumatic-tyred rolled layer (half pass)	2-35
Figure 2.48: Measured densities against measured moisture contents of second selected subgrade layer after one pass with pneumatic-tyred roller on vibratory-rolled layer	2-35
Figure 2.49: The compaction growth curve of the second selected subgrade layer of Section 3 showing the average measured dry density against the activity prior to taking the moisture/density measurements (average measured moisture content value is printed below data point)	2-36
Figure 2.50: Measured dry densities against measured moisture contents of first stabilised subbase layer after half a pass with grid roller following mixing and levelling	2-37
Figure 2.51: Measured dry densities against measured moisture contents of first stabilised subbase layer after one pass with grid roller	2-37
Figure 2.52: Measured dry densities against measured moisture contents of first stabilised subbase layer after half a pass with vibratory roller on grid-rolled layer	2-38
Figure 2.53: Measured dry densities against measured moisture contents of first stabilised subbase layer after one pass of vibratory roller on grid-rolled layer	2-38
Figure 2.54: Measured dry densities against measured moisture contents of first stabilised subbase layer after half a pass with pneumatic-tyred roller on vibratory-rolled layer	2-39

LIST OF FIGURES (Continued)

	<u>PAGE</u>	
Figure 2.55:	Measured dry densities against measured moisture contents of first stabilised subbase layer after one full pass with pneumatic-tyred roller on vibratory-rolled layer	2-39
Figure 2.56:	The compaction growth curve of the first stabilised subbase layer of Section 8 showing measured dry densities against the activity prior to taking the moisture/density measurements (average measured moisture content is printed below data point)	2-40
Figure 2.57:	The compaction growth curve of the first stabilised subbase layer of Section 7 showing the average measured dry density against the activity prior to taking the moisture/density measurements (average measured moisture content is printed below data point)	2-40
Figure 2.58:	The compaction growth curve of the first stabilised subbase layer of Section 9 showing the average dry density against the activity prior to taking the moisture/density measurements (average measured moisture content value is printed below data point)	2-41
Figure 2.59:	The compaction growth curve of the first stabilised subbase layer of Section 10 showing the average measured dry density against the activity prior to taking the moisture/density measurements (average measured moisture content value is printed below data point)	2-41
Figure 2.60:	Measured dry densities against measured moisture contents of first stabilised subbase layer of Section 9 after one and a half passes with pneumatic-tyred roller	2-42
Figure 2.61:	Measured dry densities against measured moisture contents of second stabilised subbase after half a pass with grid roller following mixing and levelling of layer	2-43
Figure 2.62:	Measured dry densities against measured moisture contents of second stabilised subbase layer after one pass with grid roller following mixing and levelling of layer	2-43

LIST OF FIGURES (Continued)

	<u>PAGE</u>	
Figure 2.63:	Measured dry densities against measured moisture contents of second stabilised subbase layer after one and a half passes with grid roller following mixing and levelling of layer	2-44
Figure 2.64:	Measured dry densities against measured moisture contents of second stabilised subbase layer after half a pass with vibratory roller on grid-rolled layer	2-44
Figure 2.65:	Measured dry densities against measured moisture contents of second stabilised subbase layer after one pass with vibratory roller on grid-rolled layer	2-45
Figure 2.66:	The compaction growth curve of the second stabilised subbase of Section 4 showing the average dry density against the activity prior to taking the moisture/density measurements (average measured moisture content value is printed below data point)	2-45
Figure 2.67:	The compaction growth curve of the second stabilised subbase of Section 1 showing the average measured dry density against the activity prior to taking the moisture/density measurements (average measured moisture content is printed below data point)	2-46
Figure 2.68:	Measured dry densities against measured moisture contents of the crushed stone base course layer after levelling with grader	2-47
Figure 2.69:	Measured dry densities against measured moisture contents of the crushed stone base course layer after half a pass with the grid roller on the graded layer	2-47
Figure 2.70:	Measured dry densities against measured moisture contents of the crushed stone base course layer after one pass with the grid roller on the graded layer	2-48
Figure 2.71:	Measured dry densities against measured moisture contents of the crushed stone base course after half a pass with the vibratory roller on the grid-rolled layer	2-48

LIST OF FIGURES (Continued)

	<u>PAGE</u>
Figure 2.72: Measured dry densities against measured moisture contents of the crushed stone base course after one pass with the vibratory roller and half a pass with pneumatic tyred roller on the grid-rolled layer	2-49
Figure 2.73: The compaction growth curve of the crushed stone base course of Section 5 showing the average measured dry density against the activity prior to taking the moisture/density measurements (average measured moisture content value is printed below data point)	2-49
Figure 2.74: The compaction growth curve of the crushed stone base course of Section 3 showing the average measured dry density against the activity prior to taking the moisture/density measurements (average measured moisture content value is printed below data point)	2-50
Figure 2.75: The compaction growth curve of the crushed stone base course of Section 1 showing the average measured dry density against the activity prior to taking the moisture/density measurements (average measured moisture content value is printed below data point)	2-50
Figure 2.76: Measured dry densities against measured moisture contents on fill layer after half a pass with grid roller following mixing and levelling	2-54
Figure 2.77: Measured dry densities against measured moisture contents on fill layer after one pass with grid roller	2-54
Figure 2.78: Measured dry densities against measured moisture contents on fill layer after half a pass with vibratory roller following on grid roller	2-55
Figure 2.79: Measured dry densities against measured moisture contents on fill layer after one pass with vibratory roller	2-55
Figure 2.80: The compaction growth curve of the fill layer of section near large cutting showing the average measured dry density against the activity prior to taking the moisture/density measurements (average moisture content value is printed below data point)	2-56

LIST OF FIGURES (Continued)

PAGE

Figure 2.81:	The compaction growth curve of the fill layer next to previous section in Figure 2.81 showing the average measured dry density against the activity prior to taking the moisture/density measurements (average moisture content value is printed below data point)	2-56
Figure 2.82:	The compaction growth curve of the fill layer on Section 1 showing the average measured dry density against the activity prior to taking the moisture/density measurements (average moisture content value is printed below data point)	2-57
Figure 2.83:	Measured dry densities against measured moisture contents on lower selected subgrade layer after levelling with grader	2-58
Figure 2.84:	Measured dry densities against measured moisture contents on lower selected subgrade layer after half a pass with grid roller following levelling	2-59
Figure 2.85:	Measured dry densities against measured moisture contents on lower selected subgrade layer after one pass with grid roller	2-59
Figure 2.86:	Measured dry densities against measured moisture contents on lower selected subgrade layer after half a pass with vibratory roller following on grid roller	2-60
Figure 2.87:	Measured dry densities against measured moisture contents on lower selected subgrade layer after one pass with vibratory roller	2-60
Figure 2.88:	The compaction growth curve of the lower selected subgrade layer on Section 1 showing the average measured dry density against the activity prior to taking the moisture/density measurements (average moisture content value is printed below data point)	2-61
Figure 2.89:	The compaction growth curve of the lower selected subgrade layer on Section 2 showing the average measured dry density against the activity prior to taking the moisture/density measurements (average moisture content value is printed below data point)	2-61

LIST OF FIGURES (Continued)

	<u>PAGE</u>
Figure 2.90: The compaction growth curve of the lower selected subgrade layer on Section 3 showing the average measured dry density against the activity prior to taking the moisture/density measurements (average moisture content value is printed below data point)	2-62
Figure 2.91: The compaction growth curve of the lower selected subgrade layer on Section 4 showing the average measured dry density against the activity prior to taking the moisture/density measurements (average moisture content value is printed below data point)	2-62
Figure 2.92: Measured dry densities against measured moisture contents on lower selected subgrade layer after one pass with vibratory roller on Section 3	2-63
Figure 2.93: Measured dry densities against measured moisture contents on lower selected subgrade layer after one and a half passes with vibratory roller on Section 4	2-63
Figure 2.94: Measured dry densities against measured moisture contents on upper selected subgrade layer after half a pass with grid roller following mixing and levelling	2-64
Figure 2.95: Measured dry densities against measured moisture contents on upper selected subgrade layer after one pass with grid roller	2-65
Figure 2.96: Measured dry densities against measured moisture contents on upper selected subgrade layer after two passes with grid roller	2-65
Figure 2.97: Measured dry densities against measured moisture contents on upper selected subgrade layer after half a pass with vibratory roller following on grid roller	2-66
Figure 2.98: Measured dry densities against measured moisture contents on upper selected subgrade layer after one pass with vibratory roller	2-66
Figure 2.99: Measured dry densities against measured moisture contents on upper selected subgrade layer after one and half passes with vibratory roller	2-67

LIST OF FIGURES (Continued)

	<u>PAGE</u>	
Figure 2.100:	The compaction growth curve of the upper selected subgrade layer on Section 2 showing the average measured dry density against the activity prior to taking the moisture/density measurements (average moisture content value is printed below data point)	2-67
Figure 2.101:	The compaction growth curve of the upper selected subgrade layer on Section 1 showing the average measured dry density against the activity prior to taking the moisture/density measurements (average moisture content value is printed below data point)	2-68
Figure 2.102:	The compaction growth curve of the upper selected subgrade layer on Section 3 showing the average measured dry density against the activity prior to taking the moisture/density measurements (average moisture content value is printed below data point)	2-68
Figure 2.103:	The compaction growth curve of the upper selected subgrade layer on Section 4 showing the average measured dry density against the activity prior to taking the moisture/density measurements (average moisture content value is printed below data point)	2-69
Figure 2.104:	Measured dry densities against measured moisture contents on upper selected subgrade layer after one pass with vibratory roller on Section 4	2-69
Figure 2.105:	Measured dry densities against measured moisture contents on lower stabilized subbase layer after half a pass with grid roller following mixing and levelling	2-71
Figure 2.106:	Measured dry densities against measured moisture contents on lower stabilized subbase layer after one pass with grid roller	2-71
Figure 2.107:	Measured dry densities against measured moisture contents on lower stabilized subbase layer after two passes with grid roller	2-72
Figure 2.108:	Measured dry densities against measured moisture contents on lower stabilized subbase layer after half a pass with vibratory roller following on grid roller	2-72
Figure 2.109:	Measured dry densities against measured moisture contents on lower stabilized subbase layer after one pass with vibratory roller	2-73

LIST OF FIGURES (Continued)

	<u>PAGE</u>
Figure 2.110: The compaction growth curve of the lower stabilized subbase layer on Section 2 showing the average measured dry density against the activity prior to taking the moisture/density measurements (average moisture content value is printed below data point)	2-73
Figure 2.111: The compaction growth curve of the lower stabilized subbase layer on Section 1 showing the average measured dry density against the activity prior to taking the moisture/density measurements (average moisture content value is printed below data point)	2-74
Figure 2.112: The compaction growth curve of the lower stabilized subbase layer on Section 3 showing the average measured dry density against the activity prior to taking the moisture/density measurements (average moisture content value is printed below data point)	2-74
Figure 2.113: The compaction growth curve of the lower stabilized subbase layer on Section 4 showing the average measured dry density against the activity prior to taking the moisture/density measurements (average moisture content value is printed below data point)	2-75
Figure 2.114: Measured dry densities against measured moisture contents on lower stabilized subbase layer of Section 1 after one pass with vibratory roller at the end of the compaction cycle	2-75
Figure 2.115: Measured dry densities against measured moisture contents on lower stabilized subbase layer of Section 3 after one pass with vibratory roller at the end of the compaction cycle	2-76
Figure 2.116: Measured dry densities against measured moisture contents on lower stabilized subbase layer of Section 4 after one and a half passes with vibratory roller at the end of the compaction cycle	2-76
Figure 2.117: Measured dry densities against measured moisture contents on upper stabilized subbase layer after half a pass with grid roller following mixing and levelling	2-78
Figure 2.118: Measured dry densities against measured moisture contents on upper stabilized subbase layer after one pass with grid roller	2-78

LIST OF FIGURES (Continued)

	<u>PAGE</u>
Figure 2.119: Measured dry densities against measured moisture contents on upper stabilized subbase layer after one and a half passes with grid roller	2-79
Figure 2.120: Measured dry densities against measured moisture contents on upper stabilized subbase layer after two passes with grid roller	2-79
Figure 2.121: Measured dry densities against measured moisture contents on upper stabilized subbase layer after half a pass with vibratory roller following on grid roller	2-80
Figure 2.122: Measured dry densities against measured moisture contents on upper stabilized subbase layer after one pass with vibratory roller	2-80
Figure 2.123: Measured dry densities against measured moisture contents on upper stabilized subbase layer after one and a half passes with vibratory roller	2-81
Figure 2.124: The compaction growth curve of the upper stabilized subbase layer on Section 3 showing the average measured dry density against the activity prior to taking the moisture/density measurements (average moisture content value is printed below data point)	2-81
Figure 2.125: The compaction growth curve of the upper stabilized subbase layer on Section 1 showing the average measured dry density against the activity prior to taking the moisture/density measurements (average moisture content value is printed below data point)	2-82
Figure 2.126: The compaction growth curve of the upper stabilized subbase layer on Section 2 showing the average measured dry density against the activity prior to taking the moisture/density measurements (average moisture content value is printed below data point)	2-82
Figure 2.127: The compaction growth curve of the upper stabilized subbase layer on Section 4 showing the average measured dry density against the activity prior to taking the moisture/density measurements (average moisture content value is printed below data point)	2-83

LIST OF FIGURES (Continued)

	<u>PAGE</u>
Figure 2.128: Measured dry densities against measured moisture contents on crushed stone base layer after half a pass with vibratory roller following mixing and levelling	2-84
Figure 2.129: Measured dry densities against measured moisture contents on crushed stone base layer after one pass with vibratory roller	2-85
Figure 2.130: Measured dry densities against measured moisture contents on crushed stone base layer after one and a half passes with vibratory roller	2-85
Figure 2.131: Measured dry densities against measured moisture contents on crushed stone base layer after two passes with vibratory roller	2-86
Figure 2.132: Measured dry densities against measured moisture contents on crushed stone base layer after two and half passes with vibratory roller	2-86
Figure 2.133: The compaction growth curve of the crushed stone base layer on Section 1 showing the average measured dry density against the activity prior to taking the moisture/density measurements (average moisture content value is printed below data point)	2-87
Figure 2.134: The compaction growth curve of the crushed stone base layer on Section 2 showing the average measured dry density against the activity prior to taking the moisture/density measurements (average moisture content value is printed below data point)	2-87
Figure 2.135: The compaction growth curve of the crushed stone base layer on Section 3 showing the average measured dry density against the activity prior to taking the moisture/density measurements (average moisture content value is printed below data point)	2-88
Figure 2.136: The compaction growth curve of the crushed stone base layer on Section 4 showing the average measured dry density against the activity prior to taking the moisture/density measurements (average moisture content value is printed below data point)	2-88
Figure 3.1: Measured dry densities against measured moisture contents for crushed stone base course on Section 1 (Site 2)(92/93) showing the effect of the moisture content on the dry density that can be achieved at the end of the compaction sequence	3-2

LIST OF ABBREVIATIONS

AASHTO	-	American Association of State Highway and Transportation Officials
ARD	-	Apparent Relative Density
BRD	-	Bulk Relative Density
CMC	-	Critical Moisture Content
DD	-	Dry Density
Grader	-	Levelling with grader
Grade(I)	-	Initial levelling with grader
Grade(F)	-	Final levelling with grader
Grid	-	Grid Roller
HVS	-	Heavy Vehicle Simulator
Impact	-	Five-sided impact roller
MC	-	Moisture Content
MDD	-	Maximum Dry Density
MDD(mod.AASHTO)	-	Maximum Dry Density (modified AASHTO compactive effort)(laboratory)
MDD(vib)	-	Maximum Dry Density (vibratory table compactive effort)(laboratory)
Mixed	-	After mixing of water
OMC	-	Optimum Moisture Content
PTR	-	Pneumatic-Tyred Roller
SBD	-	Shakedown Bulk Density (collective influence of particle shape and texture)
SD	-	Solid Density (determined as a weighted value of the Dry Bulk Density of the plus 4,75 mm material (TMH Method B14) and the Apparent Density of the minus 4,75 mm material (TMH Method B15) according to their contribution to the total grading)
Spec	-	Specification requirement
Tamp Vib	-	Tampingfoot Vibratory Roller
Vib	-	Vibratory Roller (Smooth drum)
VibH	-	Vibratory Roller (High amplitude/Low frequency mode)
WA	-	Water Absorption(%) by porous aggregate
WFD	-	Weighted Fractional Density (fractional influence of particle shape and texture)
VibL	-	Vibratory Roller (Low amplitude/High frequency mode)
ZAVDD	-	Zero Air Voids Dry Density
ZAVMC	-	Zero Air Voids Moisture Content
100 % mod	-	100 % MDD(mod.AASHTO)(lab)
97 % mod	-	97 % MDD(mod.AASHTO)(lab)
95 % mod	-	95 % MDD(mod.AASHTO)(lab)
93 % mod	-	93 % MDD(mod.AASHTO)(lab)
90 % mod	-	90 % MDD(mod.AASHTO)(lab)
(0.5x)	-	Half a roller pass (one direction only)
(1x)	-	One full roller pass (forward and back on same path)
(1.5x)	-	One and a half roller passes (on same roller path)

LIST OF ABBREVIATIONS (Continued)

- (2x) - Two full roller passes (on same roller path)
- (3x) - Three full roller passes (on same roller path)
- (2xExt) - Two extra roller passes (on same roller path)(etc)
- G + PTR(1x) - One pass each with Grid Roller and PTR (etc)
- G(2) + PTR(1) - Two passes with Grid Roller and one pass with PTR
- G1 + V0.5x - First levelling with Grader and half a pass with Vibratory Roller
- G1 + V1x - First levelling with Grader and one full pass with Vibratory Roller
- G2 + V0.5x - Second levelling with Grader and half a pass with Vibratory Roller
- G2 + V1x - Second levelling with Grader and one full pass with Vibratory Roller

SUMMARY

Earlier laboratory research into the material properties that influence the compactability and bearing capacity of untreated roadbuilding materials showed that the mod.AASHTO compaction test generally does not compact these materials to their optimum dry density. This is so because the grading of the material is the single most important factor that influences both the MDD and moisture regime (i.e. OMC, ZAVMC and CMC) of untreated roadbuilding materials. Since the mod.AASHTO test requires all particles to pass the 19 mm sieve, the laboratory grading is often finer than the field grading leading to more internal voids. This in turn leads to a lower MDD and higher moisture regime (i.e. higher OMC, ZAVMC and CMC), the values of which are then used on site for compaction control. Furthermore, because compaction of undisturbed samples on the vibratory compaction table could be compacted to higher maximum dry densities (MDDs) than the MDD(mod.AASHTO) values, it was recommended that our present compaction standards, in terms of mod.AASHTO, should be checked in the field to determine whether it is possible to increase the dry densities of actual layerwork on actual road construction projects as well.

The report basically covers this field investigation over a period of three years. The original aim had been to monitor one construction project in each of the 4 provinces for 3 years. However, in the very first year no projects could be obtained at all because of the substantial cutback on road construction by the Government. In the original proposal it was also stated that the provincial authorities would do the site monitoring while the laboratory evaluation would be done at the Division in order to reduce subsistence and travel costs. However, the road authorities were no longer available to do the site monitoring. For these reasons it was decided, in joint discussions with the Department, that both the site and laboratory work would be done by the Division. To limit subsistence and travel costs it was also decided to use construction sites as close as possible to the CSIR and to test more than one section on a particular project.

To make up for the loss of the 91/92 period, two sites were covered in the period 92/93. This work was reported on in the interim report (IR 91/199). The site monitoring on both sites showed that process control, concerning the moisture content during compaction, was for all practical purposes, nonexistent. However, for the proper compaction of untreated roadbuilding materials (i.e. using water as lubricant) the single most important factor, apart from the gradation uniformity of the material, was the proper control of the moisture content during the compaction process. The field investigation also showed that when the moisture content was controlled at its optimum level, most roadbuilding materials could be compacted to substantially higher dry densities, in terms of mod.AASHTO, in less than 3 full passes of a large vibratory roller followed by less than 3 full passes of a large pneumatic-tyred roller. The work also showed that the grid roller was not effective for compaction and should generally only be used to adjust the grading of the material by crushing over-sized particles until the material is well-graded(i.e. a wide range of particle sizes). Excessive grid-rolling causes excessive breakdown of the material leading to finer gradings, lower MDDs, higher moisture requirements and lower bearing capacities

owing to lower dry densities, as well as higher construction costs due to unnecessary rolling. Unnecessary releveling of the layerwork with the grader also brought the dry densities back to the original values after the layer had been levelled the first time following watering and mixing. On account of these observations it was proposed that an effort should be made in the last year of the project to control the compaction moisture content more optimally by means of nuclear density/moisture gauges, as well as to roll all layerwork on the controlled sections to refusal density (i.e. the point at which further compactive effort does not increase the measured dry densities or causes a slight drop in the measured dry densities).

In the period 93/94 the TPA construction site between Bronkhorstspuit and Bapsfontein (i.e. the second site of the period 92/93) was re-used because of its location. Although an effort was made to implement the recommendations of the interim report, this was not always possible owing to constraints on site, such as the non-availability of a pneumatic-tyred roller for most of the time, as well as serious problems with the water supply on site. This meant that most sections were rolled only with the grid and vibratory rollers and some sections were compacted at moisture contents below the recommended OMC. Even so, the measured dry densities showed, once again, that if the moisture content is accurately monitored and controlled by means of a nuclear density/moisture gauge or some other rapid method, it is possible to compact most layerwork to substantially greater dry densities within a limited number of roller passes (i.e. less than 3 full passes with the vibratory roller followed by less than 3 full passes of the pneumatic-tyred roller). Material samples were also compacted in a single layer on the vibratory compaction table to determine their MDD and OMC values without grading changes. This was done to determine whether it was possible to achieve the substantially higher densities, obtained with vibratory compaction in the laboratory, on site. These results were also compared with the predicted results of the Compactability Software Package, developed from the earlier laboratory investigation, which uses the material's actual grading, Atterberg limits and linear shrinkage, and ARDs and BRDs of the +4,75 mm and -4,75 mm fractions as input information. This was done to verify whether these models could generally be used to estimate the required moisture content and MDDs. The predicted results proved to be very close to OMCs and MDDs as measured on the vibratory compaction table in most cases, confirming that these models can effectively be used in identifying possible causes for compaction problems or to estimate the OMC and MDD of a material when no laboratory values are available.

The final conclusions of this project are:

- It is absolutely essential that the moisture content of the material be controlled more accurately to ensure optimal compaction within a minimum number of roller passes.
- Unnecessary rolling with the grid roller should be avoided. It should be used as a tool to improve the quality of the grading (i.e. bringing the grading closer to the "ideal grading") and not as a compaction tool.
- Unnecessary releveling of the layer should be avoided.

- Uniformity in the composition and grading of the material is essential because the grading determines the moisture requirement for optimal compaction.
- It is possible to estimate the moisture requirement of a material reasonably accurately from its grading, Atterberg limits, Linear Shrinkage, and ARDs and BRDs of the coarse and fine fractions by means of the Compactability software package.
- Excessive rolling can be detrimental. The optimal rolling pattern should be determined for each new material by observing the compaction growth curve during the construction of a test strip with each new material at the correct moisture content for the particular grading.
- Because of the lack of process control during compaction in general, it is felt that it would be premature to lay down fixed standards for the different layers at this stage.

The recommendations are:

- The present specified compaction requirements should be maintained as the absolute minimum requirement. However, each layer is to be compacted to refusal density at the correct moisture content for the particular grading with the specified equipment. The correct moisture content may be predicted by means of the Compactability Software Package, which can be bought from CICTRAN, and uses the grading, Atterberg limits, Linear Shrinkage, and ARDs and BRDs of the coarse and fine fractions of the material, or the determination of OMC from the dry density/moisture content curve for samples compacted on the vibratory compaction table.
- More emphasis should be placed on process control during construction rather than acceptance control. The moisture content of the material should be accurately controlled within certain limits for each material. The optimal rolling pattern for each material should also be determined for each new material used and this rolling pattern should be used on subsequent sections constructed from the same material after it has been ascertained by accurate measurement (nuclear method or rapid drying method presently) that the moisture content is within the required range. Documented proof of this control should be submitted to the Resident Engineer for each layer on each section before any acceptance control testing is done.
- A training programme on the correct use of rollers should also be embarked upon.
- Once the correct construction procedures are generally followed it is proposed that the acceptance control densities (i.e. measured) of projects be evaluated for a two-year period to assist in laying down new minimum specification requirements for the dry densities of layerwork.
- The replacement of the mod.AASHTO compaction test with a compaction test which does not require the material grading to be altered, such as the vibratory compaction table, should be seriously considered.

1. INTRODUCTION

During the investigation into the compactability of untreated roadbuilding materials (RDAC 88/030/2) it was found that the laboratory standard for compaction namely the modified AASHTO compaction test does not optimally compact untreated roadbuilding materials (see Figure 1)¹.

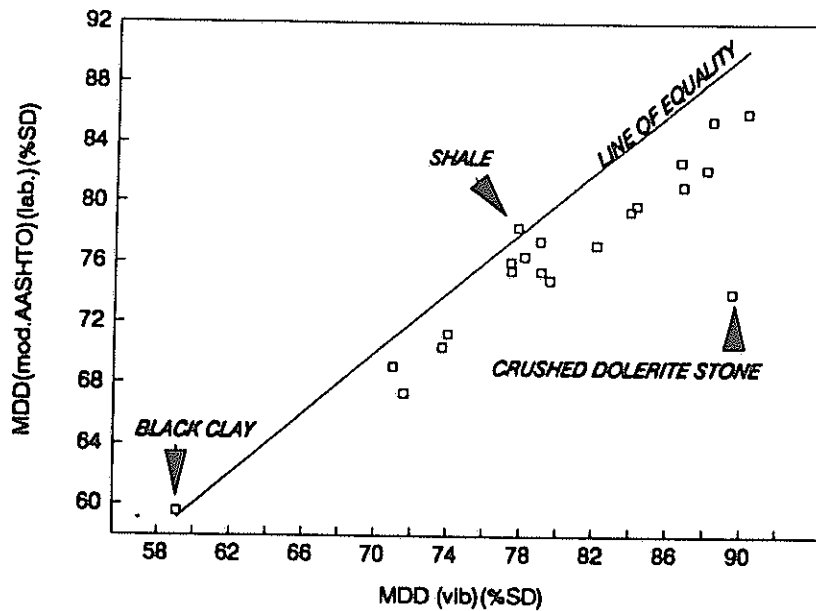


Figure 1.1: The relation between MDD(mod.AASHTO)(laboratory)(%SD) and MDD(vibratory compaction table)(%SD)

A comparison of density measurements from HVS sites before and after the HVS tests with the predicted densities of the compactability model showed that the predicted 100 % mod.AASHTO value (using the total grading and Atterberg limits) agreed well with the original density before the HVS test. The predicted optimal density also agreed well with the measured densities after the HVS tests (see Table 1.1).

Table 1.1: Comparison of the measured and predicted densities of materials in different layers on some HVS sites

SITE	Initial Density (kg/m ³)		MDD(vib)lab	End Density (kg/m ³)	
	In situ DD	MDD(mod)*		In situ DD	MDD(vib)*
ROOI3(G6)	1989	1957,4		1986	2038,6
ROOI3(G6)	1962	1957,4		1996	2038,6
ROOI3(G6)	1962	1957,4		1982	2038,6
ROOI3(G6)	1916	1957,4		1930	2038,6
ROOI3(G6)	1856	1957,4		1896	2038,6
ROOI3(G6)	1893	1957,4		1918	2038,6
ROOI4(G5)	1959	1965,8		2027	2063,8
ROOI4(G5)	2023	1965,8		2038	2063,8
ROOI4(G5)	1927	1965,8		1942	2063,8
UMK01(G2)	2283	2195,0		2368	2330,5
BULT3(G6)	1944	2016,4		2080	2080,2
BULT3(G6)	2012	2016,4		2059	2080,2
BULT3(G6)	1995	2016,4		2081	2080,2
BULT3(G6)	1929	2016,4		2190	2080,2
BULT3(G6)	2068	2016,4		2082	2080,2
BULT4(G6)	1772	2002,4		1789	2054,3
BULT4(G6)	2012	2002,4		2059	2054,3
BULT4(G6)	1930	2002,4		1982	2054,3
BULT4(G6)	1893	2002,4		1966	2054,3
RICH1(G2)	2446,5	2449,7		2560,5	2580,6
RICH2(G4)	1909,5	2112,9	2130	1997,5	2206,3
RICH3(G6)	1860	1882,6		1910	1939,1
RICH3(G6)	1891,5	1882,6		1932	1939,1
RICH4(G5)	1909,5	1920,2		1947	1981

* Only one grading and Atterberg limits available for prediction of MDD of a particular layer.

The results in Table 1.1 clearly show that, if the compactive forces of road traffic are great enough, the granular roadbuilding materials will be compacted to their optimal density as determined by their total gradings and Atterberg limits.

In a report on the permanent deformation in pavements with granular bases and subbases, Shackleton² concluded that the amount of rutting taking place during the bedding phase of the pavement could shorten the pavement design life of 20 years (normal rut depth 20 mm) by between one and eight years. This amounts to a loss of service life of between 5 - 40 %. Most of this loss could be avoided if all pavement layers are optimally compacted. The estimated extra compaction costs should not exceed 1 % of the project costs. Shackleton also pointed out that apart from the extra service life because of optimal compaction, the optimal compaction will also contribute to :

"Saving brought about by being able to delay maintenance.

Higher serviceability of the pavement throughout its life.

Reduced vehicle operating costs throughout the pavement's life.

Better safety (less ponding) for the road user." ²

The investigation into the optimisation of compaction specifications for different pavement layers is, therefore, warranted.

2. ACTUAL SITE WORK

2.1 INTRODUCTION

When the original project proposal was submitted to RDAC in 1990, the idea was that one test section would be monitored in each of the four provinces for the next three years, giving a total of 12 test sections. It was furthermore proposed and accepted that the provincial road authorities would take responsibility for site control while the laboratory work and data processing would be done by the Division of Roads and Transport Technology to save on travel and subsistence costs. However, owing to the severe cutback of government expenditure on roads, most of the road authorities were unable to assist and no provincial sites were available in 91/92.

As the Division was now responsible for both site monitoring and doing the laboratory work, it was agreed that construction sites as close as possible to the Division should be used and that more than one section would be monitored on each construction project. It was also agreed that the number of sections to be investigated would be determined by the budget, which could mean possibly fewer than four per annum. To counter the unavailability of construction sites in 1991/92 it was proposed to try and cover eight sections in 1992/93.

2.2 **SITE 1 (THE PRETORIA END OF THE PRETORIA-RUSTENBURG TOLL ROAD)**

The Department of Transport granted permission for this project to be monitored. Permission was given in June 1992. Immediate negotiations were started with both the consulting engineer's (BKS) site personnel as well as the contractor's (Basil Read) site personnel to explain what the objectives of the research were, as well as how the research would be done.

As proposed in the original document the provincial road authorities (see Appendix A), it was proposed that the vibratory roller should be balanced to ensure uniform compaction results over the full width of the roll. Each side of the on-site vibratory roller's roll was weighed ; the drum drive side (right-hand side) was found to be about 300 kg heavier than the left-hand side of the roll. A design drawing of the plate to supply the extra mass on the left hand side was supplied to Basil Read. However, by the middle of September it became clear that the contractor did not intend to make this plate. It was therefore decided to do the experimental work with the existing construction equipment instead of waiting any longer, as only small sections of construction still remained on this site.

As different teams were constructing different layers, it was decided to try and cover as many of the different layer types as possible. Only a small section of fill and selected subgrade had not been constructed by that time, so the information on these layers is rather limited. Other layers that were covered in this investigation were the first and second stabilized subbases as well as the crushed stone base course (before slushing).

Rain or breakdown of equipment caused delays from time to time. Rolling was very often delayed to late in the afternoon which unfortunately meant that the research team could not always stay to the end of the final rolling of a particular layer.

Furthermore, the contractor's site personnel very often decided to follow their own approach rather than that suggested. Despite this deviation from the proposed approach, it was decided to monitor the effectiveness of the rolling techniques used rather than reduce the number of sites monitored.

The results are, therefore, grouped together in layer type, rather than discussed under a particular section. The different layers will be discussed in sequential order from the bottom up. As it would be impractical to show all the results, an extract has been made to show the general trend for each layer.

2.3 THE METHOD OF COMPACTION AND CONTROL PROCEDURE FOLLOWED

The actual technique followed was to determine the compaction growth curve by means of a nuclear moisture/density gauge. This allows for a large number of readings to be recorded in quick succession without delaying the compaction process excessively. The recommended compaction procedure as proposed by the Division of Roads and Transport Technology (see Appendix A for more detail) entailed the following general sequence :

- (a) Vibratory roller (high amplitude - low frequency combination).
- (b) Vibratory roller (low amplitude - high frequency combination).
- (c) Pneumatic-tyred roller.

The change-over between roller types had to occur as soon as it was established that the operating roller type and technique did not show a substantial increase or otherwise a decrease in density between successive roller passes. Although this technique was generally followed for the final compaction after the final levelling had been done by the grader, the contractor seemed to prefer to use the grid roller as the initial compaction tool and in many cases as many as 6 grid roller passes were applied before the final levelling. In the case of fill material, use was made of a

vibratory tamping-foot roller for the initial compaction and a five sided impact roller for the final compaction (20 passes). The fill was constructed according to a method specification rather than a density specification.

For the purpose of achieving uniform density levels the Division recommends that the same compaction sequence and the same number of passes should be applied to each part of the layer. This means that only one roller should be used at a time or that the compaction of the layer should have proceeded far enough for the next roller (e.g. the pneumatic-tyred roller) to start rolling without the rollers interfering with one another. However, as researchers had to depend on the cooperation of the contractor (without any binding authority), it happened on this site that the contractor sometimes used all three main roller types (grid, vibratory and pneumatic-tyred rollers) all at the same time and in a haphazard manner.

2.4 THE DENSITY RESULTS MEASURED

2.4.1 Fill

Only two relatively small sections of fill material, a yellow broken-down shale, remained by the time the actual research work started. Figure 2.1 shows the measured densities after 6 passes with the vibratory tamping-foot roller. Note that the densities ranged from 1 900 kg/m³ at a moisture content of 12 % to 1 400 kg/m³ at a moisture content of 24 %, emphasizing the important effect of moisture content on the densities that can be achieved.

Figure 2.2 shows the measured densities after 20 passes with the five-sided impact roller. The densities ranged from 2 100 kg/m³ at a moisture content of 7 % to about 1 800 kg/m³ at a moisture content of 15 %. The measured density results are once again approximately parallel to the zero air voids dry density line (ZAVDD)(i.e. line of total saturation), showing that even the high compactive forces react in the same way to pore pressure build up. The variation in the measured dry density results also point to one of the pitfalls of a method specification when no limits are placed on the level of the moisture content. Figure 2.3 shows the average measured dry densities for different layer thicknesses of fill. This figure illustrates that it is possible to compact thicker layers of material to uniform densities using impact compaction.

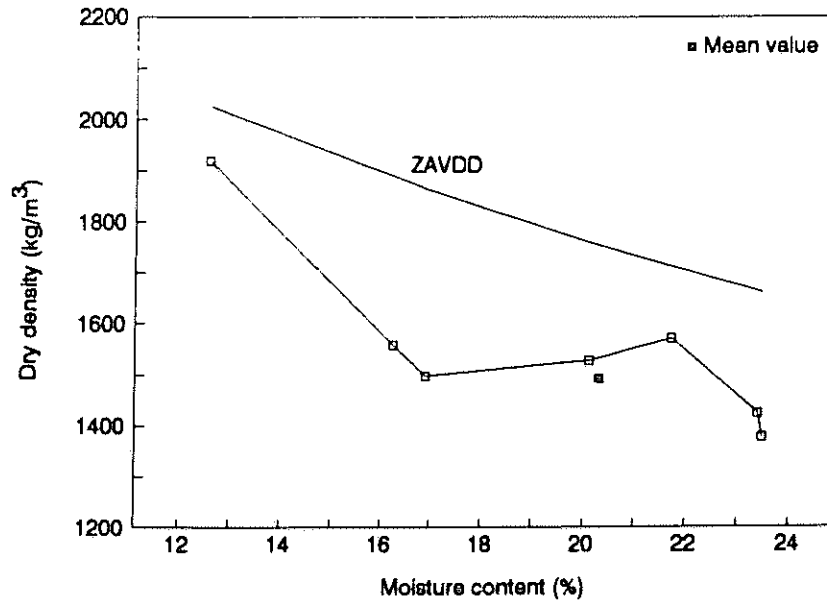


Figure 2.1: Measured dry densities against measured moisture contents on fill compacted with a vibratory tamping-foot roller (6 passes)

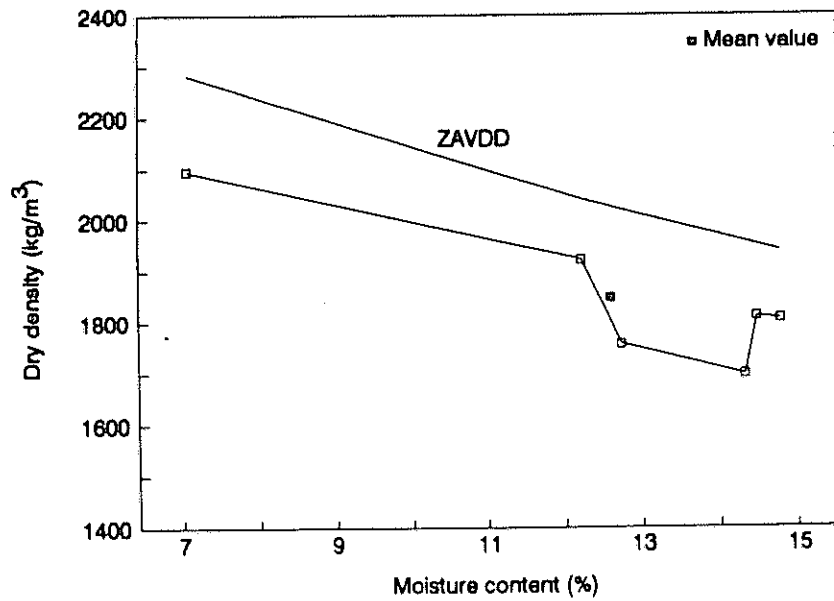


Figure 2.2: Measured dry densities against measured moisture contents on fill compacted with a five-sided impact roller (20 passes) (250 mm layer)

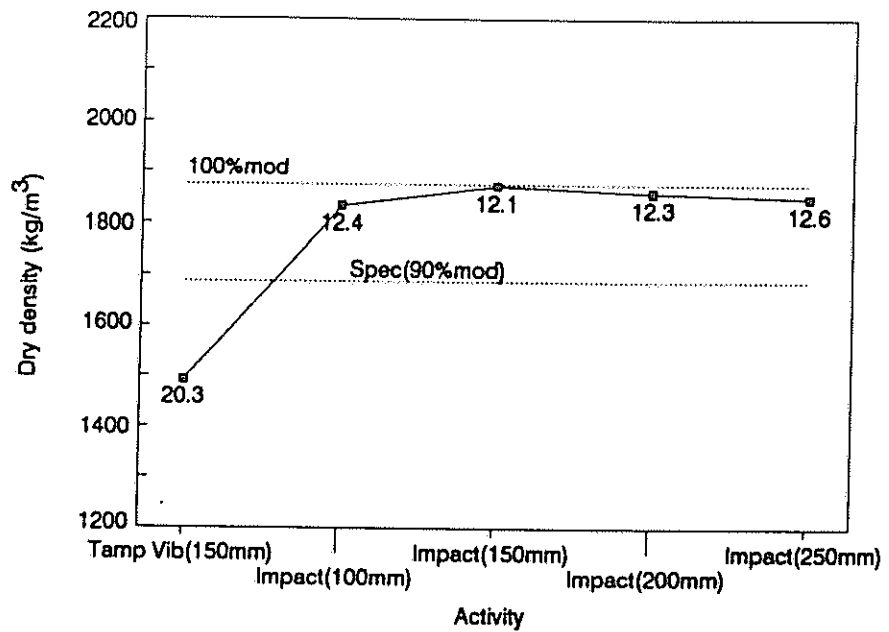


Figure 2.3: Average measured dry densities for different layer thicknesses of fill as well as method of compaction

2.4.2 Selected subgrade

Only two sections of subgrade, consisting of 200 mm layer of G6 material obtained SABRIX quarry and had to be compacted 90% mod.AASHTO, were left. Owing to time delays both sections could not be properly monitored through the compaction phases. However, it is still possible to gain some information from the measured results. Figure 2.4 shows the measured dry densities against the measured moisture contents for two similar gauges at the same measuring points. Although there are smaller differences between the measured values of the two gauges, the results agree well with each other. It also shows that the optimum compaction is achieved when the material is nearly saturated. This confirms the results of the vibratory compaction table.

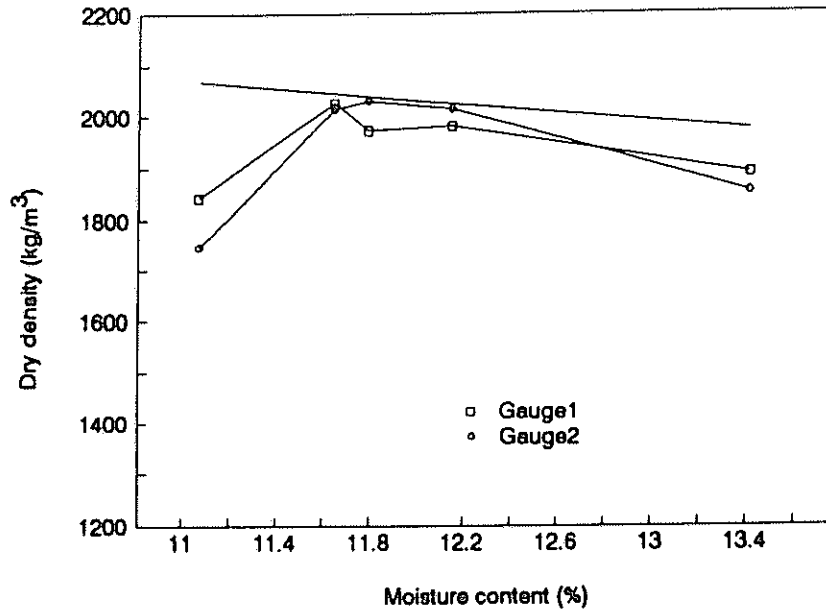


Figure 2.4: Measured dry densities against measured moisture contents for compacted selected subgrade materials using two CPN nuclear gauges

Figure 2.5 shows the compaction growth curve for the second section as far as it was monitored. The measured results show that the effect of the vibratory roller had reached its effective limit. The roller operators were advised apply on one full roller pass with the pneumatic-tyred roller after the vibratory roller.

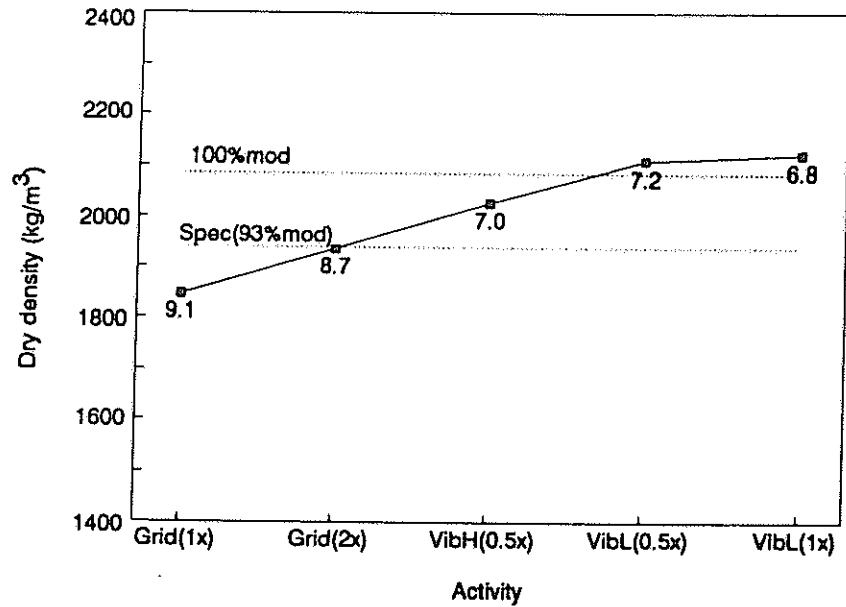


Figure 2.5: The compaction growth curve of the selected subgrade layer

2.4.3

Lower cement stabilized subbase (125 mm thick)

This layer consisted of crushed stone, a G4 material with nominal maximum stone size of 37,5 mm, from Olifantsfontein quarry to which an amount of fines from another source was added and stabilized with 2,5 % ordinary Portland cement (OPC). Three sections of this particular layer were monitored during compaction. The specification required that this layer be compacted to 95 % mod.AASHTO density. Figures 2.6 to 2.12 show the influence of the different activities on the dry density on Section 2.

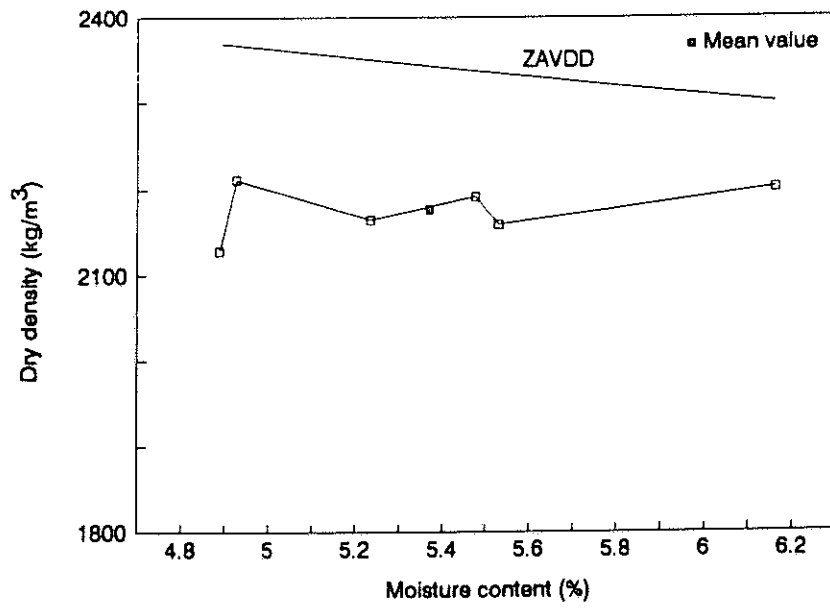


Figure 2.6: Measured dry densities against measured moisture contents for the lower cement stabilized subbase after two passes with grid roller

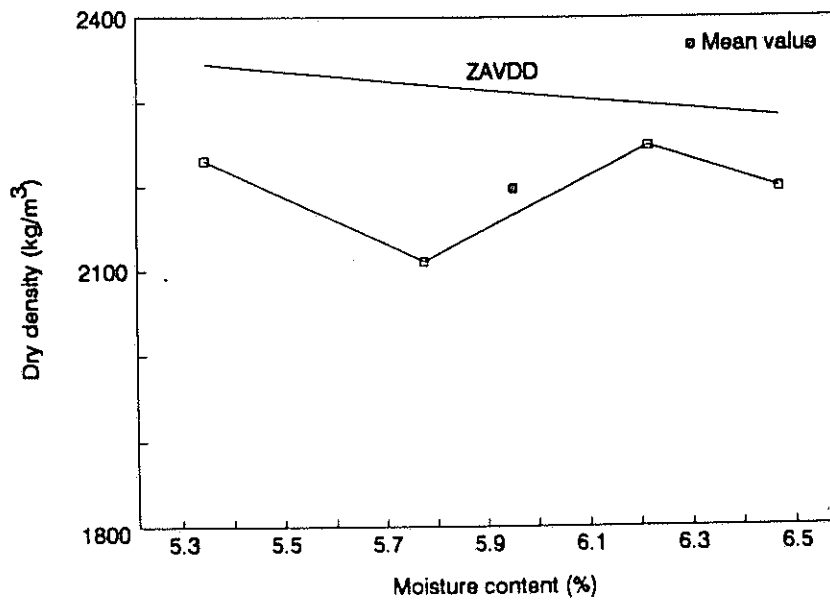


Figure 2.7: Measured dry densities against measured moisture contents for the lower cement stabilized subbase after grading the grid-rolled section

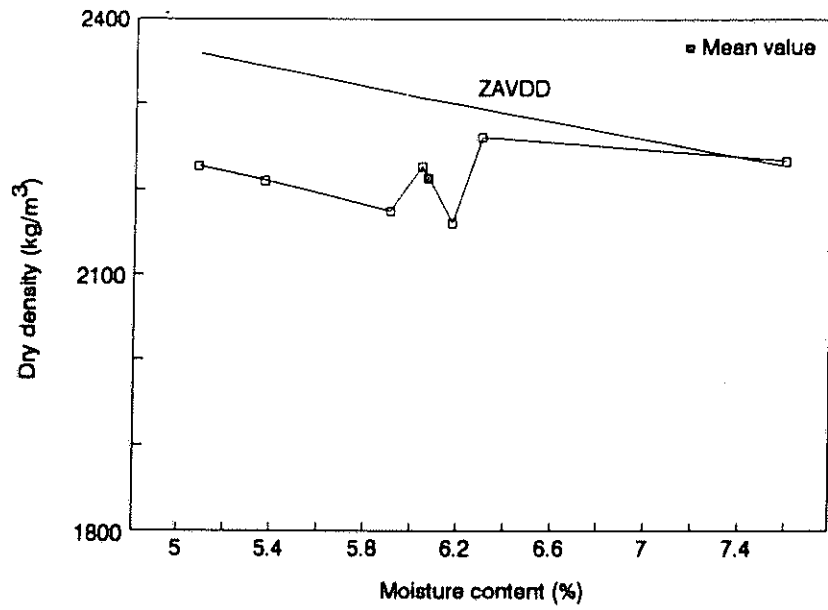


Figure 2.8: Measured dry densities against measured moisture contents for the lower cement stabilized subbase after two extra grid roller passes on graded section

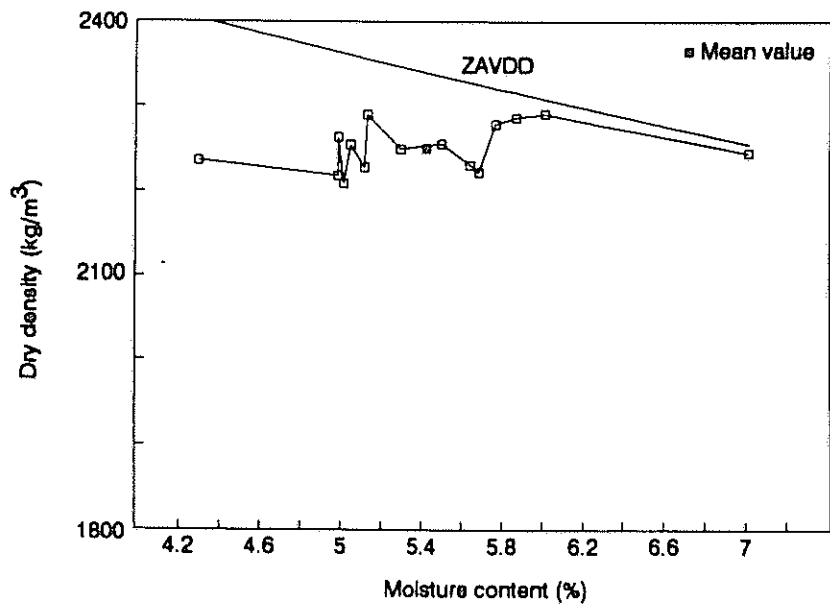


Figure 2.9: Measured dry densities against measured moisture contents for the lower cement stabilized subbase after a second grading and one full pass with vibratory roller (G2 + V1)

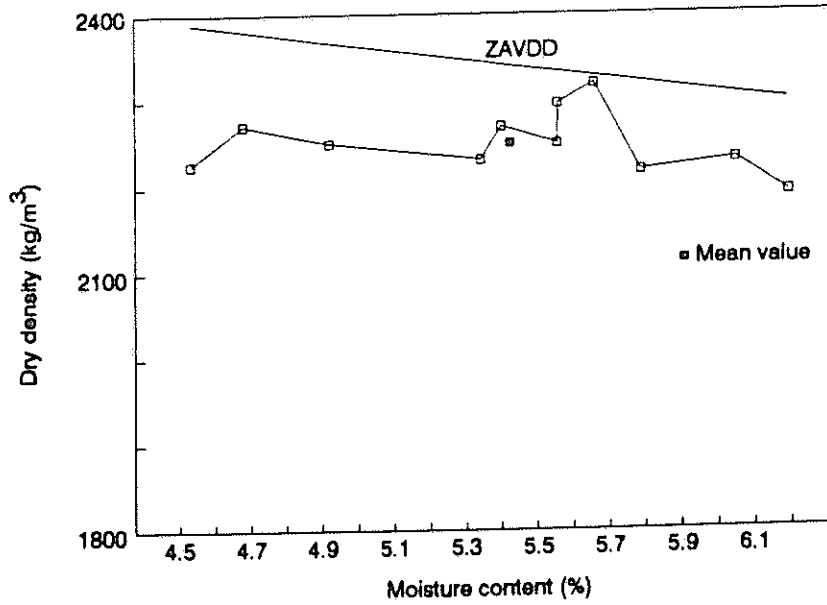


Figure 2.10: Measured dry densities against measured moisture contents for the lower cement stabilized subbase after one pass with pneumatic-tyred roller (PTR) on the vibratory compacted section

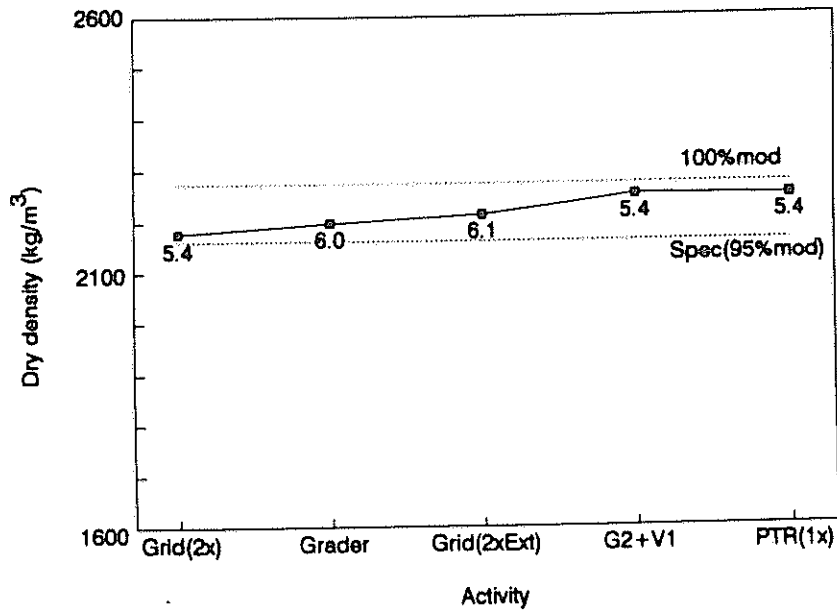


Figure 2.11: The compaction growth curve of the lower cement stabilized subbase of Section 2 showing the average dry densities (measured) against the activity prior to taking the density measurements (average moisture content value is printed below data point)

Figure 2.11 shows that no excessive compactive effort was required to achieve acceptable results. Figures 2.12 and 2.13 show the compaction growth curves for the other two sections. Figure 2.12 shows that four passes with the grid roller were applied after grading, before the vibratory roller started. Note that the vibratory roller was not very effective, because the moisture content of the material was too low (i.e. close to CMC value where maximum cohesive forces occur). There was no water sprayer available on site at this stage (approximately 18:00). After obtaining the services of such a sprayer and spraying and rolling with the pneumatic-tyred roller, an immediate increase in the layer dry density was achieved. Note, however, that if too much water is applied it could lead to a lowering of the in situ dry density levels.

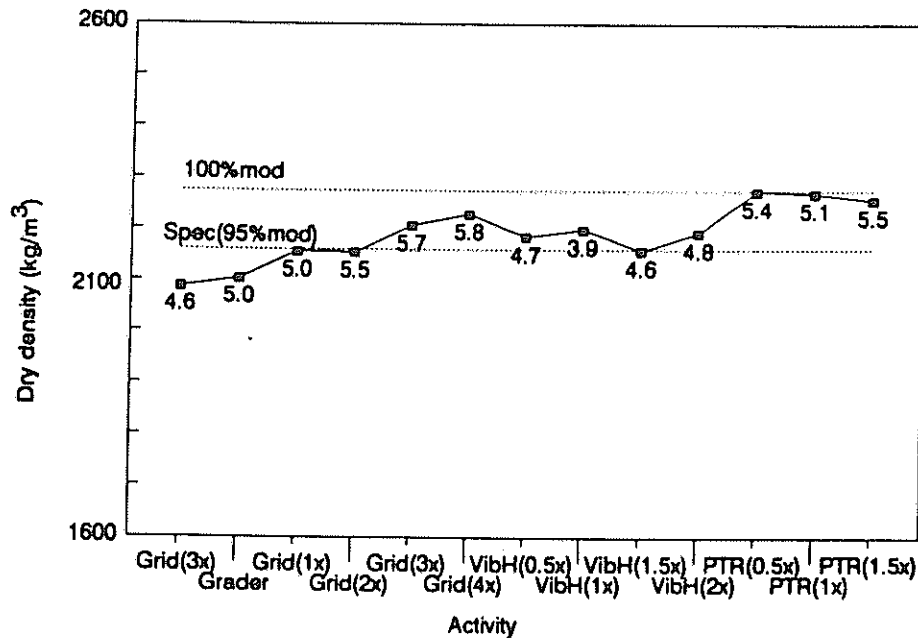


Figure 2.12: The compaction growth curve of Section 3 showing the average dry densities (measured) against the activity prior to taking the density measurements (average moisture content value is printed below data point)

For Section 6 the use of the vibratory roller for initial compaction was strongly suggested. However, the grader operator (in charge of the team in the absence of a foreman) insisted on doing half a pass with the grid roller before the half pass of the vibratory roller was applied after which the section was levelled with the grader (G1 in Figure 2.13). A full pass with the vibratory roller was then applied as the first phase of the final compaction this the section. However, the grader operator started grading the section again (G2) insisting that he had not finally graded the section the previous time. Once again a water sprayer had to be obtained before finalizing the compaction. It should be emphasized that at all times the moisture content level was only visually assessed by the construction team but never measured.

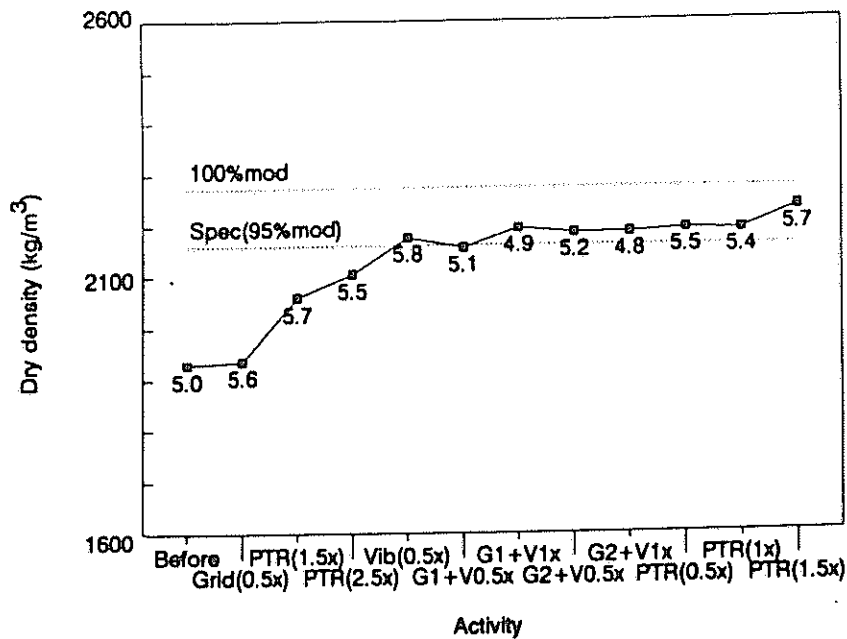


Figure 2.13: The compaction growth curve of Section 6 showing the average dry densities (measured) against the activity prior to taking the density measurements (average moisture content value is predicted below data point)

Note that with all the extra rolling of the last two sections (see Figures 2.12 and 2.13) the results were not markedly better than that of the first section (see Figure 2.11). This clearly shows that visual assessment of compaction criteria is not very effective at all, even where experienced personnel are involved.

2.4.4 Upper cement stabilized subbase (125 mm thick)

The compaction of this layer, consisting of the same material as the previous layer and treated in the same manner, was monitored on six sections (Sections 1 and 2 were done at the same time).

The required density was, however, increased to 97 % mod.AASHTO. The research team was advised of this only after the first section (Section 6), using 95 % mod.AASHTO as criteria. Figures 2.14 to 2.19 show the compaction sequence activities for this particular section. Problems were experienced in compacting this section; it was later discovered that a different source of fines had been added to this section which influenced the grading.

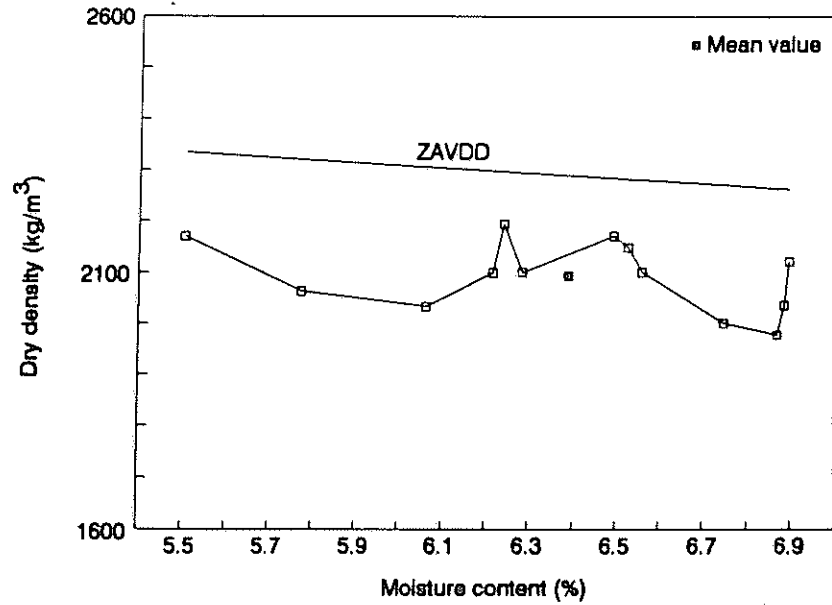


Figure 2.14: Measured dry densities against measured moisture contents for upper cement stabilized subbase after one and a half passes with pneumatic-tyred roller

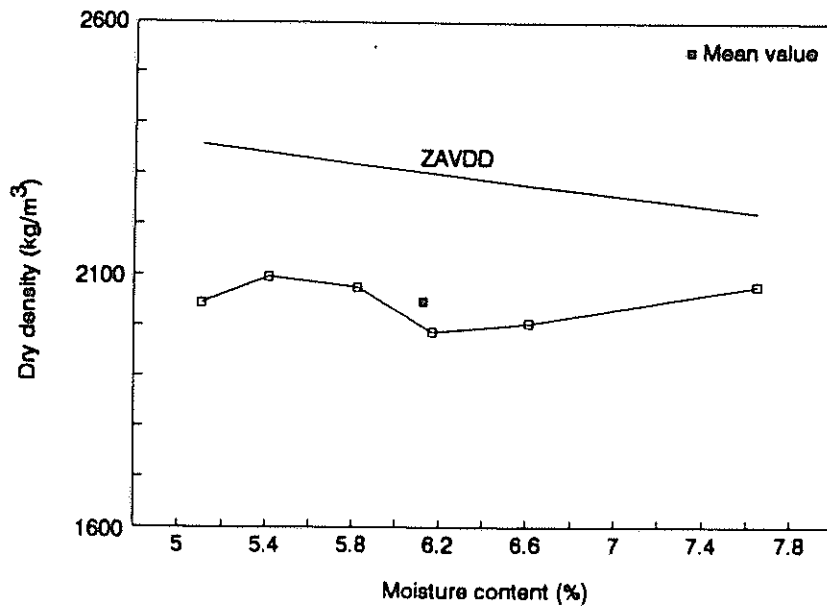


Figure 2.15: Measured dry densities against measured moisture contents for upper cement stabilized subbase after grading the pneumatic-tyred rolled section

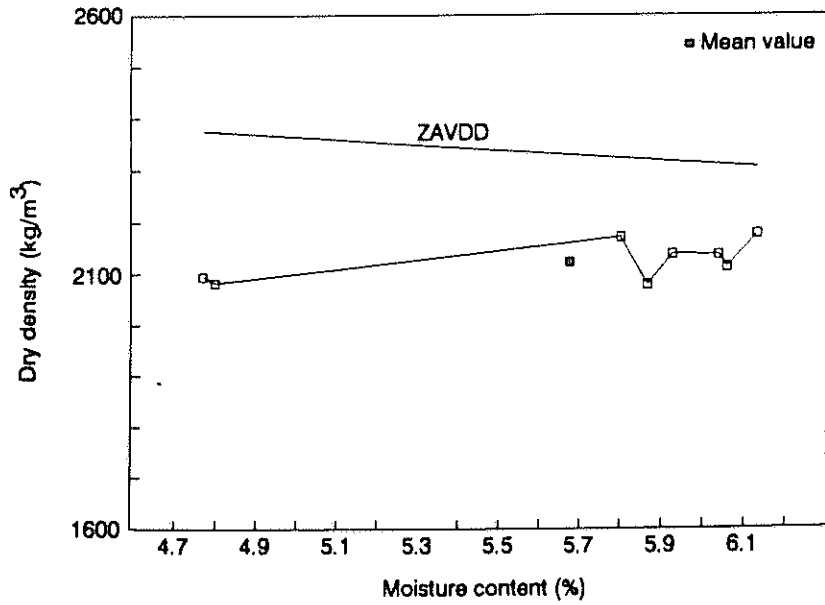


Figure 2.16: Measured dry densities against measured moisture contents for upper cement stabilized subbase after half a pass with the vibratory roller (high amplitude/low frequency) on the graded section

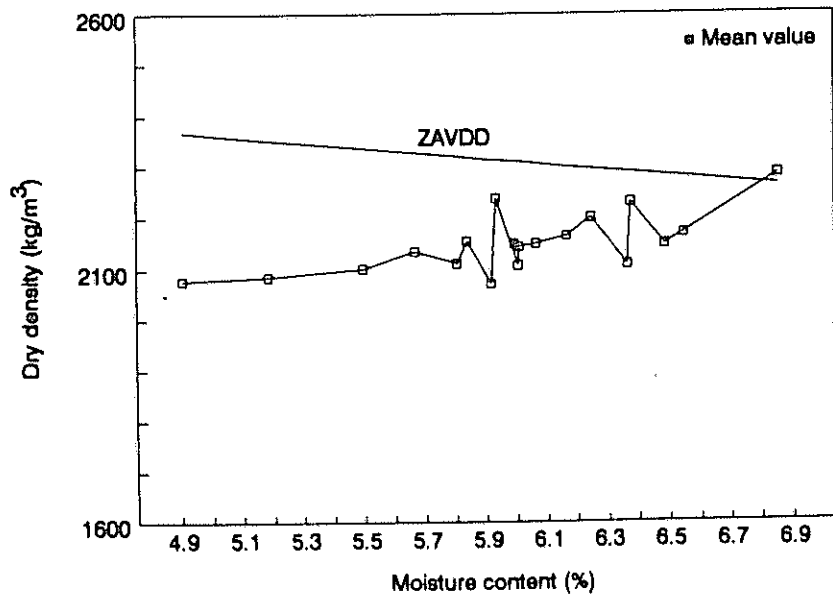


Figure 2.17: Measured dry densities against measured moisture contents for upper cement stabilized subbase after another half a pass with the vibratory roller (low amplitude/high frequency)

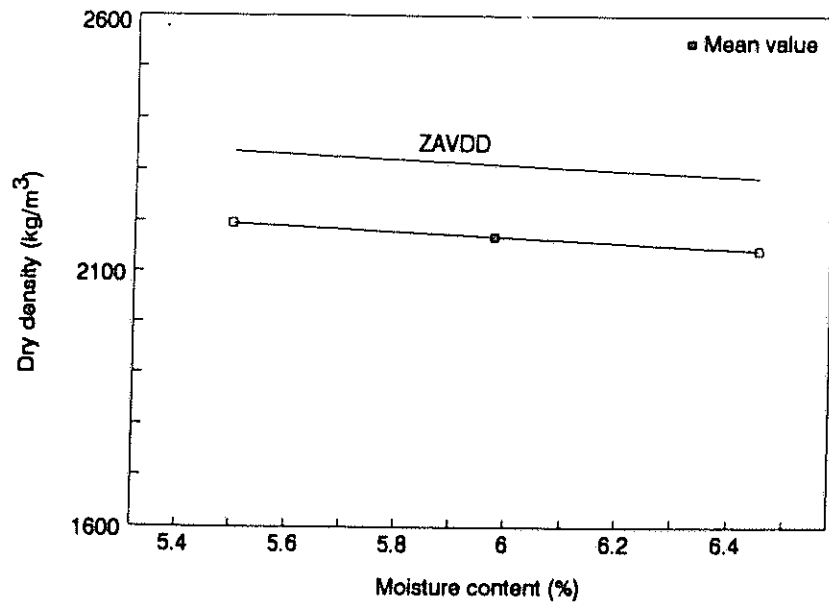


Figure 2.18: Measured dry densities against measured moisture contents for upper cement stabilized subbase after half a pass with pneumatic-tyred roller on the vibratory-rolled section

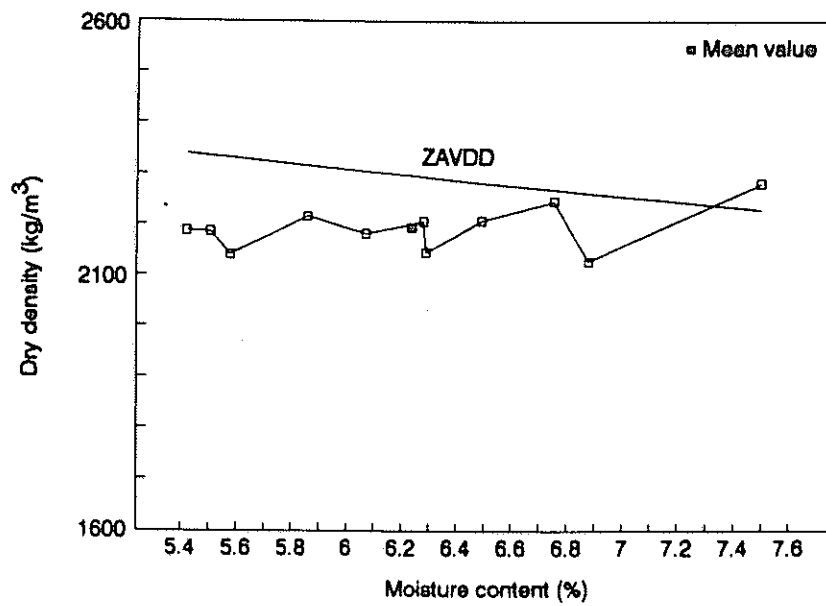


Figure 2.19: Measured dry densities against measured moisture contents for upper cement stabilized subbase after one full pass with the pneumatic-tyred roller

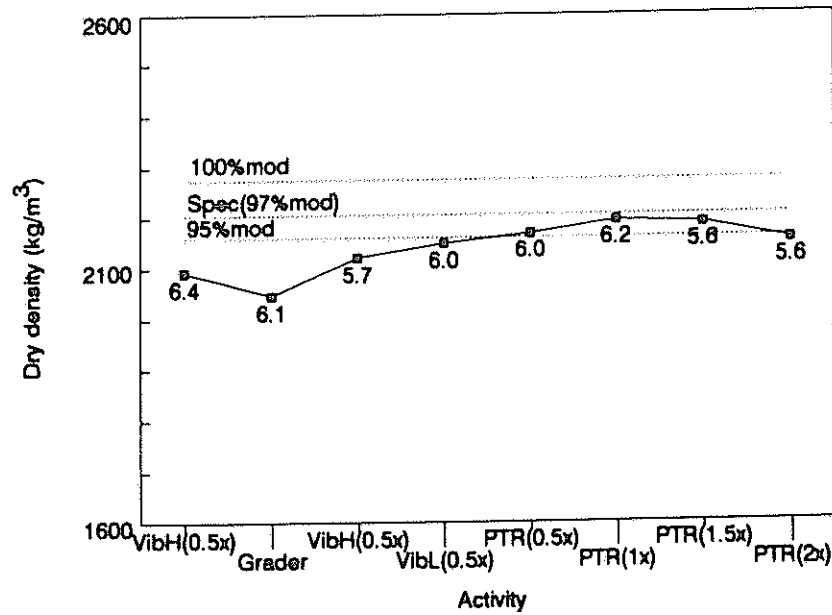


Figure 2.20: The compaction growth curve of the upper cement stabilized subbase of Section 6 showing the average measured dry density against the activity prior to taking the moisture/density measurements (average measured moisture content value is printed below data point)

Note that the maximum dry densities are always achieved near to the zero air voids dry density line (i.e. the material is totally saturated) (see Figures 2.17 and 2.19). Because the density results were lower than those of the lower cement stabilized subbase, the pneumatic-tyred roller operator was instructed to apply another pass on one lane to see whether this would increase the density. When it was noted that the extra effort actually lowered the density, the operator was instructed to apply only one pass to the rest of the section. Figure 2.20 shows that the average dry density is above 95 % mod.AASHTO after one pass with the pneumatic-tyred roller, but lower than 97 % mod.AASHTO. It was only the next day that it was noted that the compaction criteria for this layer was 97 % mod.AASHTO. When the section initially failed to pass the acceptance requirement, more acceptance tests were done by the consultants and the layer had subsequently passed the specification requirements. The compaction growth curves of this layer for the other sections are shown in Figure 2.21 to 2.24.

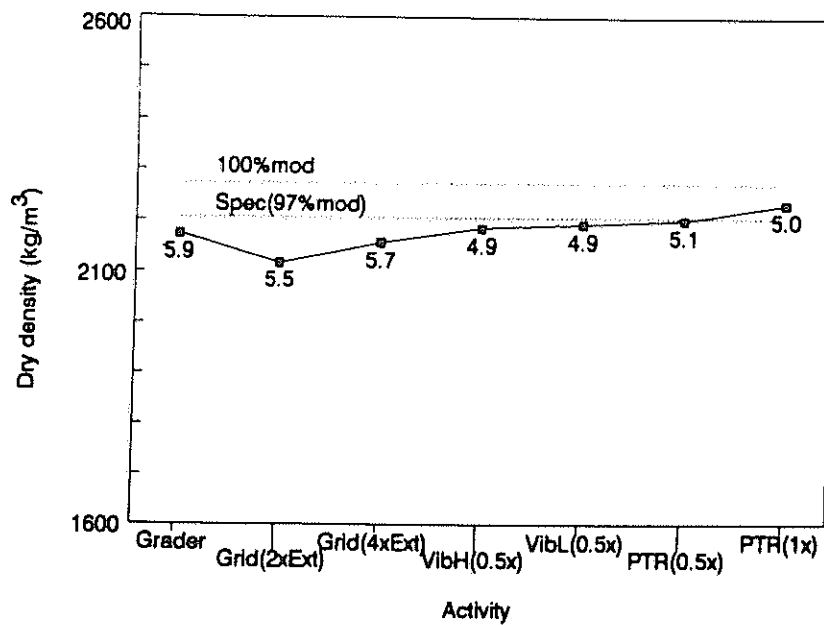


Figure 2.21: The compaction growth curve of the upper cement stabilized subbase of Sections 1 and 2 showing the average measured dry density against the activity prior to taking the moisture/density measurements (average measured moisture content value is printed below data point)

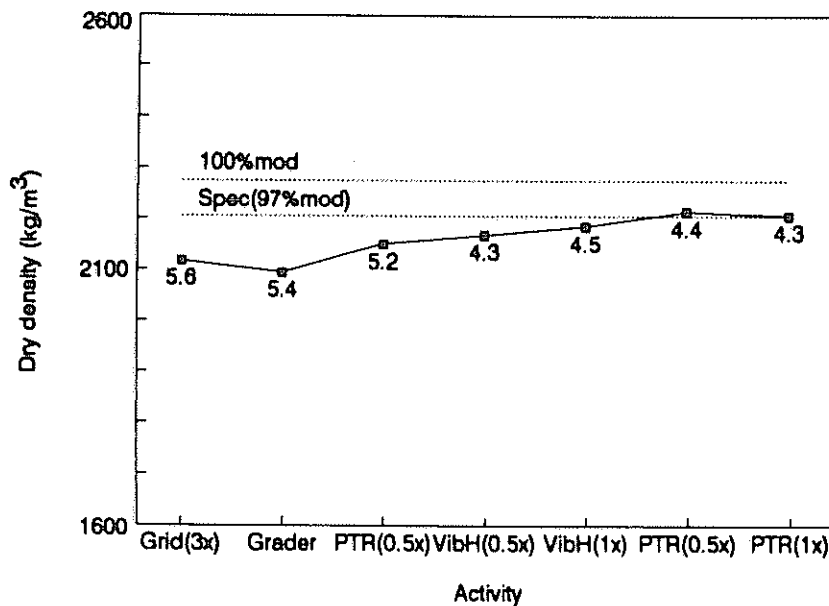


Figure 2.22: The compaction growth curve of the upper cement stabilized subbase of Section 3 showing the average measured dry density against the activity prior to taking the moisture/density measurements (average measured moisture content value is printed below data point)

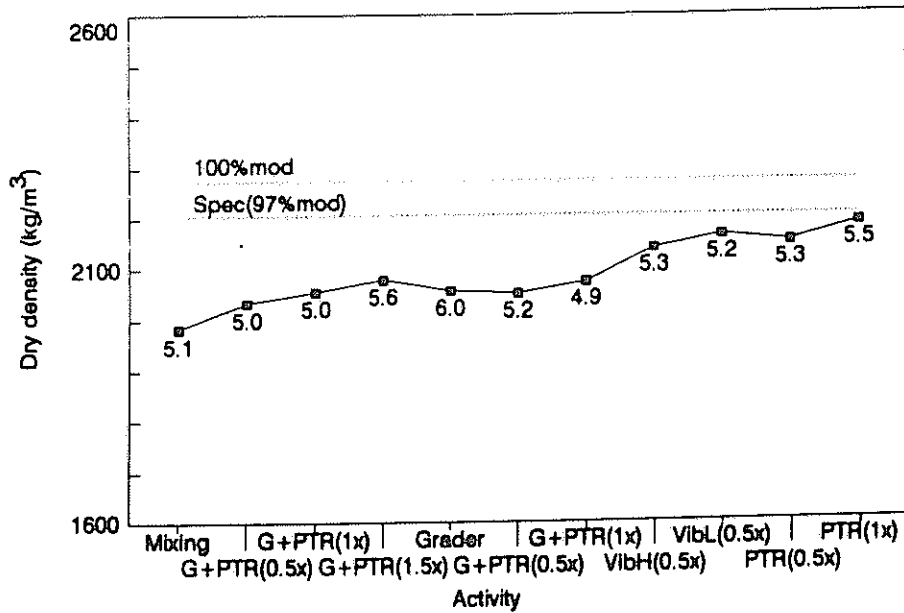


Figure 2.23: The compaction growth curve of the upper cement stabilized subbase of Section 5 showing the average measured dry density against the activity prior to taking the moisture/density measurements (average measured content value is printed below data point)

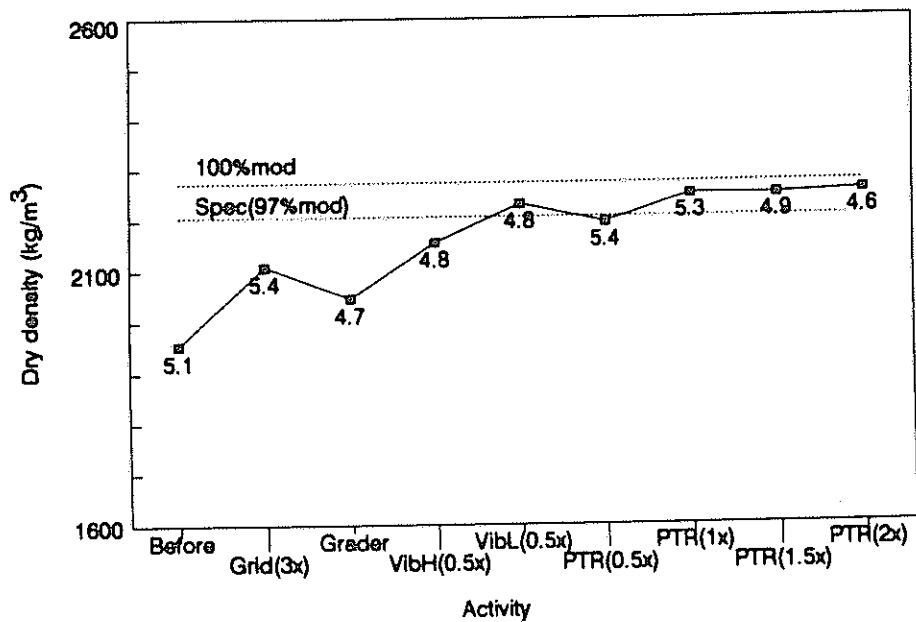


Figure 2.24: The compaction growth curve of the upper cement stabilized subbase of Section 7 showing the average measured dry density against the activity prior to taking the moisture/density measurements (average measured content value is printed below data)

The reason why the average dry density for Section 7 is lower after 0.5 passes with the pneumatic-tyred roller is because at least half the measurements were taken in the edge lane of the road (see Figure 2.25). The compaction growth curve without taking account of these edge lane measurements is shown in Figure 2.26.

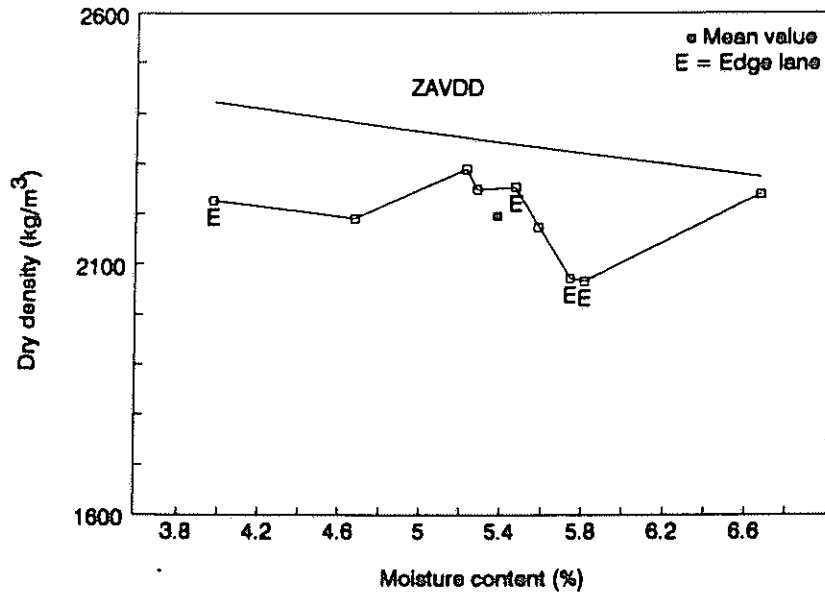


Figure 2.25: Measured dry densities against measured moisture contents of upper cement stabilized subbase after half a pass with the pneumatic-tyred roller on the vibratory-rolled section

The cause of the lower edge lane densities probably lies in a combination of the following:

- (a) The material on the edge of a layer is not as well mixed as rest of layer (grading and moisture content).
- (b) The edge lane is sometimes contaminated with some material from the previous layer which is lying in a windrow on the shoulder of the completed layer work.

The rise in the density growth curve from VibH(0.5x) to VibL(0.5x) in Figure 2.26 shows that on this section it would have been worthwhile to do another half a pass with the vibratory roller using the low amplitude/high frequency combination. However, on Section 1, 2, 3 and 5 (see Figures 2.21 to 2.23) the flattening out of the curve from VibH(0.5x) to VibL(0.5x) or VibH(1x) seems to indicate that one did not stand to gain much from further rolling with the vibratory roller. In the

case of Section 3, (see Figure 2.22) the moisture content of the layer was actually too low (should have been closer to 5.0), and the pneumatic-tyred roller had most probably compacted the top 50 mm of the layer while the lower 75 mm of the layer was left uncompacted by the initial half pass of the pneumatic-tyred roller immediately after the final grading of the layer. The bridging effect of the top 50 mm could possibly have been partly overcome if the moisture content had been higher (see Figure 2.23), but the water sprayer was not available as it was being used elsewhere. In some cases the problems with compaction can also be attributed to the fact that the cement had already started to bond while compaction was still taking place (excessive time spent on mixing and levelling).

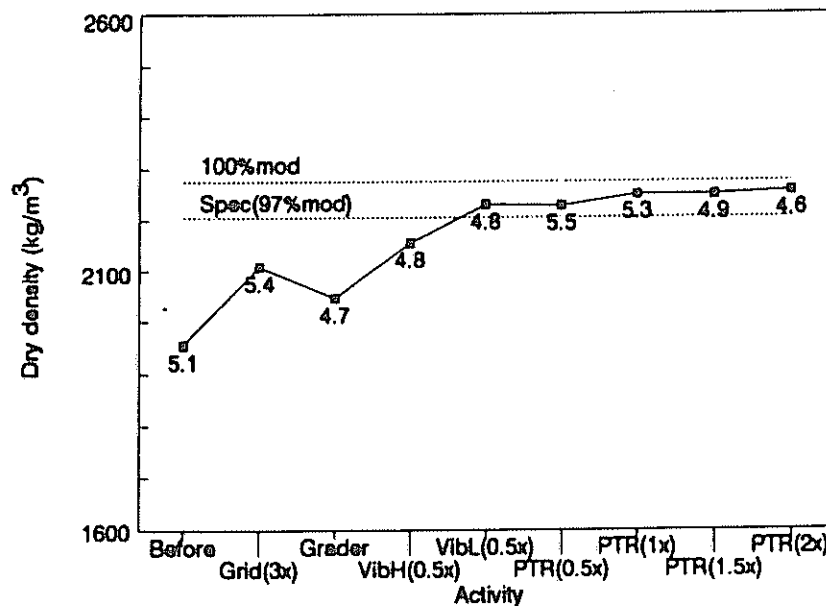


Figure 2.26: The compaction growth of the upper cement stabilized subbase of Section 7 showing the average measured dry density against the activity prior to the moisture/density measurements (minus the readings in the edge lane for 0,5 PTR) (average measured moisture content value is printed below data point)

2.4.5 Crushed stone base course (150 mm thick)

This layer consisted of a 150 mm layer of G1 crushed quartzite with a nominal maximum size of 37,5 mm from Ferro Crushers which had to be compacted to 88 %AD. However, the material seemed to have a lack of fines and permission was granted to add a fine cohesionless sand as additional fines in some cases.

Invariably the contractor tried to compact the layer first without the additional fines. Most of the time, however, the layer had to be reconstructed as it did not meet the density or grading requirements of the specification. Four sections of this layer were monitored including the construction and reconstruction of Section 3. The compaction process of this layer was only monitored in the initial compaction phase prior to slushing because the contractor and consultant did not want the research team to disturb the layer during or after slushing. For acceptance control purposes the consultant drilled the probe holes with a hammerdrill instead of knocking in the normal peg, to reduce the disturbance of the layer. Figures 2.27 to 2.28 show the compaction sequence used for compaction of the base course on Sections 1 and 2 (done simultaneously).

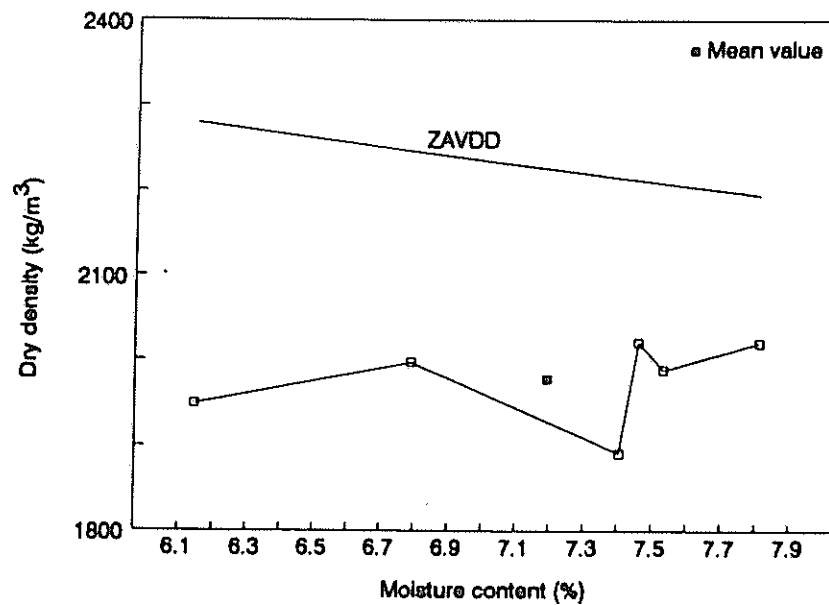


Figure 2.27: Measured dry densities against measured moisture contents for base course layer of Sections 1 and 2 after initial grading with grader

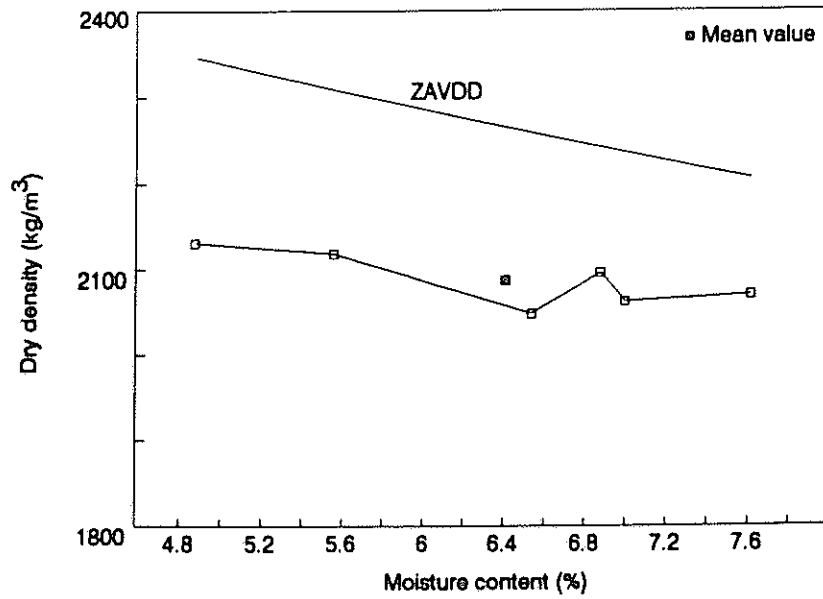


Figure 2.28: Measured dry densities against measured moisture contents for base course layer of Sections 1 and 2 after initial two passes with grid roller and one pass with pneumatic-tyred roller

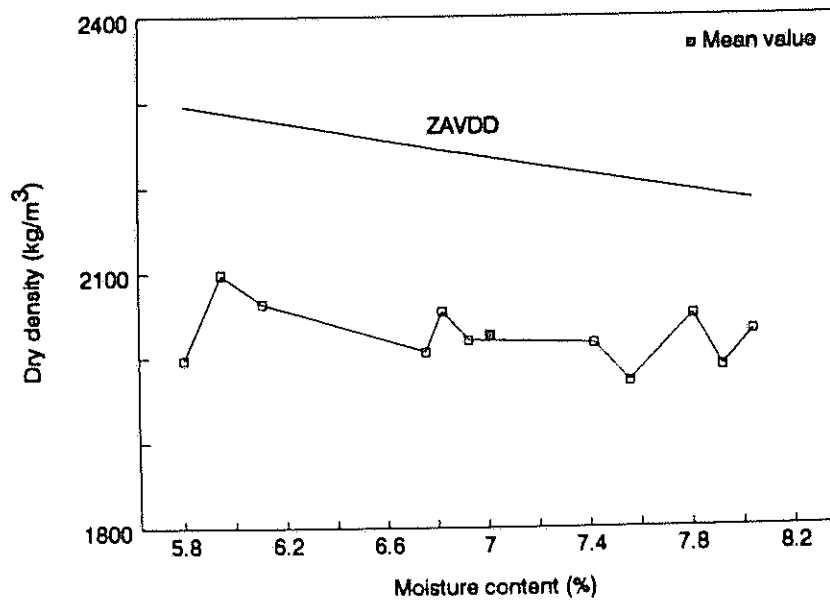


Figure 2.29: Measured dry densities against measured moisture contents for base course layer of Sections 1 and 2 after final grading with grader

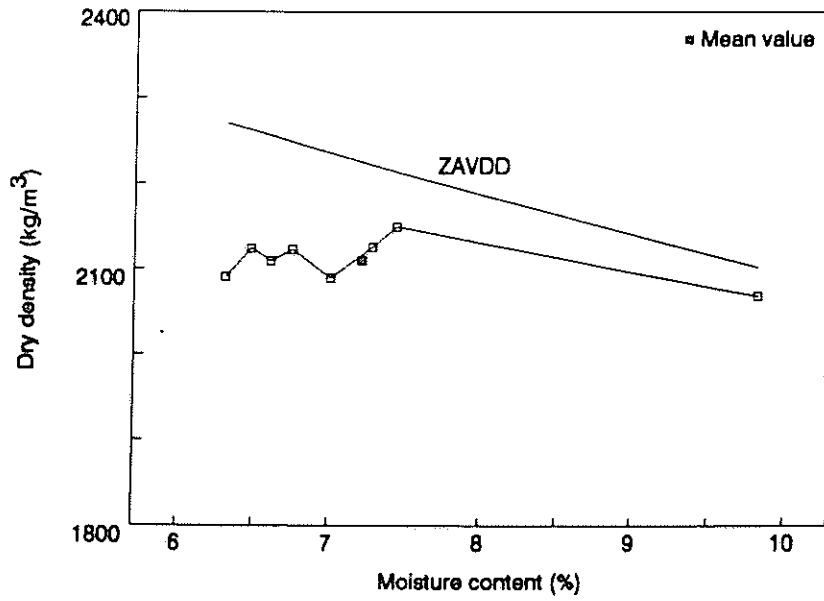


Figure 2.30: Measured dry densities against measured moisture contents for base course layer of Sections 1 and 2 after half a pass with vibratory roller (high amplitude/low frequency)

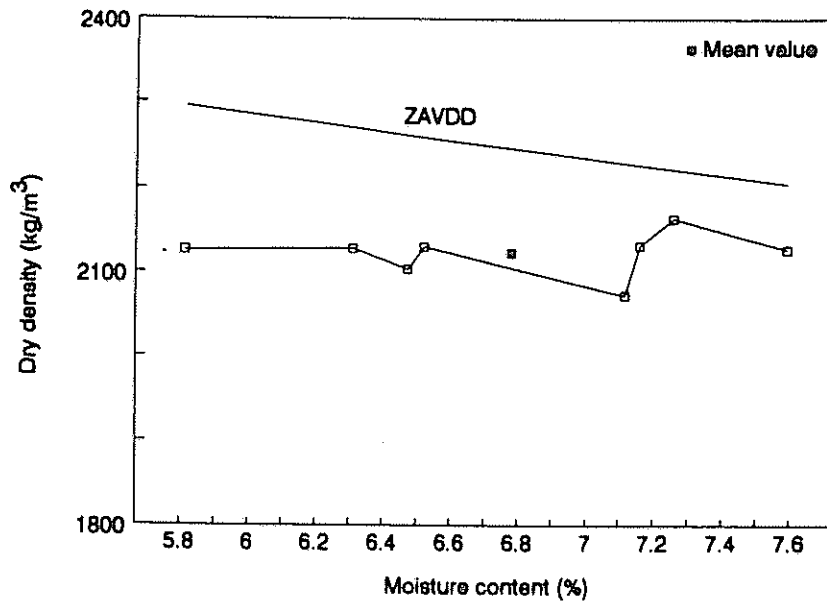


Figure 2.31: Measured dry densities against measured moisture contents for base course layer of Sections 1 and 2 after half a pass with vibratory roller (low amplitude/high frequency)

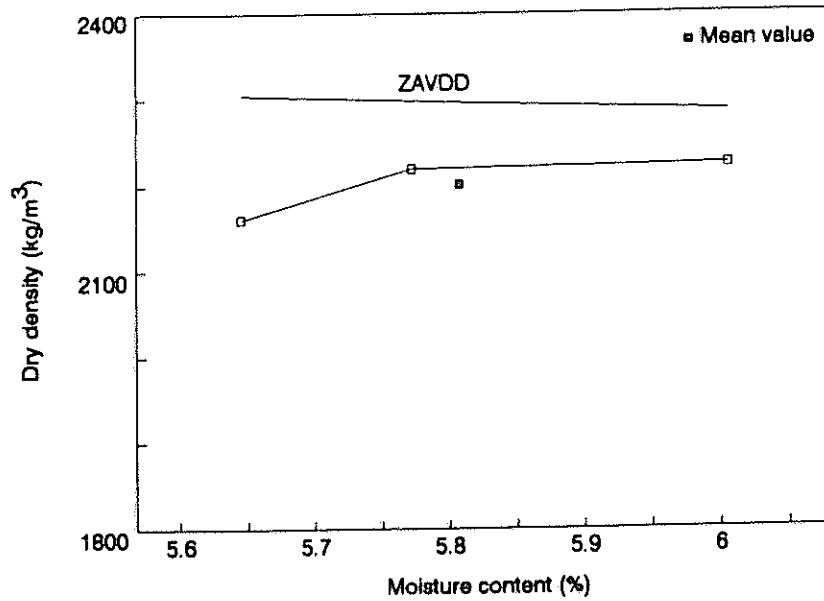


Figure 2.32: Measured dry densities against measured moisture contents for base course layer of Sections 1 and 2 after one full pass with vibratory roller (low amplitude/high frequency)

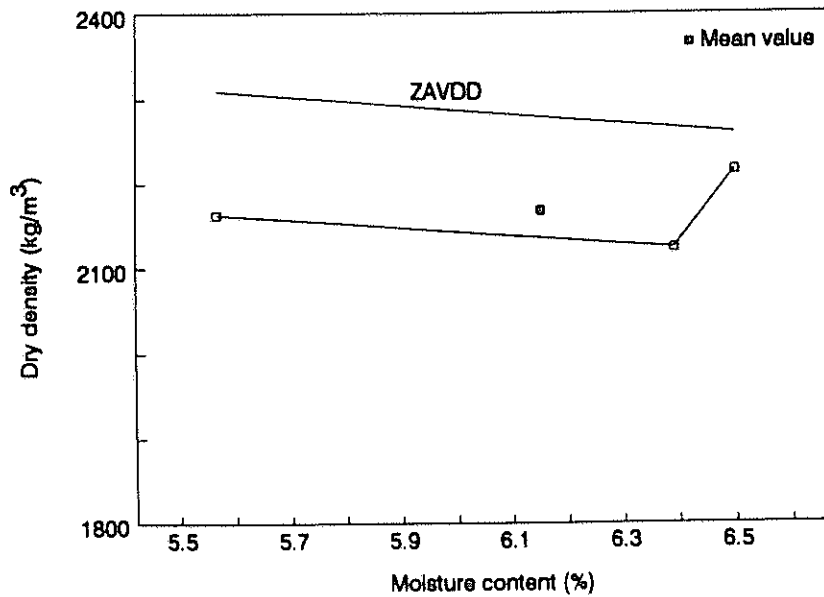


Figure 2.33: Measured dry densities against measured moisture contents for base course layer of Sections 1 and 2 after one and a half passes with vibratory roller (low amplitude/high frequency)

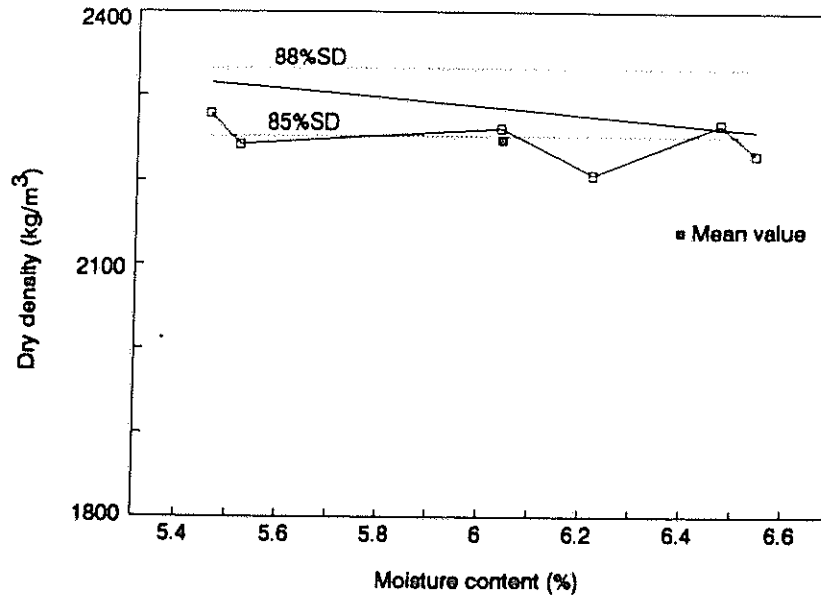


Figure 2.34: Measured dry densities against measured moisture contents for base course layer of Sections 1 and 2 after half a pass with pneumatic-tyred roller on vibratory-rolled layer

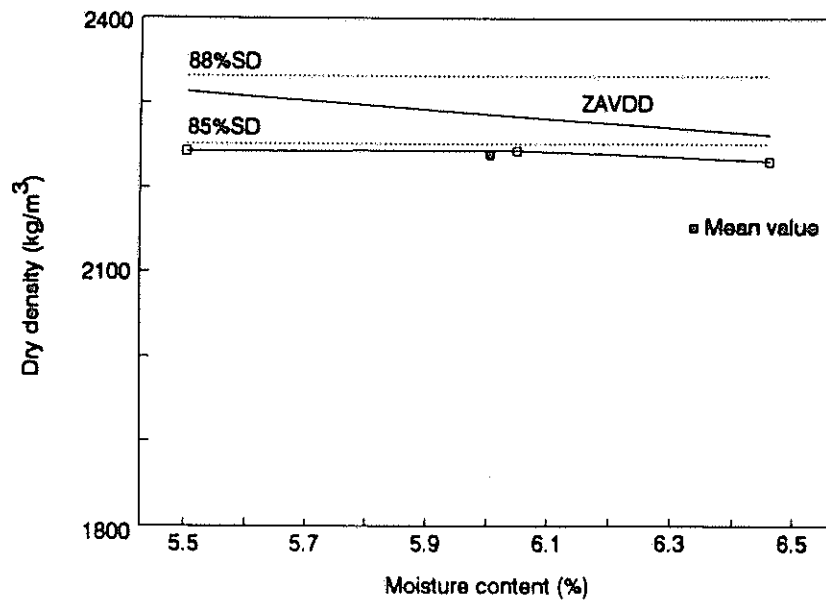


Figure 2.35: Measured dry densities against measured moisture contents for base course layer of Sections 1 and 2 after one full pass with pneumatic-tyred roller

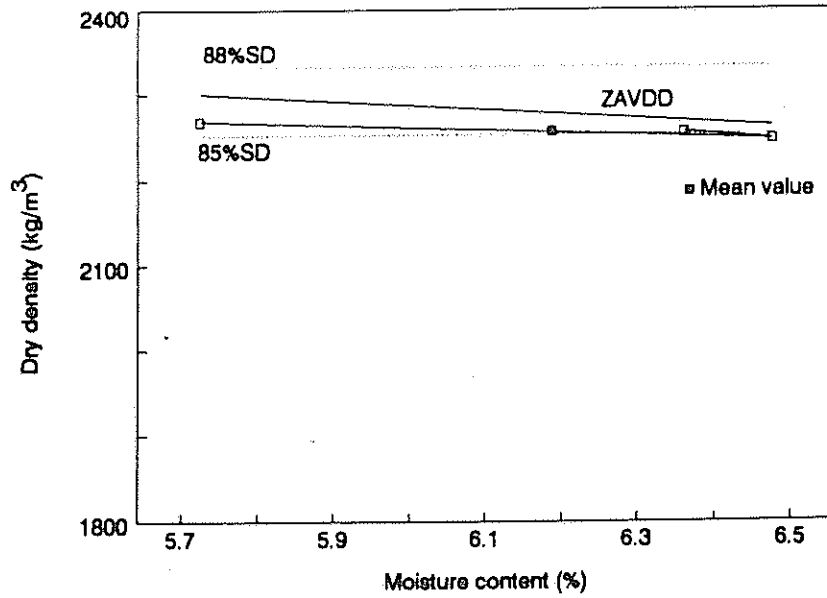


Figure 2.36: Measured dry densities against measured moisture for base course layer of Sections 1 and 2 after one and a half passes with pneumatic-tyred roller

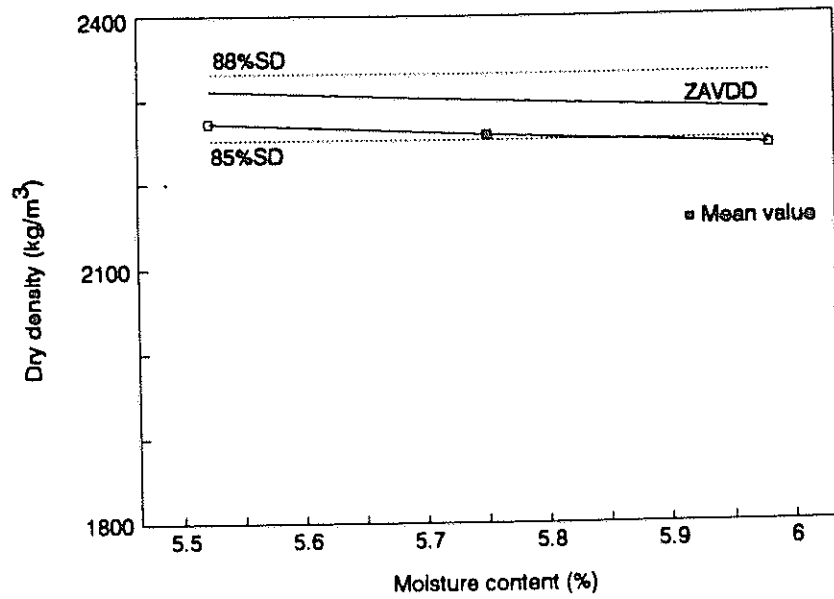


Figure 2.37: Measured dry densities against measured moisture contents for base course layer of Sections 1 and 2 after two full passes of pneumatic-tyred roller

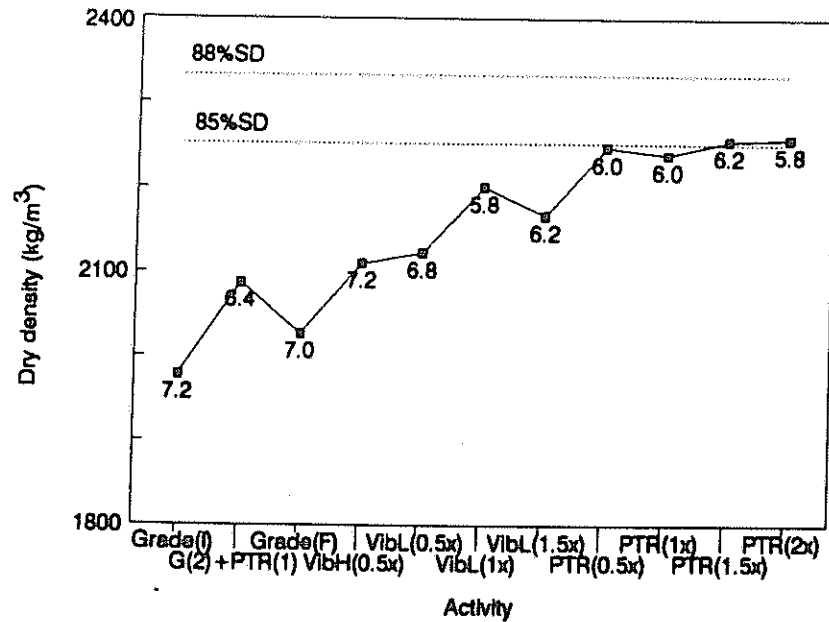


Figure 2.38: Compaction growth curve of the base course layer of Sections 1 and 2 showing the average measured dry density against the activity prior to taking the moisture/density measurements (average measured moisture content value printed below data point)

The compaction growth curves for the base course layers of Sections 7 and 3 and the reconstructed base layer of Section 3 are shown in Figures 2.39 to 2.41.

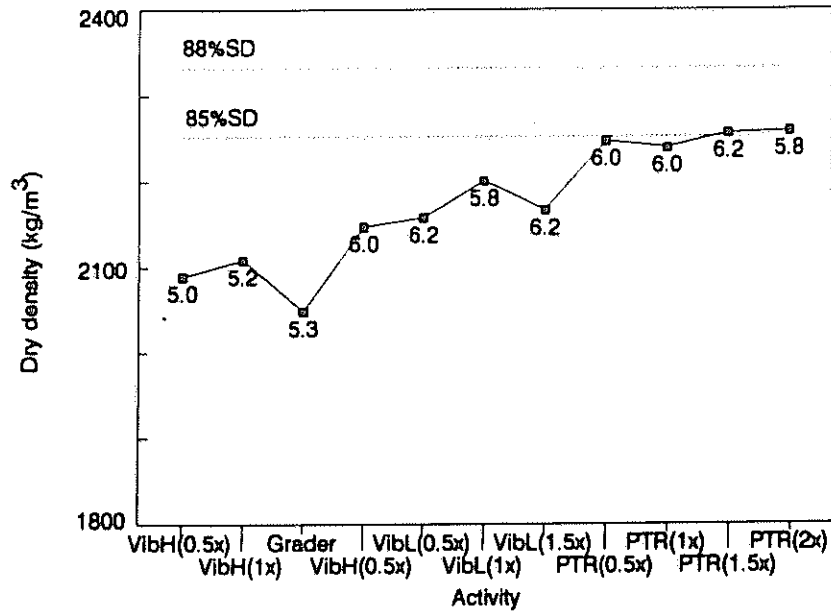


Figure 2.39: Compaction growth curve of the base course layer of Section 3 showing the average measured dry density against the activity prior to taking the moisture/density measurements (average measured moisture content value printed below data point)

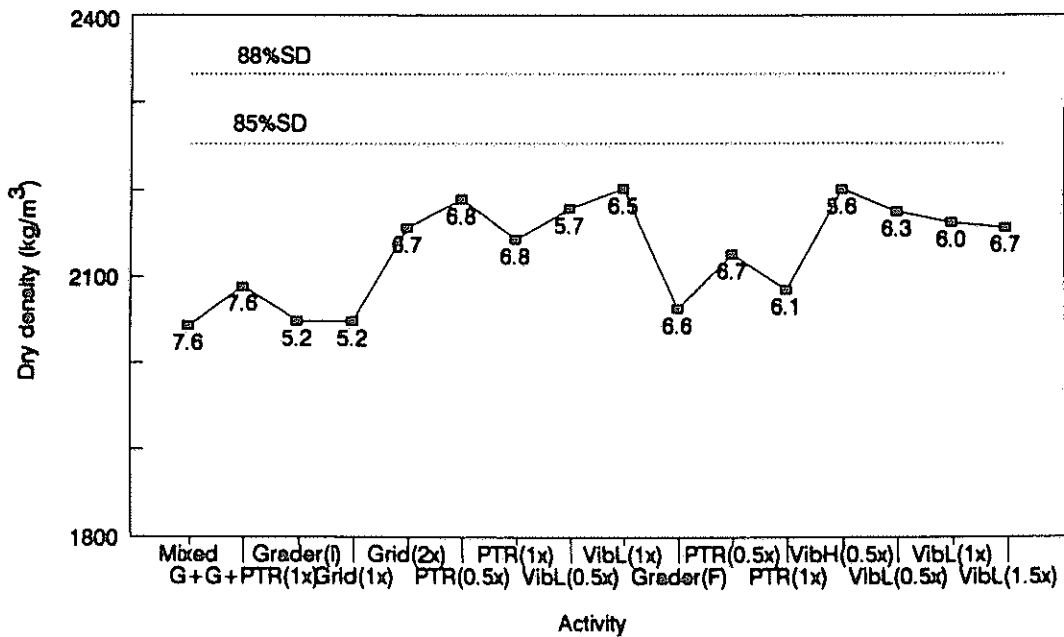


Figure 2.40: Compaction growth curve of the reconstructed base course layer of Section 3 showing the average measured dry density against the activity prior to taking the moisture/density measurements (average measured moisture content value printed below data point)

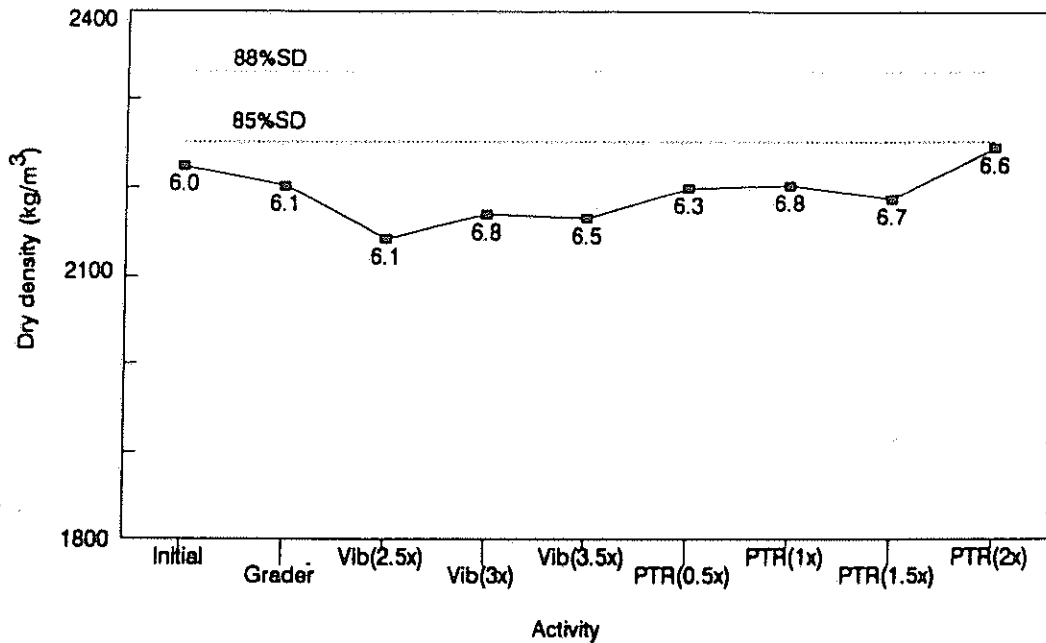


Figure 2.41: Compaction growth curve of the base course layer of Section 7 showing the average measured dry density against the activity prior to taking the moisture/density measurement (average measured moisture content value printed below data point)

Note from Figures 2.38 to 2.41 how much the layer is actually disturbed by the grading (levelling) process. Unnecessary levelling by the grader is therefore counter productive. From Figures 2.39 and 2.40 it would seem that the initial construction of the base course layer was more successful than the reconstruction. There are a number of reasons for this namely:

- (a) An excessive amount of extra fines was added to the layer as it was practically impossible to add the required amount, unless a chip-spreader was used (not available).
- (b) On the reconstructed layer the foremen insisted in over-applying the water. This also applies to Section 7.

By 18:00 when it was clear that extra rolling would still be required to compact this layer to specification requirements. The slushing process on this reconstructed layer on this section (Section 7) as well as on Sections 1 and 2, which also had to be reconstructed owing to a lack of fines, took two full days in each case to rid the layer of the excess fines. The tremendous construction effort

construction effort required to correct for small grading errors, once again emphasizes the importance of process control of the grading of G1 material prior to compaction. Similarly, the effective control of the moisture content will lead to substantial savings in the compactive effort required to compact a layer optimally.

Figure 2.42 shows the average measured densities as well as the back-calculated zone densities at the "initial stage". It should be pointed out that a substantial amount of compactive effort had already been applied at this stage. The zone density was calculated as follows (zones of 50 mm were used).

D_1	=	D_{50} (average)	D_1'	=	D_{0-50} (zone)
D_2	=	D_{100} (average)	D_2'	=	D_{50-100} (zone)
D_3	=	D_{150} (average)	D_3'	=	$D_{100-150}$ (zone)

$$D_1 = D_1'$$

$$D_2 = (D_1' + D_2')/2$$

$$D_2' = 2.D_2 - D_1' = 2.D_2 - D_1$$

$$D_3 = (D_1' + D_2' + D_3')/3$$

$$D_3' = 3.D_3 - (D_1' + D_2')$$

$$= 3.D_3 - 2.D_2$$

or $D_n' = n.D_n - (n-1).D_{n-1}$ (general equation) (2 - 1)

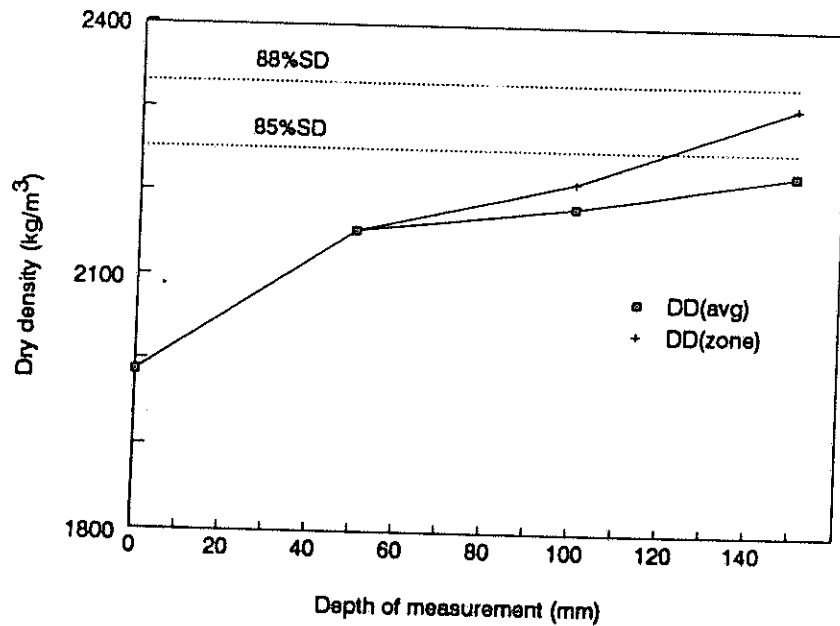


Figure 2.42: Average measured dry densities for different depths including back scatter (zero depth) as well as back-calculated average zone dry densities against depth of measurement

Figure 2.42 shows that the bottom of the layer is already well compacted (between 85 % SD and 88 % SD) while the top portion of the layer is still loose. The large difference between the back scatter method (zero depth) and direct transmission in the measured dry density results also shows why the back scatter readings are not acceptable for either process or acceptance control purposes.

2.5

SITE 2 (THE RECONSTRUCTION OF THE BRONKHORSTSPRUIT-BAPSFONTEIN PROVINCIAL ROAD)

Permission was granted in principal by the TPA Roads Department for the use of all the construction done by department as possible test sections for this particular project.

A number of other construction projects were also considered for possible use, including the reconstruction of the road between Pietersburg and Louis Trichardt and construction in the Lowveld area. However, the distance between the CSIR and these construction sites was too great to include them in the study.

Because the reconstructed road between Bronkhorstspuit and Bapsfontein covers varying material types, and is within reasonable distance from the CSIR (approximately 60 km), it was decided to

monitor more than one section on this site as well. The aim is to do the final site monitoring for the 1993/94 financial year on this project as well.

Owing to staff limitations, it was further decided to concentrate on one construction site at a time, rather than monitor both sites at the same time. Therefore, the actual investigations on Site 2 started at the beginning of December 1992. Since the period December to March falls in the rainy season, quite a number of construction delays were experienced from the beginning of December.

Prior to starting the site investigation, discussions were held with the site staff to explain the aim of the investigation, and the actual procedure that would be used on site. A special meeting was also held with site foremen, after it was found that the present compaction procedure differed from that proposed. Rollers tended to do half passes, sometimes with a different roller directly behind the first one, leading to unidirectional compaction procedures. In rushed situations, rolling would be done in a haphazard fashion, usually involving the grid and pneumatic-tyred rollers.

Information on the compaction of the following layers was gathered in the 1992/93 period:

- | | | |
|-----|---------------------------|--------------|
| (a) | Crushed stone base | (4 sections) |
| (b) | Second stabilized subbase | (2 sections) |
| (c) | First stabilized subbase | (4 sections) |
| (d) | Second selected subgrade | (1 section) |

The results on a particular layer will once again be grouped together.

2.6 THE DENSITY RESULTS MEASURED

2.6.1 Second selected subgrade (upper)

The material was obtained from one of the new cuttings of the road and consisted of sandstone rubble which had to be broken down by the grid roller. After the material had been broken down to an acceptable size (G5-G6), the final compaction of the layer was done. Figures 2.43 to 2.48 show the results obtained by the separate compaction activities, while Figure 2.49 shows the compaction growth curve of the layer.

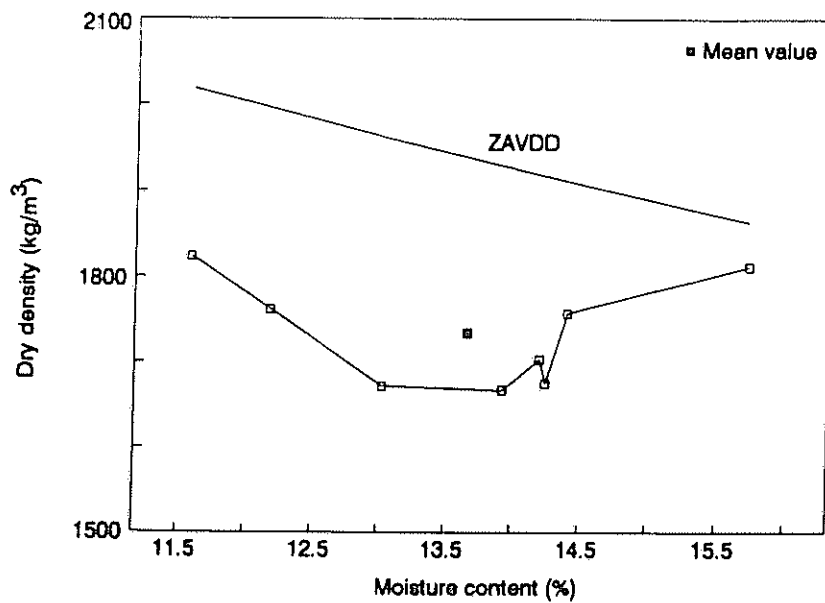


Figure 2.43: Measured dry densities against measured moisture contents on second selected subgrade layer after one pass with the grid roller following initial mixing and levelling

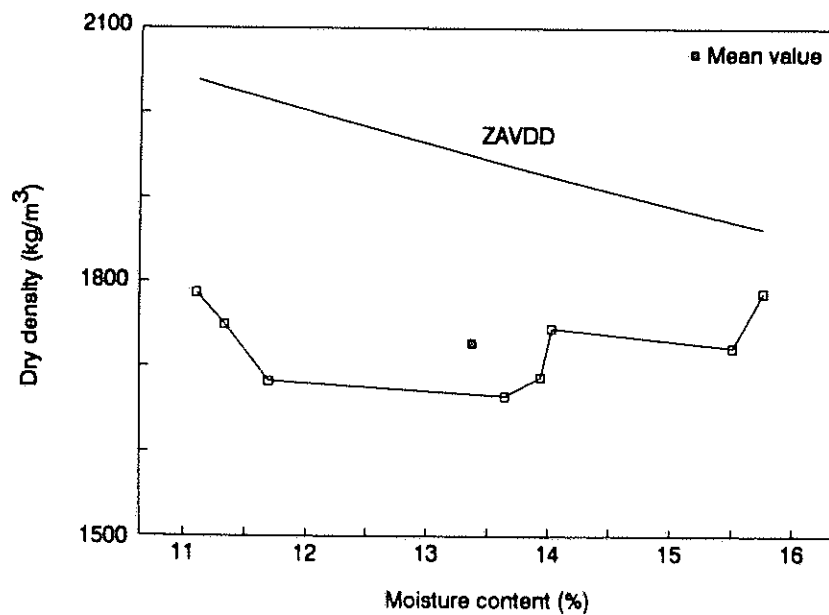


Figure 2.44: Measured dry densities against measured moisture contents on second selected subgrade after half a pass with grid roller on finally graded layer

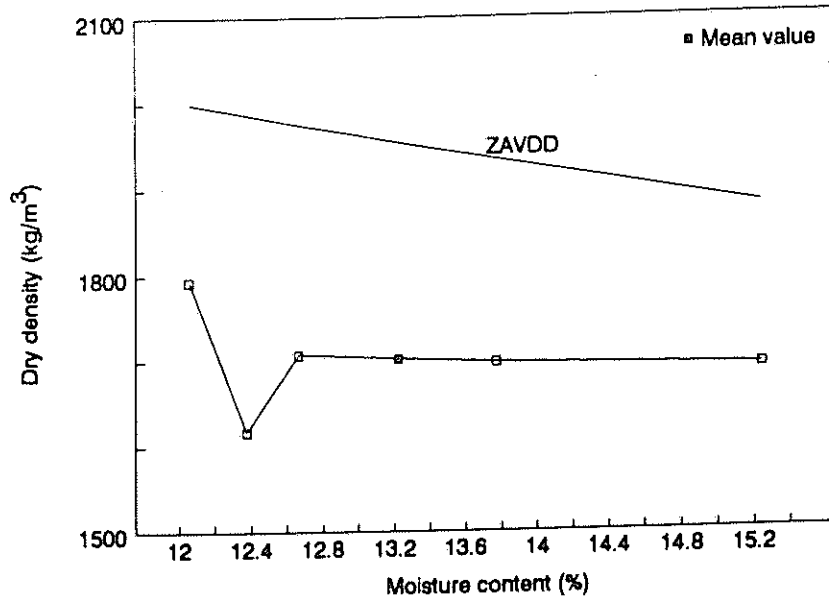


Figure 2.45: Measured dry densities against moisture contents on second selected subgrade layer after one pass with grid roller on finally graded layer

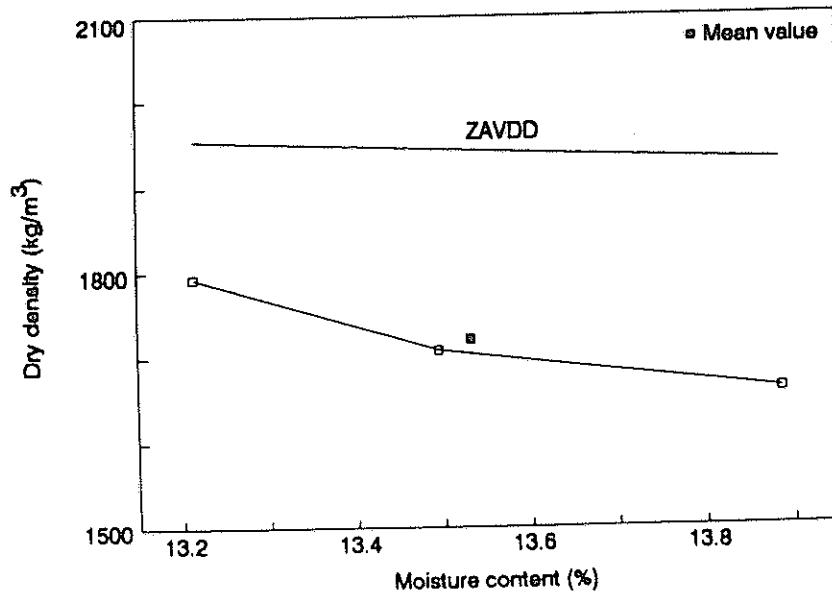


Figure 2.46: Measured dry densities against measured moisture contents of second selected subgrade after half a pass with pneumatic-tyred roller on grid-rolled layer

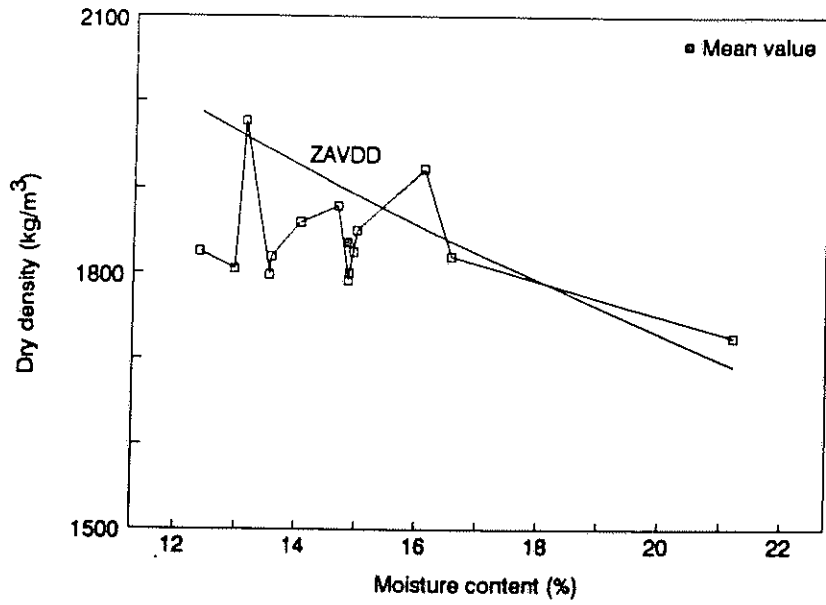


Figure 2.47: Measured dry densities against moisture contents of second selected subgrade after one pass with vibratory roller on pneumatic-tyred rolled layer (half pass)

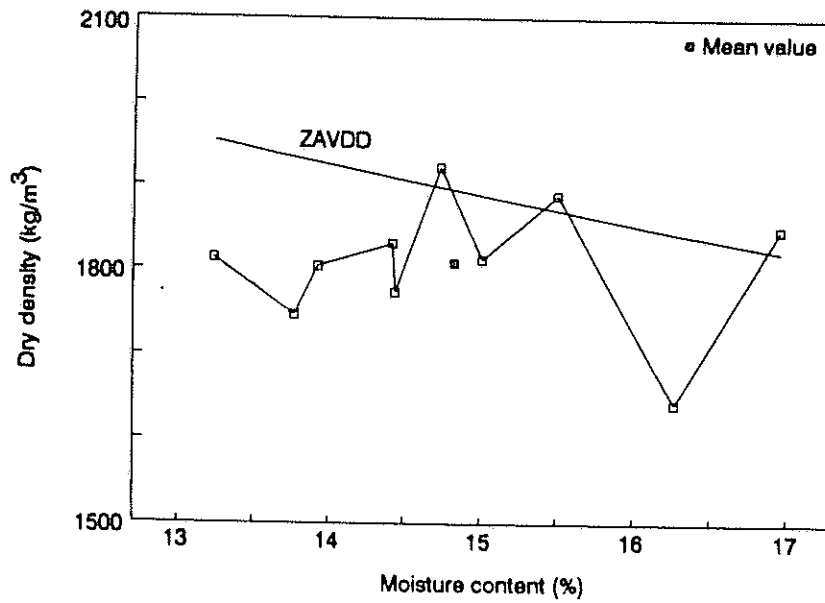


Figure 2.48: Measured densities against measured moisture contents of second selected subgrade layer after one pass with pneumatic-tyred roller on vibratory-rolled layer

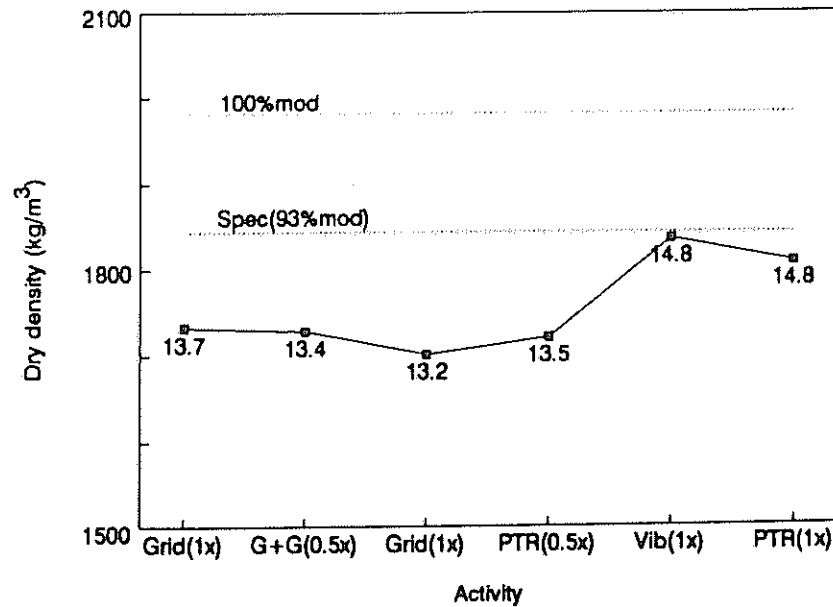


Figure 2.49: The compaction growth curve of the second selected subgrade layer of Section 3 showing the average measured dry density against the activity prior to taking the moisture/density measurements (average measured moisture content value is printed below data point)

Figure 2.49 shows that the grid and pneumatic-tyred roller do not have a significant effect on the initial compaction. However only one pass with the vibratory roller brought the dry densities right up to the zero air voids dry density line (see Figure 2.47). This once again emphasizes the fact that a test strip is necessary to determine the optimal rolling pattern.

2.6.2 First stabilized subbase (lower)

Four sections of this particular layer were monitored. The subbase material is obtained from a nearby borrowpit and consists of a hard shale material (G5-G6). Figures 2.50 to 2.55 show the results obtained by the separate compaction activities of Section 8 while Figure 2.56 shows the compaction growth curve of the section. The compaction growth curves for the other three sections are shown in Figures 2.57 to 2.59.

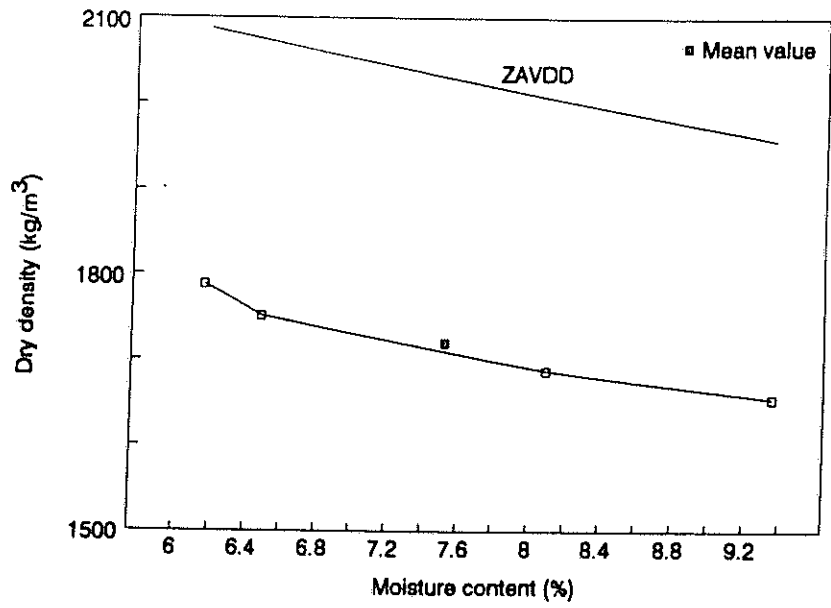


Figure 2.50: Measured dry densities against measured moisture contents of first stabilized subbase layer after half a pass with grid roller following mixing and levelling

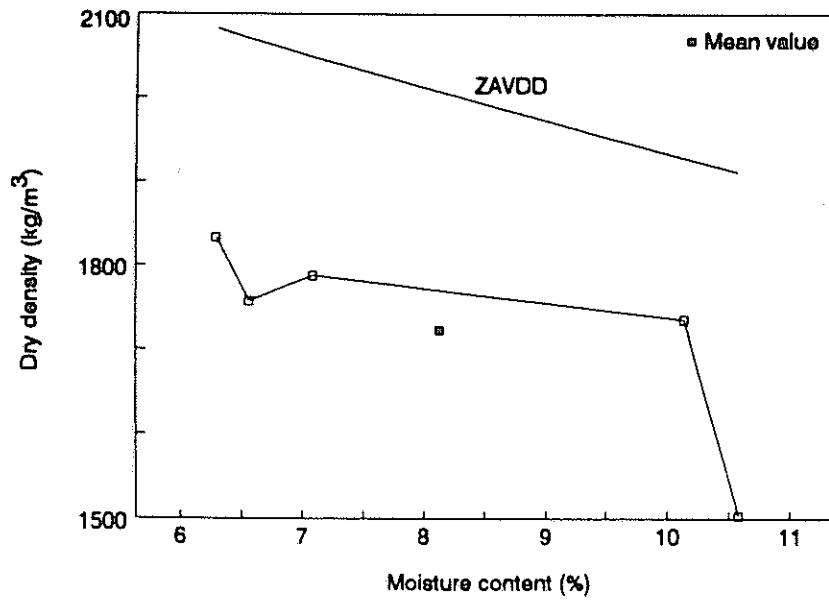


Figure 2.51: Measured dry densities against measured moisture contents of first stabilized subbase layer after one pass with grid roller

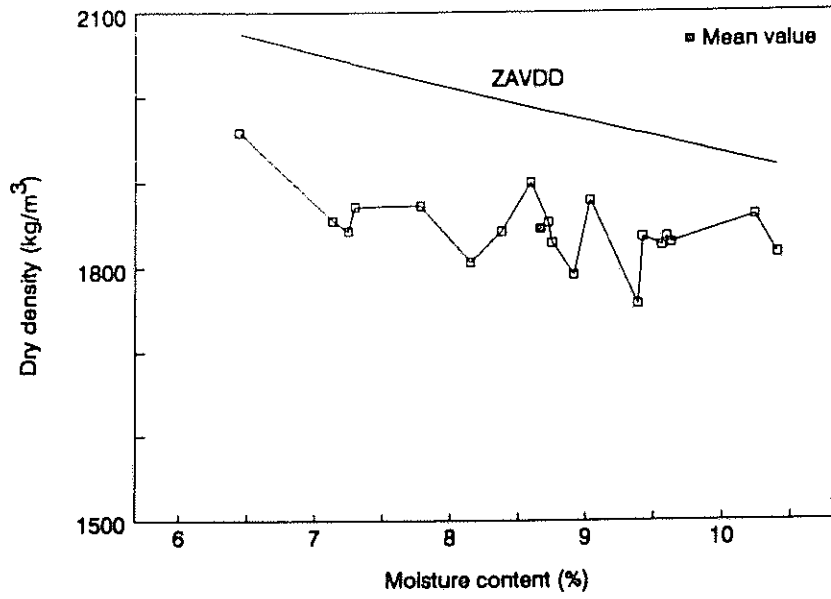


Figure 2.52: Measured dry densities against measured moisture contents of first stabilized subbase layer after half a pass with vibratory roller on grid-rolled layer

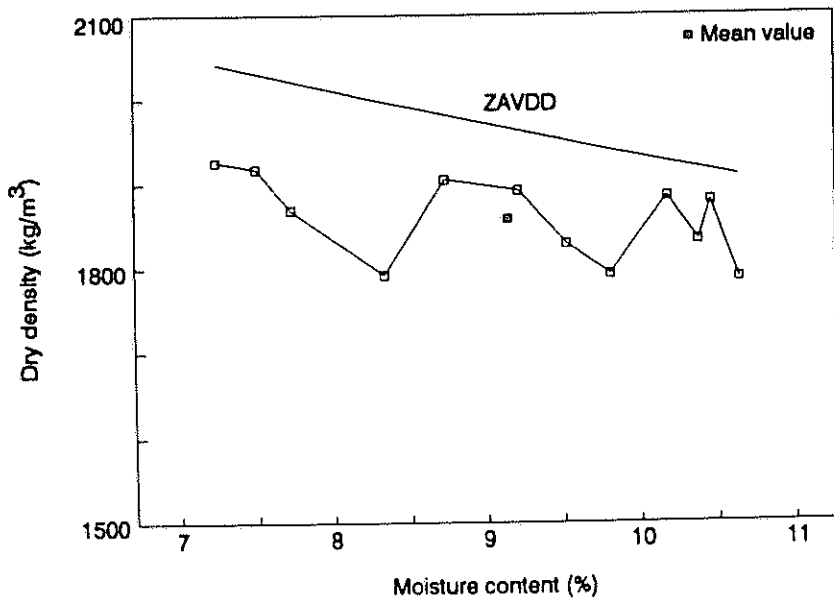


Figure 2.53: Measured dry densities against measured moisture contents of first stabilized subbase layer after one pass of vibratory roller on grid-rolled layer

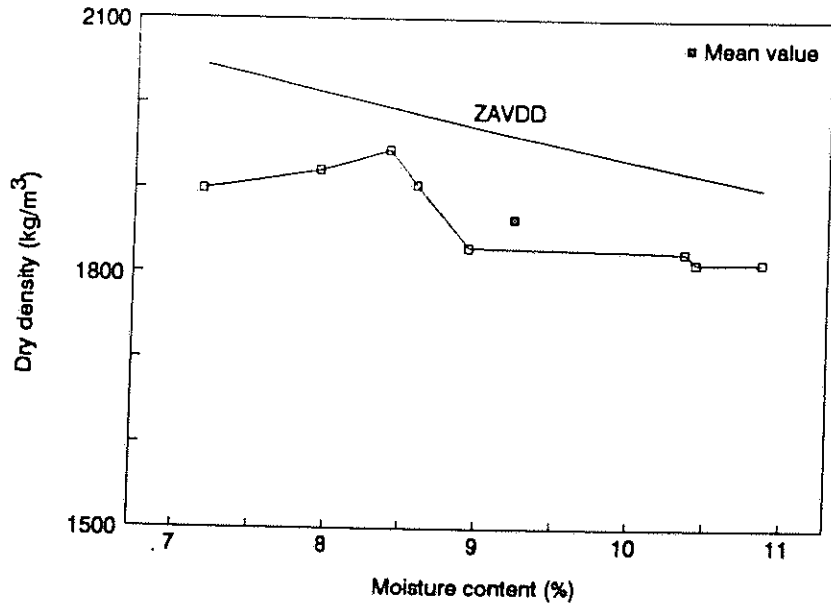


Figure 2.54: Measured dry densities against measured moisture contents of first stabilized subbase layer after half a pass with pneumatic-tyred roller on vibratory-rolled layer

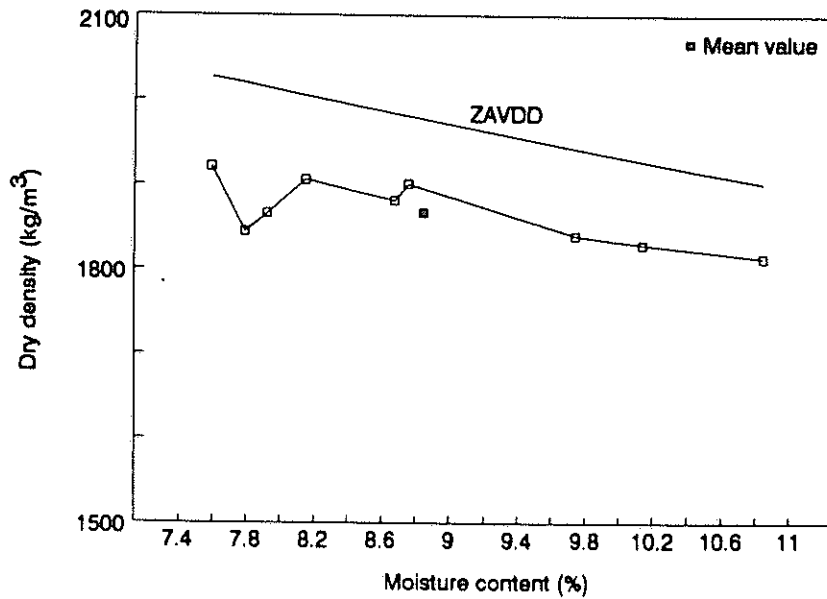


Figure 2.55: Measured dry densities against measured moisture contents of first stabilized subbase layer after one full pass with pneumatic-tyred roller on vibratory-rolled layer

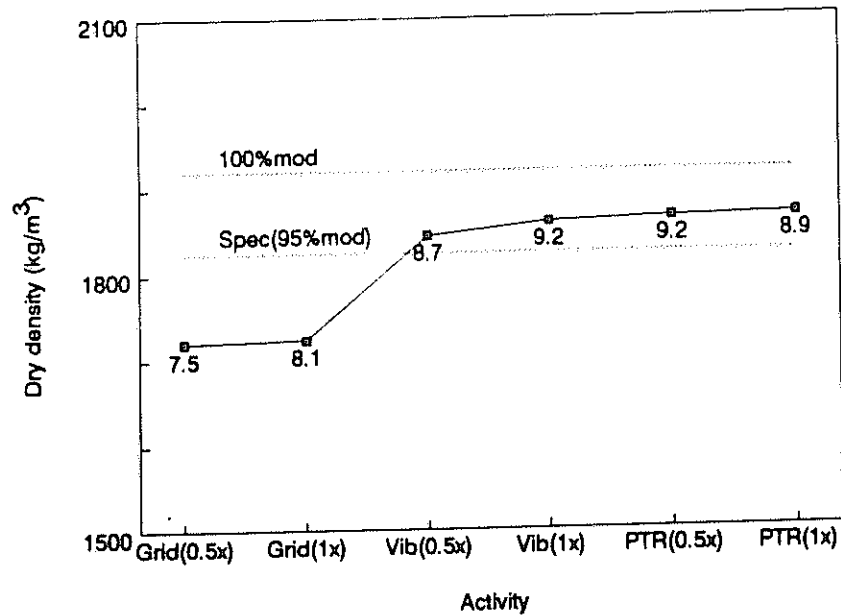


Figure 2.56: The compaction growth curve of the first stabilized subbase layer of Section 8 showing measured dry densities against the activity prior to taking the moisture/density measurements (average measured moisture content is printed below data point)

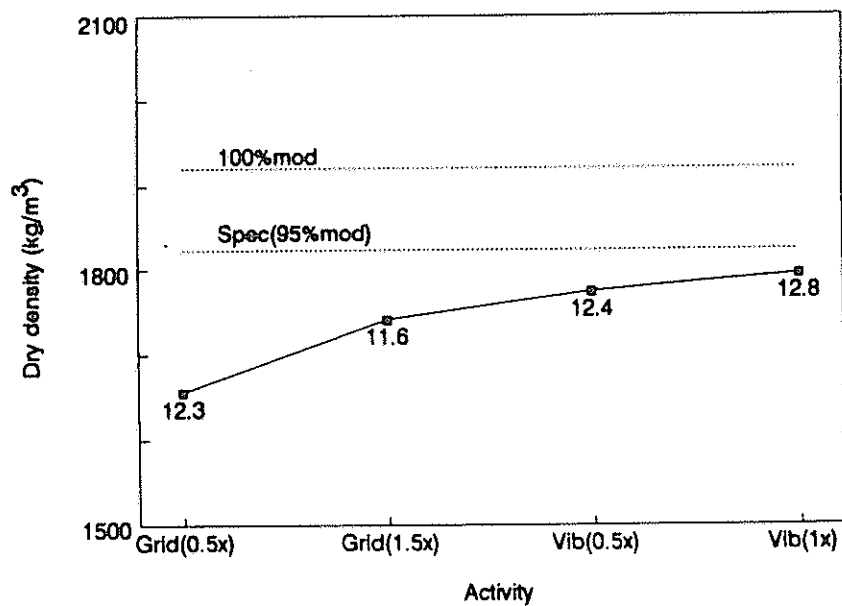


Figure 2.57: The compaction growth curve of the first stabilized subbase layer of Section 7 showing the average measured dry density against the activity prior to taking the moisture/density measurements (average measured moisture content is printed below data point)

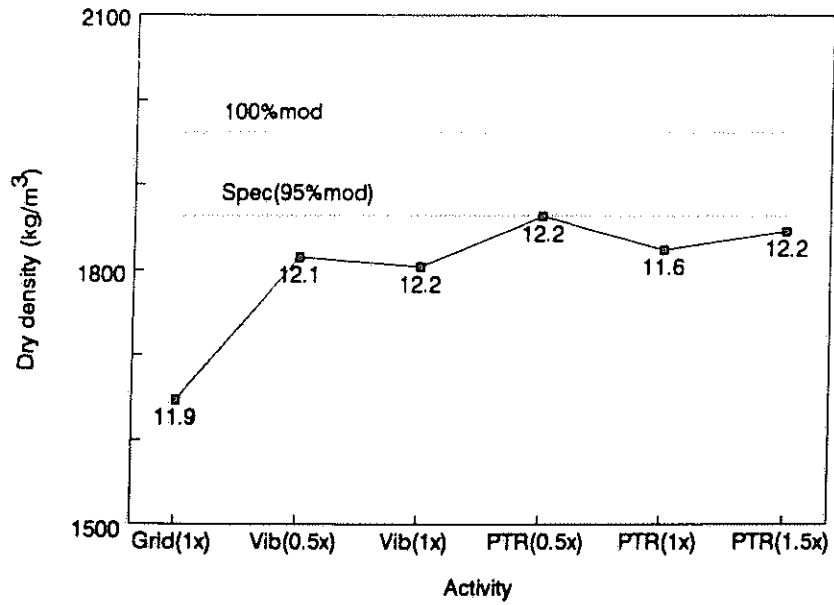


Figure 2.58: The compaction growth curve of the first stabilized subbase layer of Section 9 showing the average dry density against the activity prior to taking the moisture/density measurements (average measured moisture content value is printed below data point)

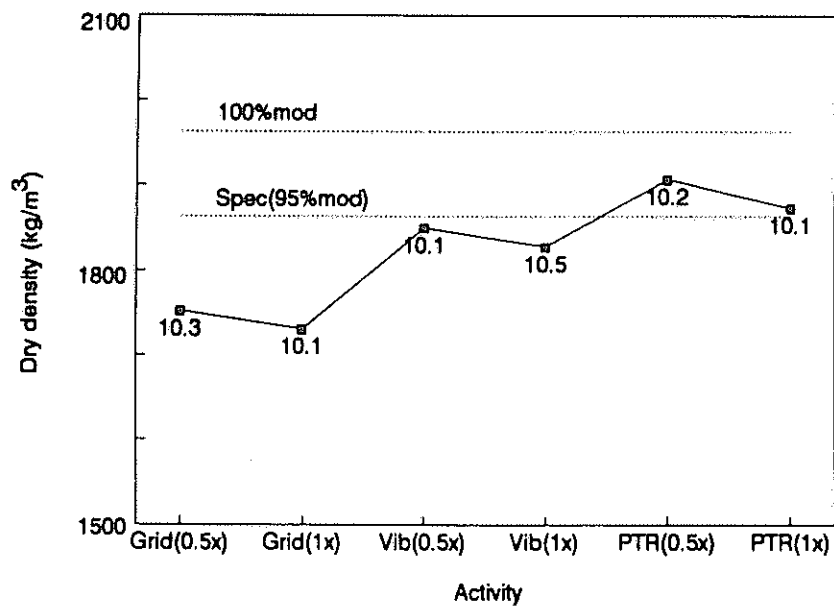


Figure 2.59: The compaction growth curve of the first stabilized subbase layer of Section 10 showing the average measured dry density against the activity prior to taking the moisture/density measurements (average measured moisture content value is printed below data point)

Although the measured dry densities of Section 8 did not quite reach the zero air voids dry density line (see Figure 2.55), the measured dry densities did meet the specification requirement of 95 % mod.AASHTO density (see Figure 2.56). On the other three sections the measured dry densities did not satisfy the density requirement even though the measured dry densities came right up to the zero air voids density line (see example for Section 9 in Figure 2.60). This clearly emphasizes the tremendous importance of proper control over the moisture content.

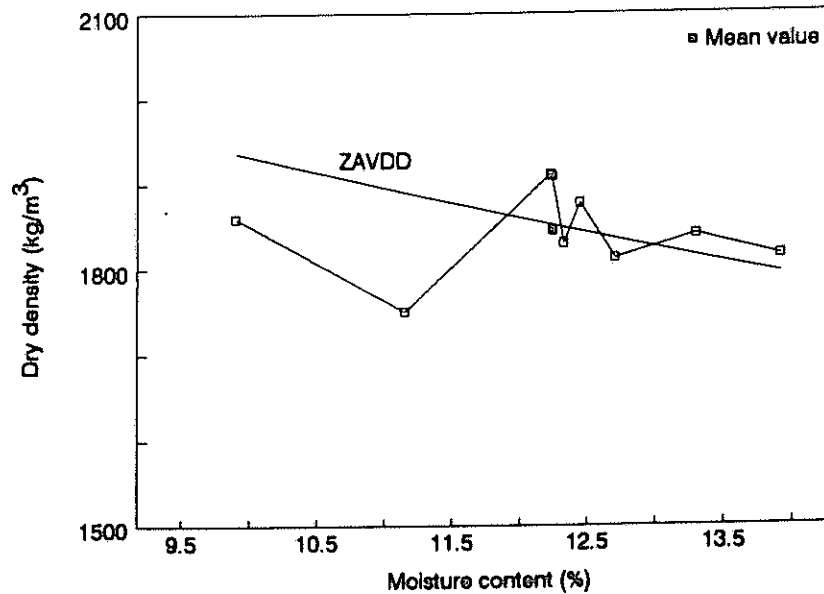


Figure 2.60: Measured dry densities against measured moisture contents of first stabilized subbase layer of Section 9 after one and a half passes with pneumatic-tyred roller

Note that although some of the measured dry densities points are above the zero air voids dry density line in Figure 2.60, this is not theoretically possible. The reason for this happening is that the estimated value of the relative solid density of the material was not totally correct. However, the fact that the measured points plot parallel to this line clearly indicates that the material is effectively saturated (i.e. all the voids are either filled with water or air which cannot be dissipated).

2.6.3. Second stabilized subbase (upper)

Two sections of this particular layer were monitored in the 1992/93 period. The layer was constructed from the same material as the first stabilized subbase layer. Figures 2.61 to 2.65 show the results obtained by the separate activities for Section 4 while Figures 2.66 and 2.67 show the compaction growth curves of the layer for both sections.

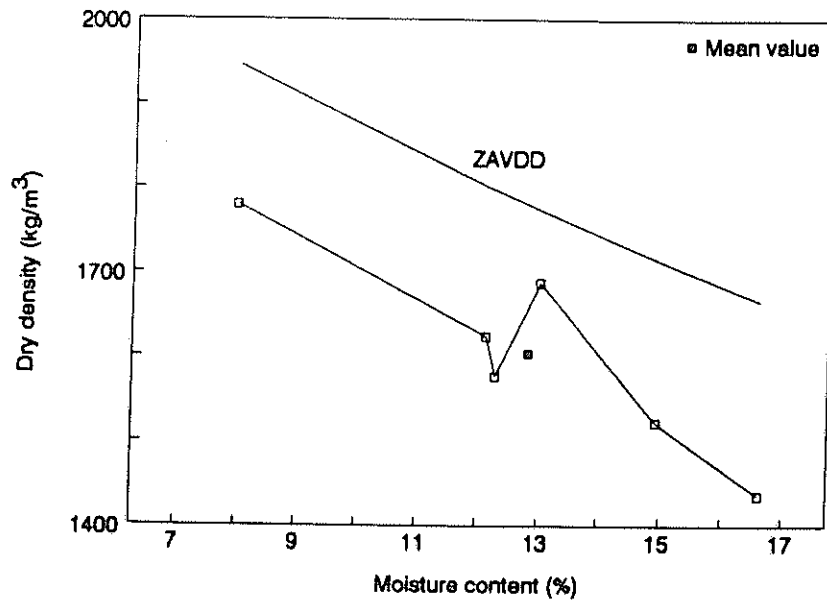


Figure 2.61: Measured dry densities against measured moisture contents of second stabilized subbase after half a pass with grid roller following mixing and levelling of layer

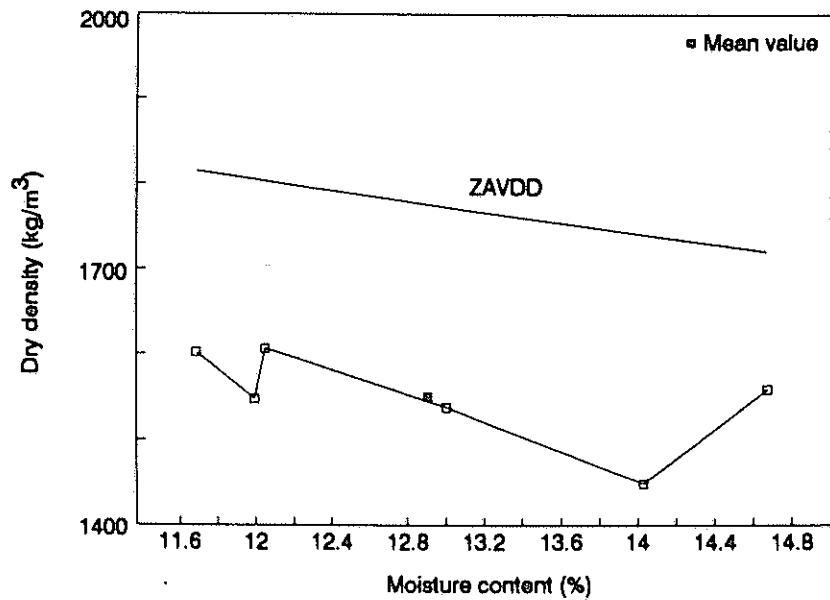


Figure 2.62: Measured dry densities against measured moisture contents of second stabilized subbase layer after one pass with grid roller following mixing and levelling of layer

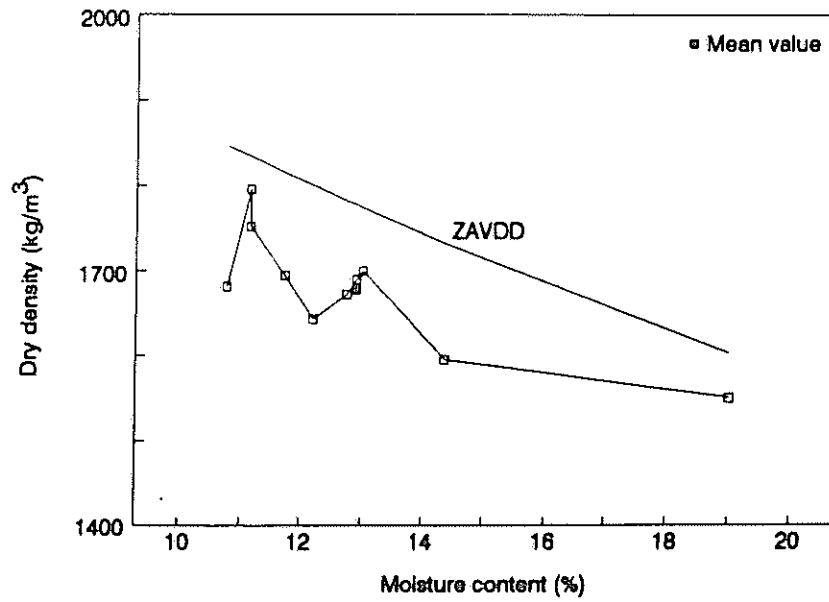


Figure 2.63: Measured dry densities against measured moisture contents of second stabilized subbase layer after one and a half passes with grid roller following mixing and levelling of layer

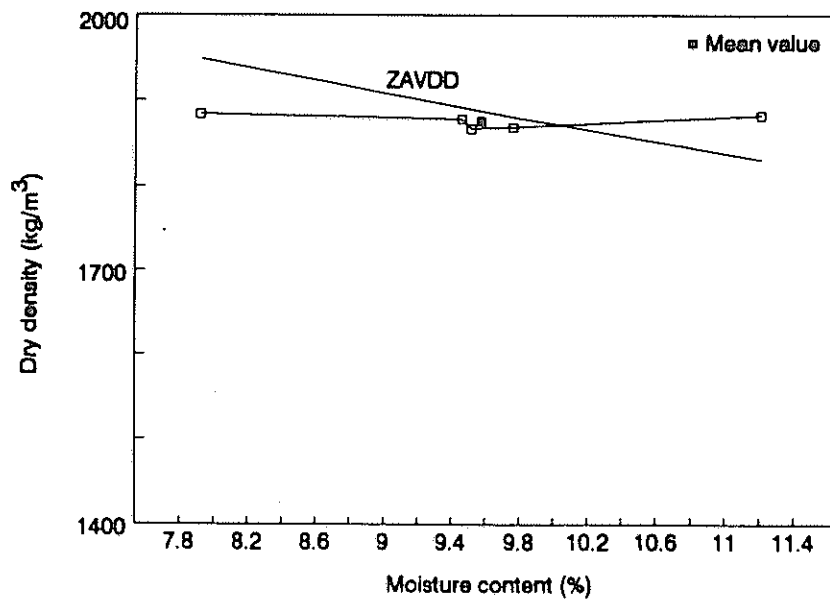


Figure 2.64: Measured dry densities against measured moisture contents of second stabilized subbase layer after half a pass with vibratory roller on grid-rolled layer

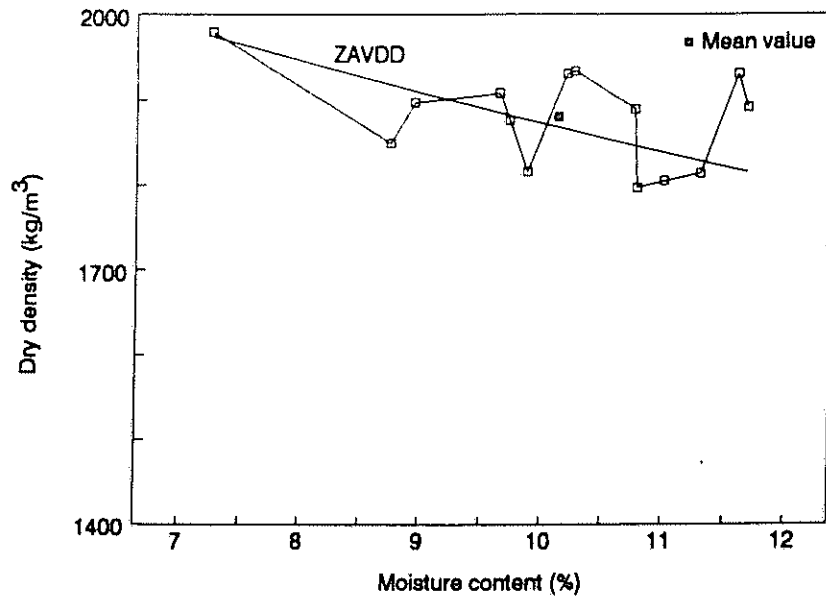


Figure 2.65: Measured dry densities against measured moisture contents of second stabilized subbase layer after one pass with vibratory roller on grid-rolled layer

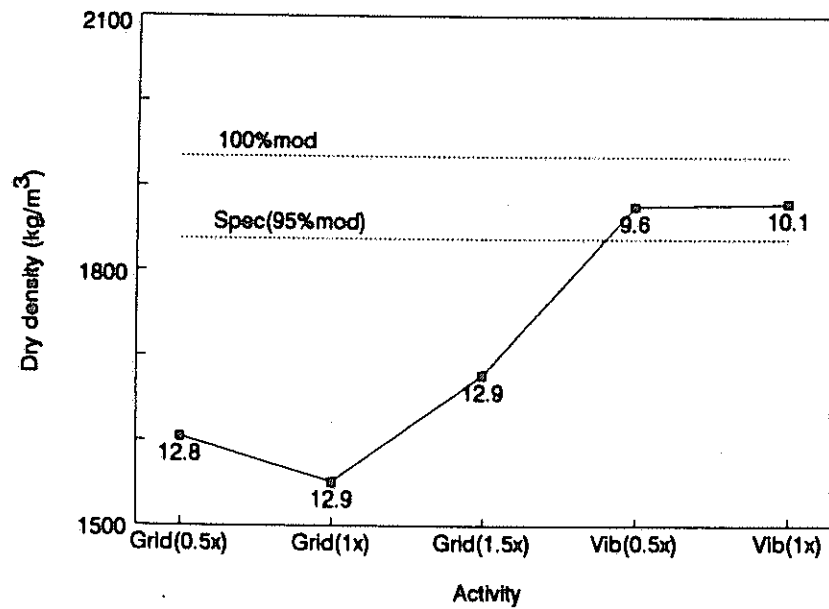


Figure 2.66: The compaction growth curve of the second stabilized subbase of Section 4 showing the average dry density against the activity prior to taking the moisture/density measurements (average measured moisture content value is printed below data point)

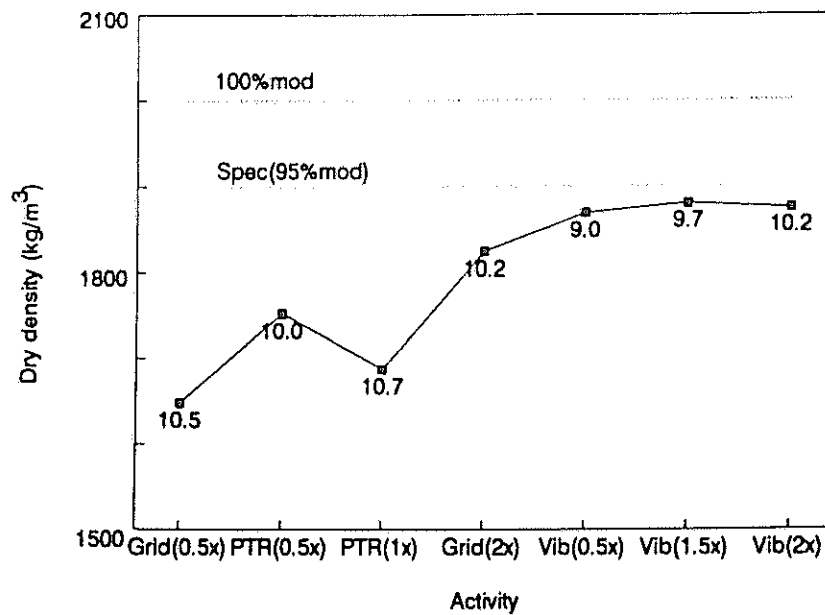


Figure 2.67: The compaction growth curve of the second stabilized subbase of Section 1 showing the average measured dry density against the activity prior to taking the moisture/density measurements (average measured moisture content is printed below data point)

Figures 2.66 and 2.67 show that neither the grid roller or the pneumatic roller are very effective for the initial compaction. In both cases the layer was not finished off with the pneumatic-tyred roller as is usually done. The particular foreman did not require a pneumatic tyred roller on his compaction team.

2.6.4. Crushed stone base course (G1)

Three sections of this particular layer were monitored in the 1992/93 period. The layer was constructed from a crushed quartzite stone obtained from a quarry at Bronkhorstspuit. Figures 2.68 to 2.72 show the compaction results obtained by the separate compaction activities for Section 5 while Figures 2.73 to 2.75 show the compaction growth curves of the layer for the three sections. Note the compaction of the base course layer was only monitored in the initial compaction phase prior to slushing.

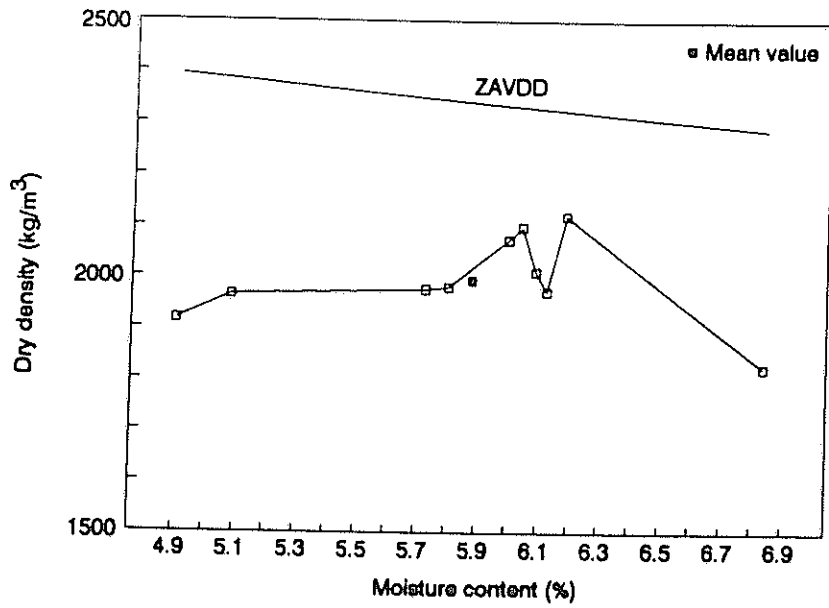


Figure 2.68: Measured dry densities against measured moisture contents of the crushed stone base course layer after levelling with grader

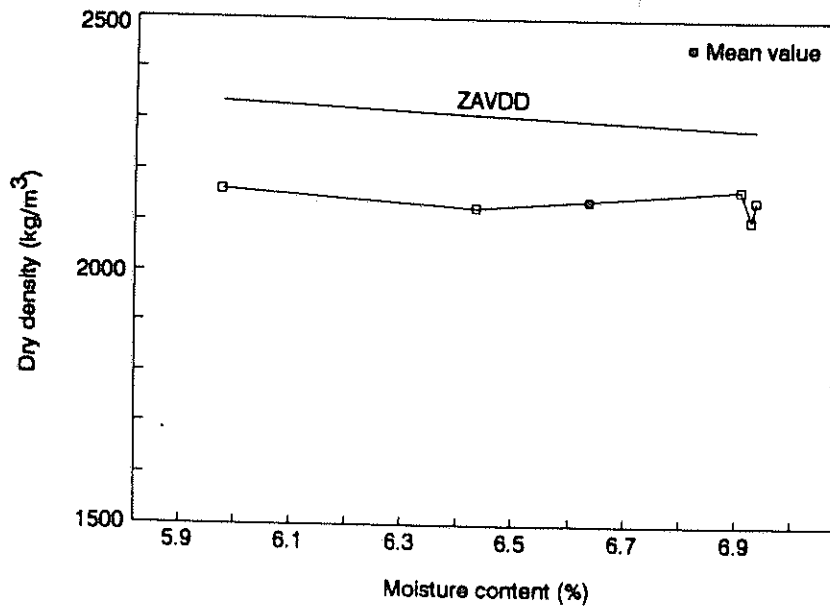


Figure 2.69: Measured dry densities against measured moisture contents of the crushed stone base course layer after half a pass with the grid roller on the graded layer

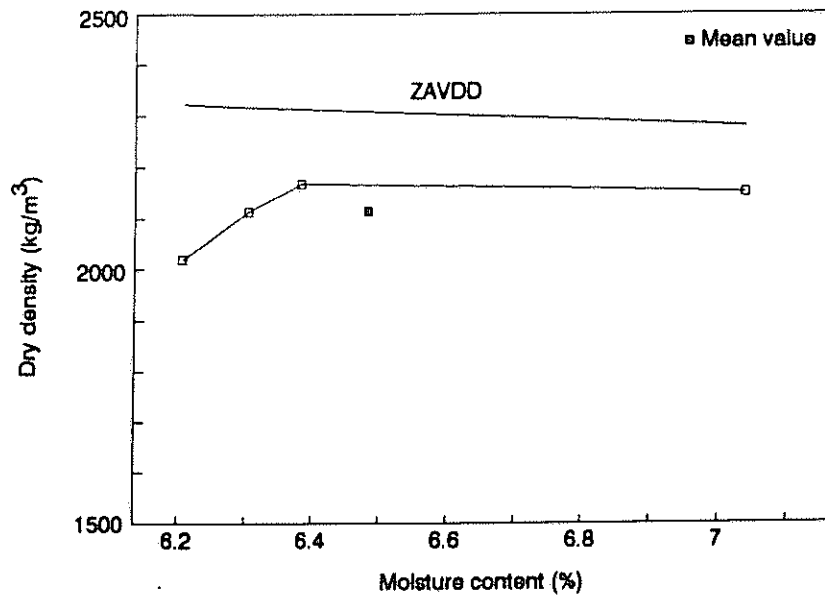


Figure 2.70: Measured dry densities against measured moisture contents of the crushed stone base course layer after one pass with the grid roller on the graded layer

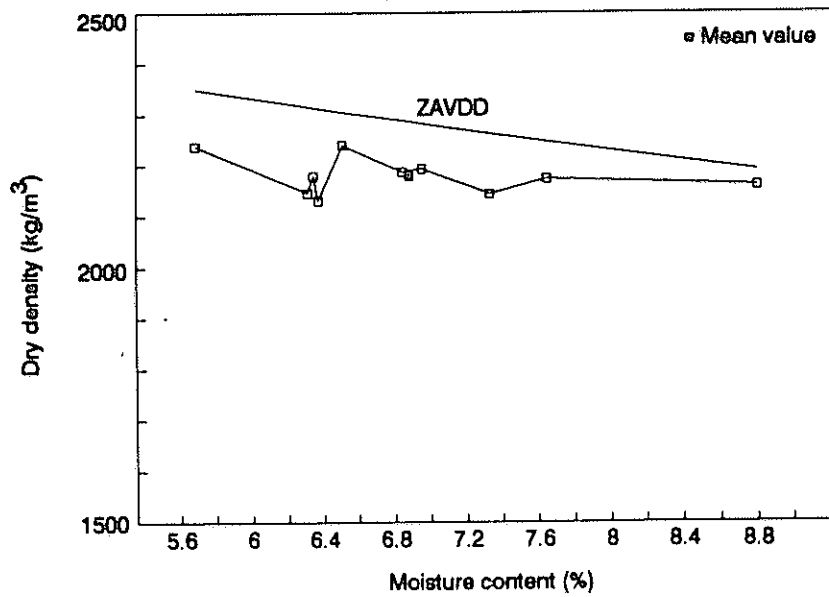


Figure 2.71: Measured dry densities against measured moisture contents of the crushed stone base course after half a pass with the vibratory roller on the grid-rolled layer

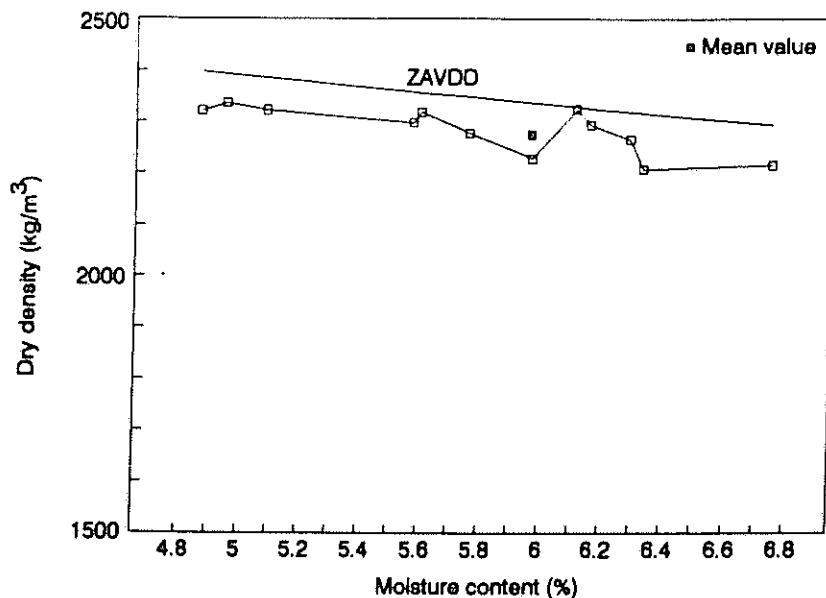


Figure 2.72: Measured dry densities against measured moisture contents of the crushed stone base course after one pass with the vibratory roller and half a pass with pneumatic-tyred roller on the grid-rolled layer

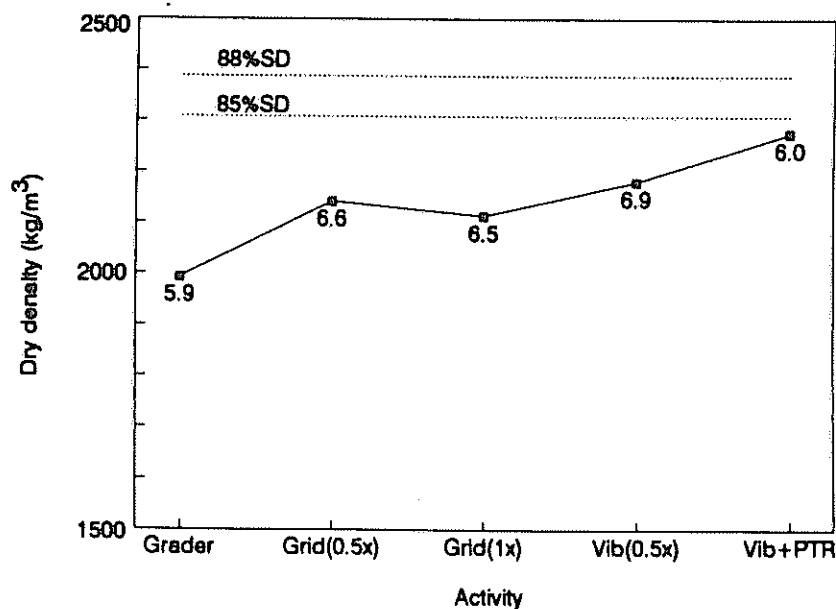


Figure 2.73: The compaction growth curve of the crushed stone base course of Section 5 showing the average measured dry density against the activity prior to taking the moisture/density measurements (average measured moisture content value is printed below data point)

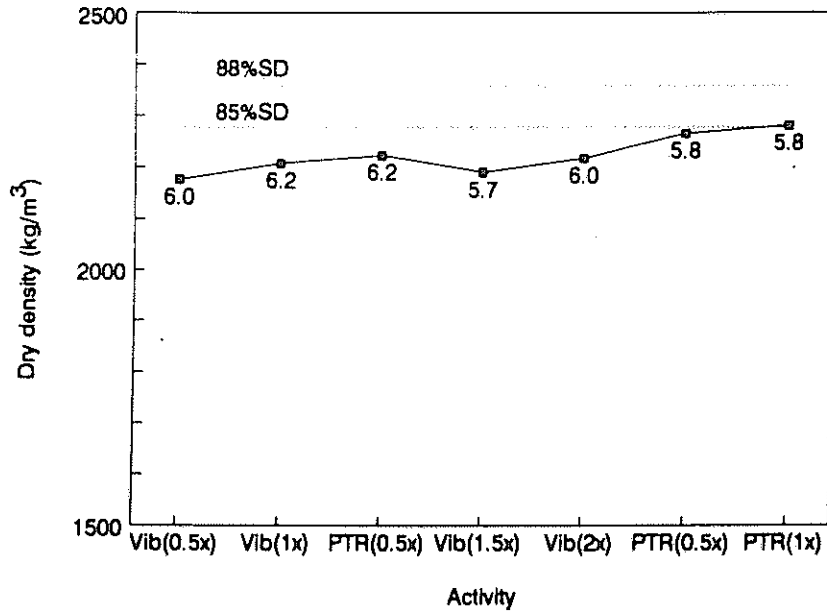


Figure 2.74: The compaction growth curve of the crushed stone base course of Section 3 showing the average measured dry density against the activity prior to taking the moisture/density measurements (average measured moisture content value is printed below data point)

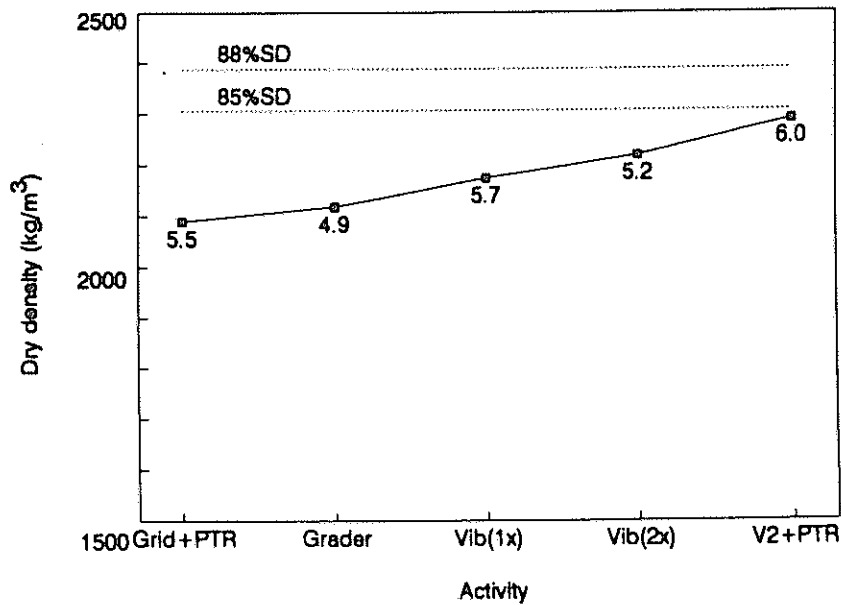


Figure 2.75: The compaction growth curve of the crushed stone base course of Section 1 showing the average measured dry density against the activity prior to taking the moisture/density measurements (average measured moisture content value is printed below data point)

THE WORK AT THE BRONKHORSTSPRUIT CONSTRUCTION SITE IN 1993/94

As mentioned earlier, the decision was taken to continue the monitoring of the compaction procedures on the TPA construction site on the road between Bronkhorstspuit and Bapsfontein in the financial year 1993/94. The main reason for this was that there were no other road construction projects close to the CSIR campus. Another reason was that cordial relations had already been established with the construction staff on this particular site, which meant that the monitoring could be effectively executed without further briefing to site personnel.

The original plan had been to obtain the after-compaction gradings, Atterberg limits, and Linear Shrinkage values for different pavement layers of the completed sections and use these together with the ARDs and BRDs of both the coarse (>4,75mm) and fine (<4,75mm) fractions, to determine the predicted values of MDD(mod.AASHTO) and MDD(vibratory) as well as the predicted values of the moisture regime (OMC(mod.AASHTO), OMC(vibratory), ZAVMC(mod.AASHTO), ZAVMC(vibratory) and CMC) for each of the layers (constructed from the same material) by means of the compactability software package. The predicted values of the OMC would then be used as the control value for moisture content on site. Actual compaction was not to commence unless the material was at OMC. Unfortunately the site laboratory had difficulty in supplying this information. Therefore use was made of the OMC (mod.AASHTO) as determined by the field laboratory. In general, the cooperation was excellent, for which the Division would like to express its sincere gratitude,

Problems experienced included:

- initial resistance from some of the site staff to new approaches. For example distrust was expressed in moisture content values measured with the nuclear density/moisture gauges when readings as high as 23% were recorded instead of the anticipated 14%.
- site staff including roller operators, being dependent on staff transport, finished work at approximately 16h15 so that the recommended rolling sequence was not completed on some sites.
- layers were compacted with a grid and/or vibratory roller only, because no pneumatic-tyred roller was available.
- severe shortage of water for compaction purposes was experienced on site at one stage. To convey water from the nearest available point took more than one hour which meant that often the material had already partially dried before the next load of water arrived. Thus the required OMC was not always reached.
- on another fairly long section, which the construction team tried to handle in toto on a very hot and dry day, the required OMC was just never reached. However, because this was a cement stabilized layer (i.e. second subbase)(Section 1), it was imperative that the layer be compacted the

same day. The construction team therefore, decided to try and compact the layer at this low moisture content. The dry density results of this section were substantially lower compared to those of the same layer for the other sections.

Positive developments included:

- reduced use of grid rollers as compaction equipment, and acceptance of this roller as a tool to improve the grading of the material.
- effort spent on grader levelling was also optimized and for most sections the layers were levelled once only before the compaction cycle was started.
- in general the compaction cycle started only after the monitoring team was satisfied that the material was very close to or at OMC for that particular layer. There were a few exceptions to this despite the problems mentioned.

On the whole the dry density results confirm that it is possible to compact roadbuilding materials (both treated and untreated) to substantially higher dry densities than the present specification requirements. Even more encouraging is the fact that the earlier observation that the amount of compactive effort required could be greatly reduced with proper moisture content control was again confirmed. This means that the compaction standards of roads can generally be improved without an increase in roadbuilding costs and that with proper moisture content control the contractor could even increase his productivity by cutting out unnecessary rolling and watering.

Initially, monitoring was undertaken regardless of the schedule of the construction team. This was very haphazard and unsatisfactory and a lack of adequate communication failed to establish whether any compaction was, in fact, scheduled so that at times fruitless site visits were made by the team. A number of meetings were subsequently held with the resident engineer and his staff and it was agreed that four specific sections would be allocated to the Division to monitor the compaction process for all constructed layers. The sections were marked and the Division advised of compaction work. The sections were at the following positions:

- Section 1: 21600 - 22200
- Section 2: 27900 - 28500
- Section 3: 29300 - 29900
- Section 4: 17300 - 17600

It may be interesting to evaluate the performance of these sections against their individual construction records with time. Apart from monitoring the compaction process, samples of the material were taken to the Division to determine its after-compaction grading, Atterberg limits,

Linear Shrinkage (LS), Shakedown Bulk Density, and the ARDs and BRDs of both the coarse (+4.75mm) and fine (-4.75mm) fractions. Because it is extremely difficult to determine the BRD of the fine fraction, it was assumed that BRD was equal to ARD of this fraction. The laboratory results of each layer were then used together with the compactability software package developed by the Division to determine the predicted MDDs and moisture regime for comparison with density results as well as the site laboratory's MDD(mod.AASHTO) and OMC(mod.AASHTO) results (see Appendix A for the above results).

The aim was to monitor the compaction process from the roadbed up to base course level. Unfortunately very little fill was left by the time the four sections were allocated; only one of these sections involved some fill construction. The pavement consisted of the following layers:

- Crushed stone base - 150 mm thick
- Upper stabilized subbase - 150 mm thick
- Lower stabilized subbase - 150 mm thick
- Upper selected subgrade - 150 mm thick
- Lower selected subgrade - 150 mm thick
- Fill

The results on a particular layer are grouped together for discussion purposes.

2.8 THE DENSITY RESULTS MEASURED

2.8.1 Fill

Although only one fill layer was monitored on one of the allocated sections, two other fill sections were monitored on other sections. The same CPN nuclear surface gauges were used on all of these sections. No bias adjustment to the measured moisture content was done at any time. Past experience with these particular instruments showed that it is generally unnecessary to adjust the moisture content reading of these instruments. The only likely exception is very heavy clay materials containing a certain amount of bound water, which is not driven off at 105°C during oven drying. The results of the fill layer near the large cutting are used as the example in this case. The measured dry density results at different stages of the compaction phase are shown in Figures 2.76 to 2.79 and the compaction growth curve in Figure 2.80. The compaction growth curves for the other two fill layers are shown in Figures 2.81 and 2.82 respectively. Fills were generally constructed from a red shale obtained from cuttings. The quality of the shale was generally G5 with a small amount of G6 and only once G7.

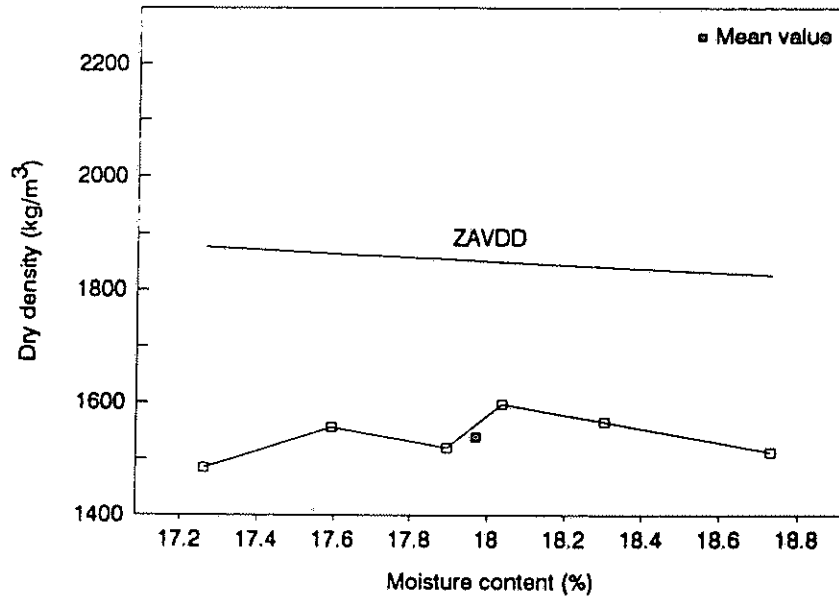


Figure 2.76: Measured dry densities against measured moisture contents on fill layer after half a pass with grid roller following mixing and levelling

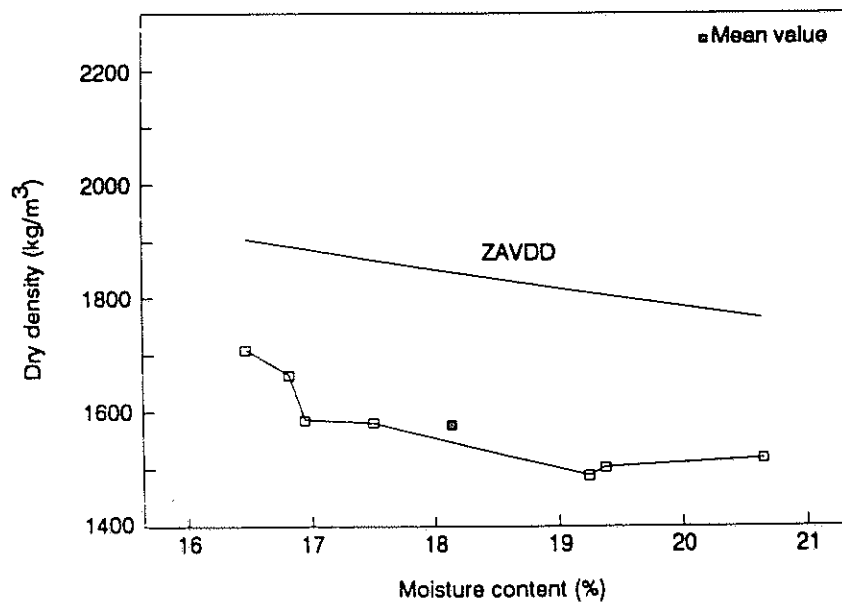


Figure 2.77: Measured dry densities against measured moisture contents on fill layer after one pass with grid roller

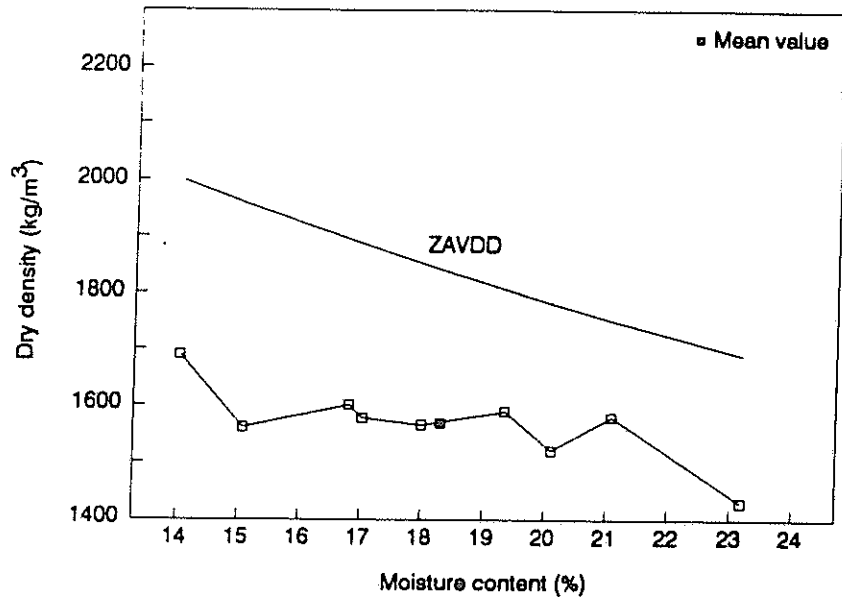


Figure 2.78: Measured dry densities against measured moisture contents on fill layer after half a pass with vibratory roller following on grid roller

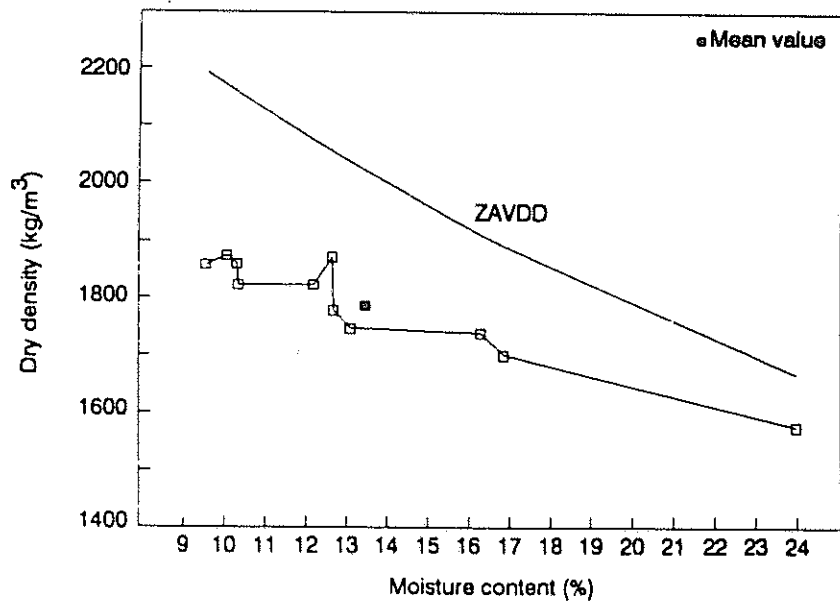


Figure 2.79: Measured dry densities against measured moisture contents on fill layer after one pass with vibratory roller

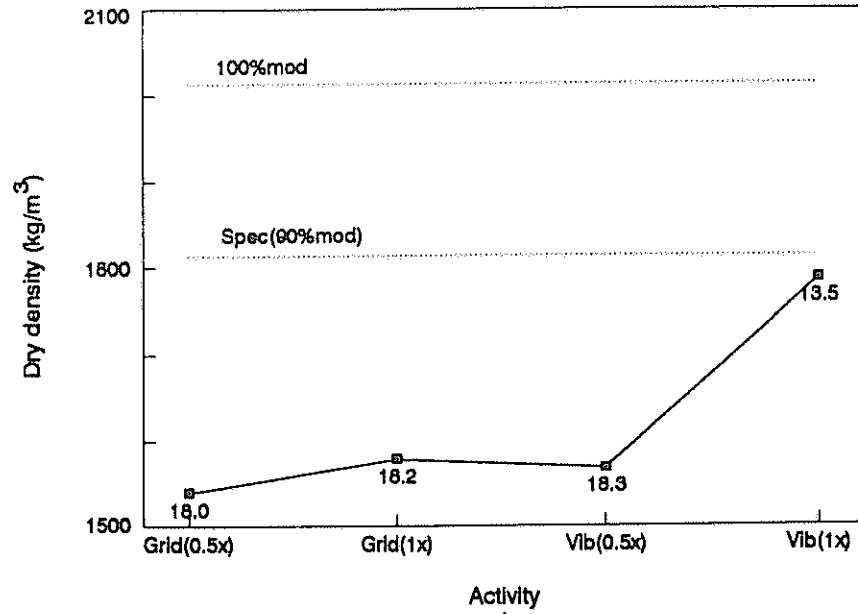


Figure 2.80: The compaction growth curve of the fill layer of section near large cutting showing the average measured dry density against the activity prior to taking the moisture/density measurements (average moisture content value is printed below data point)

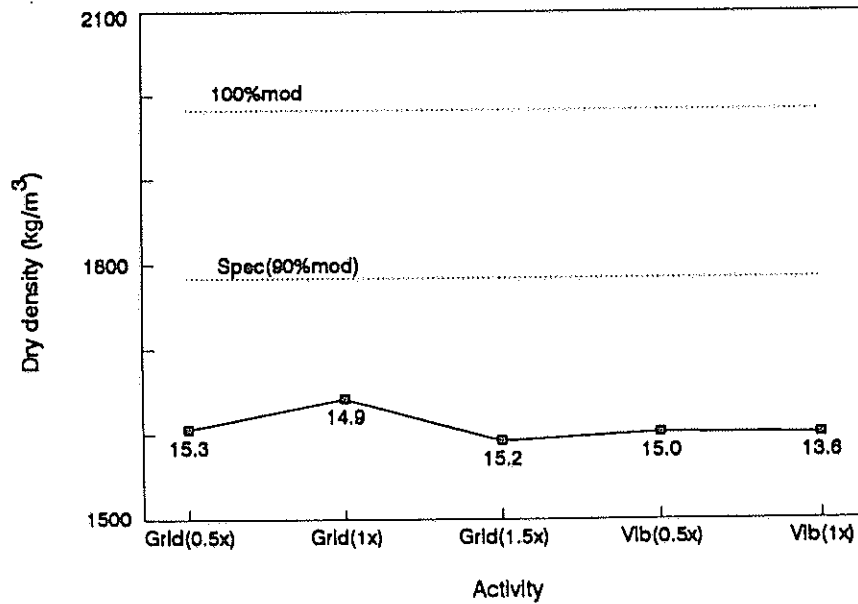


Figure 2.81: The compaction growth curve of the fill layer next to previous section in Figure 2.80 showing the average measured dry density against the activity prior to taking the moisture/density measurements (average moisture content value is printed below data point)

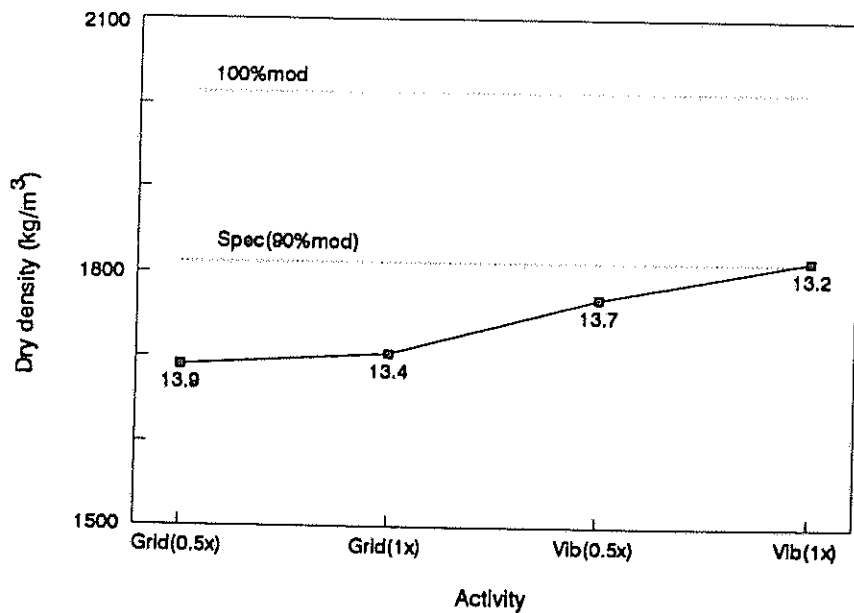


Figure 2.82: The compaction growth curve of the fill layer on Section 1 showing the average measured dry density against the activity prior to taking the moisture/density measurements (average moisture content value is printed below data point)

Figures 2.76 to 2.79 show that both the grid roller and vibratory roller had very little influence on the dry density when the material is too wet, but as soon as the moisture content was correct there was a substantial increase in dry density (see Figure 2.79). The higher dry densities were recorded on the upper side of the curve camber and the lower dry densities on the lower side of the curve camber. Thus after only one full pass of the vibratory the specification requirement of 90% mod.AASHTO density had already been met in many areas. Unfortunately the compaction process was terminated at this stage because the roller broke down. As the compaction growth curve was still rising at this stage (see Figures 2.80), it is highly likely that substantially higher density levels could have been achieved if the compaction process had continued until refusal density had been reached. Figure 2.79 shows that the moisture content of the material in some areas was already above OMC because the dry density results plot parallel and near to the zero air voids dry density (ZAVDD) line. The compaction growth curve in Figure 2.81 also shows that it is impossible to effectively compact this fill material when the moisture content is above OMC.

2.8.2 Lower selected subgrade

The lower selected subgrade layer was not constructed from the same material on all four sections. On three of the sections a red shale material (G5-G6) was used. On the fourth section (Section 2)

brown loamy soil (G5) was used. Although three of the sections were constructed from more or less similar material their MDD(mod.AASHTO) values as determined by the site laboratory differed substantial. The values were 1967, 2200 and 2050 kg/m^3 for Sections 1, 3 and 4 respectively. The measured dry densities against the measured moisture contents after different activities during the compaction sequence of this layer on Section 1 are shown in Figures 2.83 to 2.87 and the compaction growth curve in Figure 2.88. Figures 2.89 to 2.90 show the compaction growth curves for this layer on Sections 2, 3 and 4 respectively.

The growth in Figure 2.88 shows that the grid roller had very little effect in general on the compaction after the first half pass. On the other hand the vibratory roller still had a substantial influence after one pass. Unfortunately the compaction process was terminated after one full pass with the vibratory roller instead of rolling to refusal density. Figure 2.90 also shows that the effect of the grid roller on the compaction process had reached its limit after about one pass; the dry densities were still increasing after one pass with the vibratory roller when the compaction process was terminated. Note that the slope of the compaction growth curve for the vibratory roller is less steep than in Figure 2.88. This was probably because the material on Section 3 was compacted on the dry side of OMC, thereby decreasing the effectiveness of the vibratory roller. The compaction growth curve in Figure 2.91 shows a similar tendency. However, this was due to the material actually being too wet (i.e. above OMC)(see Figures 2.92 and 2.93 as well). Note that the measured dry densities plot parallel to and near to the ZAVDD line, which means that the moisture content was actually too high.

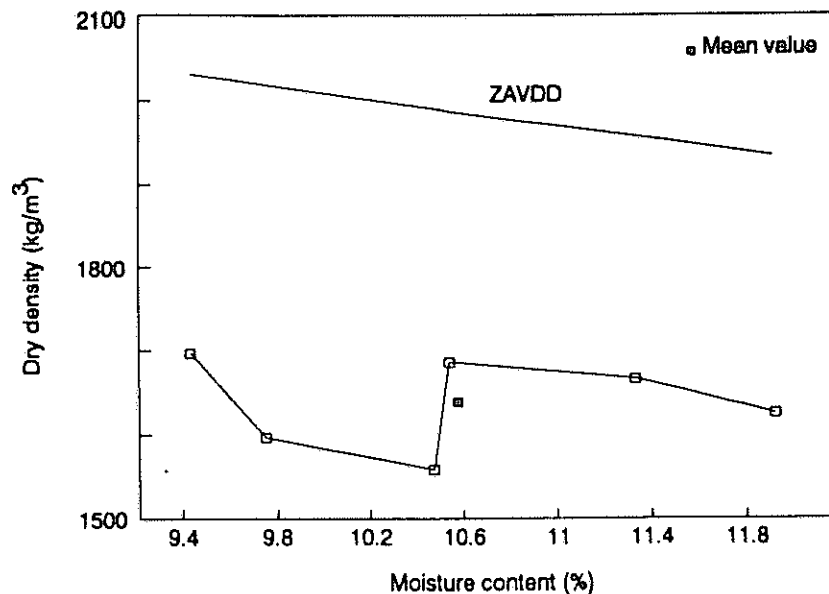


Figure 2.83: Measured dry densities against measured moisture contents on lower selected subgrade layer after levelling with grader

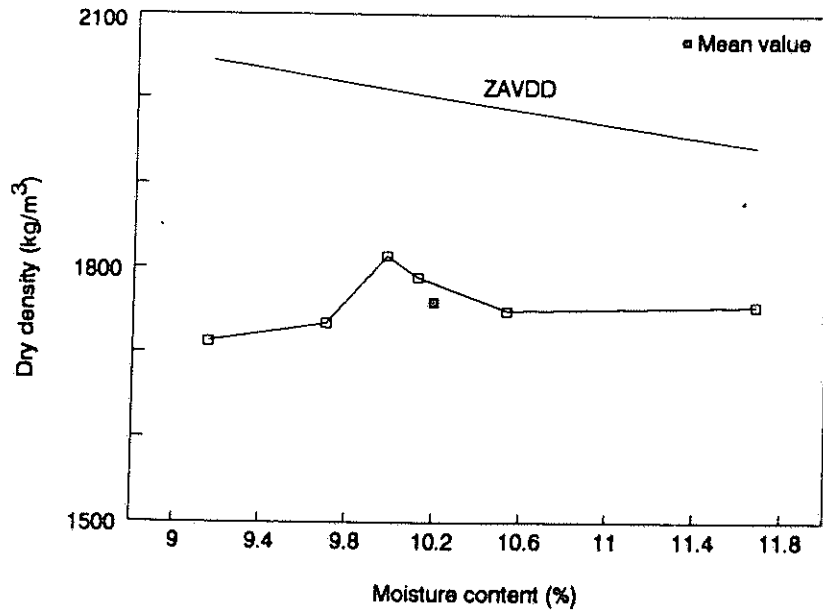


Figure 2.84: Measured dry densities against measured moisture contents on lower selected subgrade layer after half a pass with grid roller following levelling

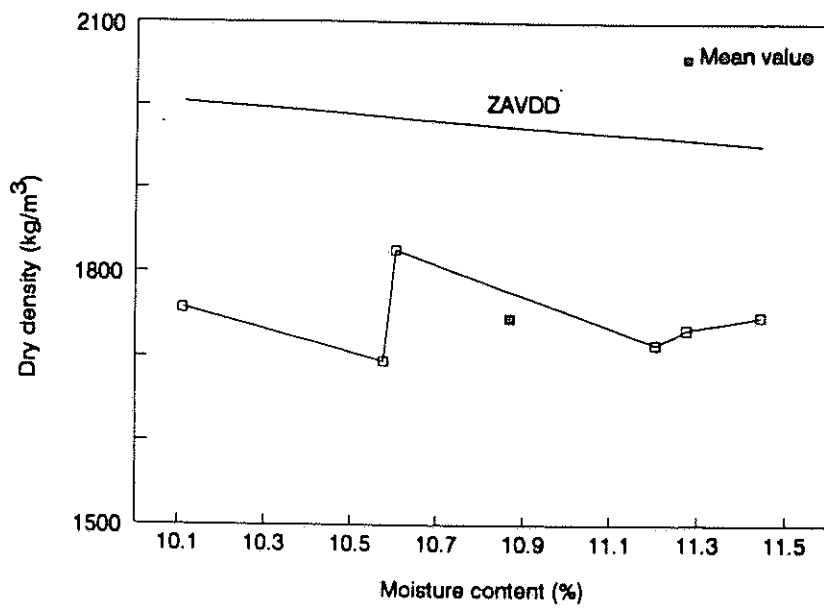


Figure 2.85: Measured dry densities against measured moisture contents on lower selected subgrade layer after one pass with grid roller

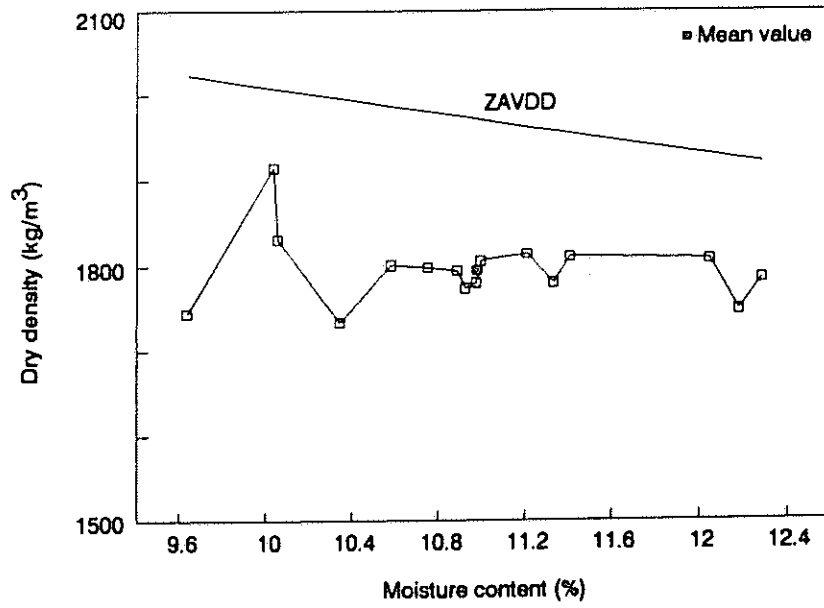


Figure 2.86: Measured dry densities against measured moisture contents on lower selected subgrade layer after half a pass with vibratory roller following on grid roller

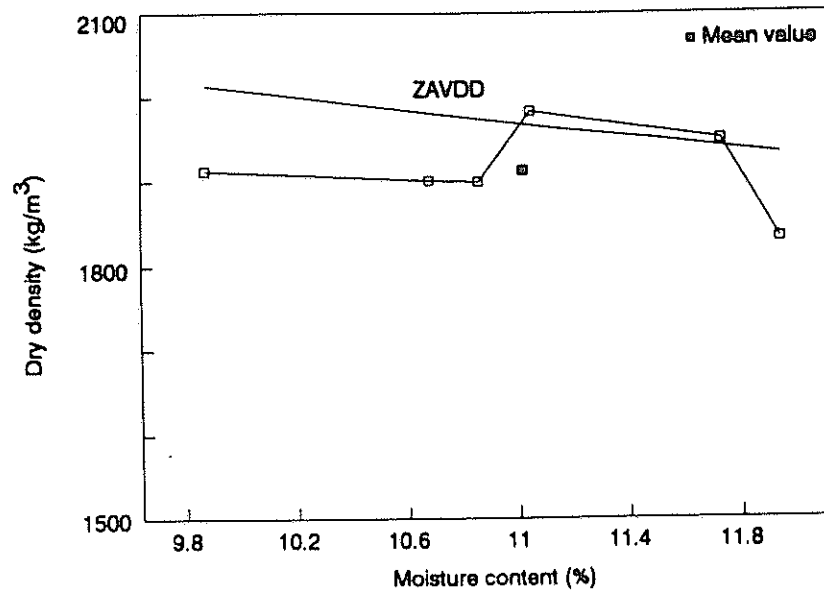


Figure 2.87: Measured dry densities against measured moisture contents on lower selected subgrade layer after one pass with vibratory roller

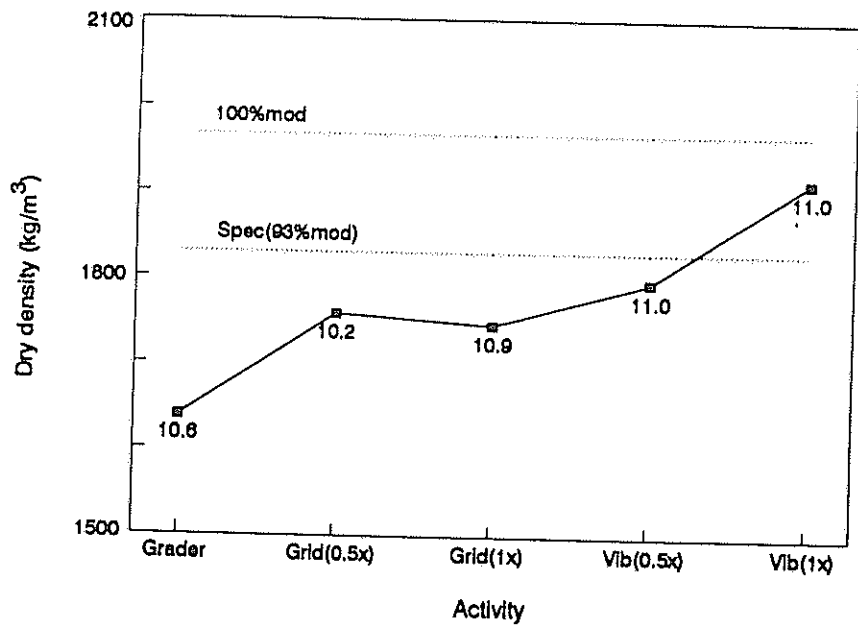


Figure 2.88: The compaction growth curve of the lower selected subgrade layer on Section 1 showing the average measured dry density against the activity prior to taking the moisture/density measurements (average moisture content value is printed below data point)

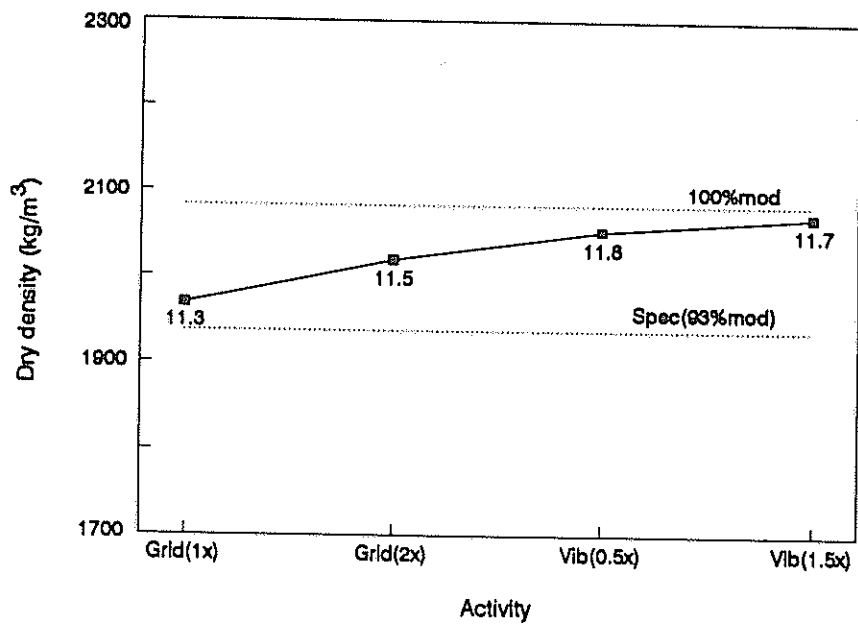


Figure 2.89: The compaction growth curve of the lower selected subgrade layer on Section 2 showing the average measured dry density against the activity prior to taking the moisture/density measurements (average moisture content value is printed below data point)

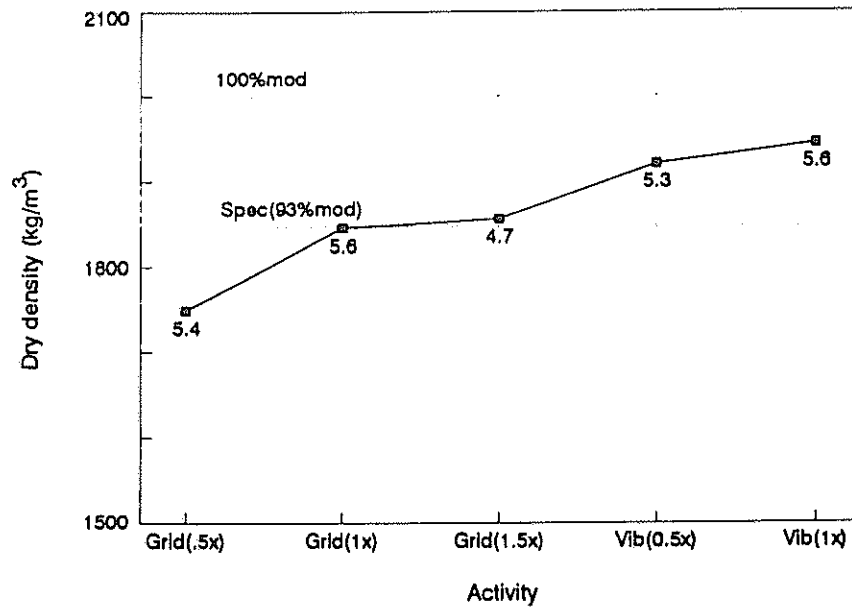


Figure 2.90: The compaction growth curve of the lower selected subgrade layer on Section 3 showing the average measured dry density against the activity prior to taking the moisture/density measurements (average moisture content value is printed below data point)

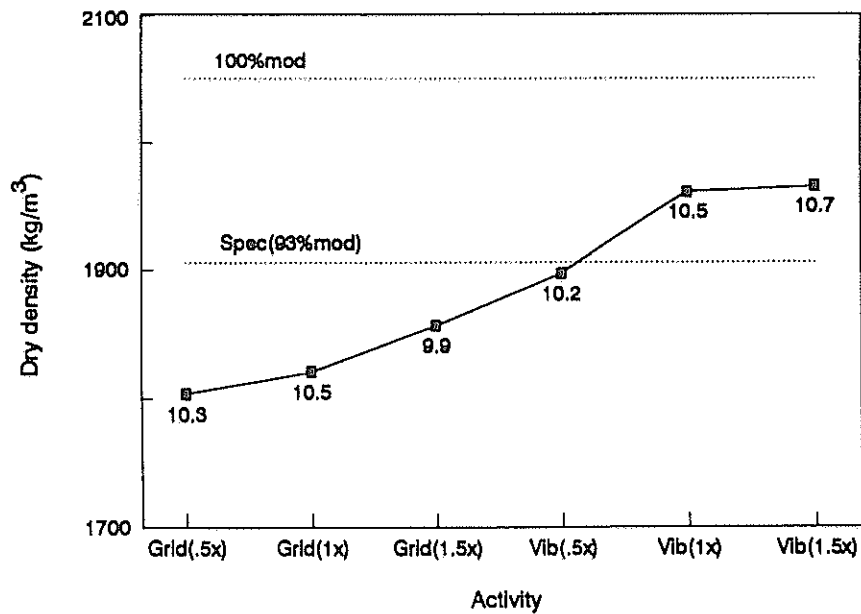


Figure 2.91: The compaction growth curve of the lower selected subgrade layer on Section 4 showing the average measured dry density against the activity prior to taking the moisture/density measurements (average moisture content value is printed below data point)

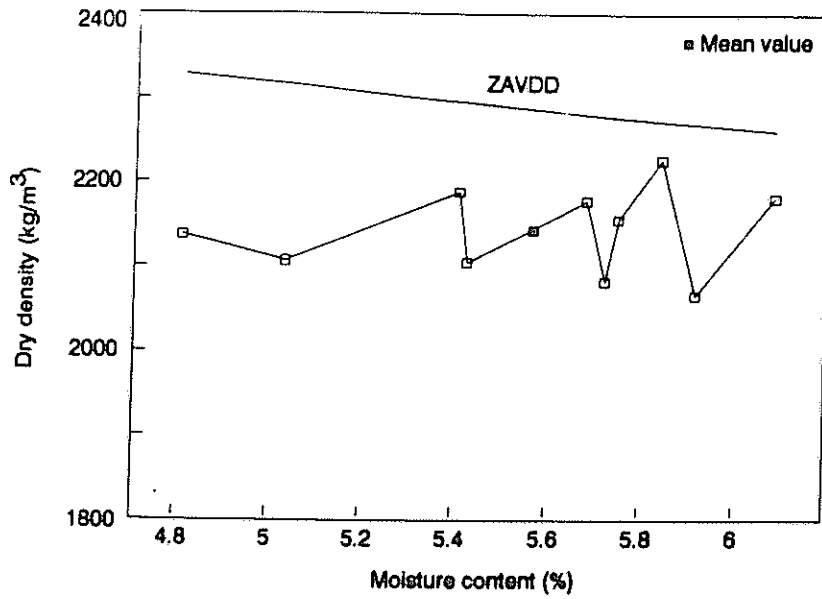


Figure 2.92: Measured dry densities against measured moisture contents on lower selected subgrade layer after one pass with vibratory roller on Section 3

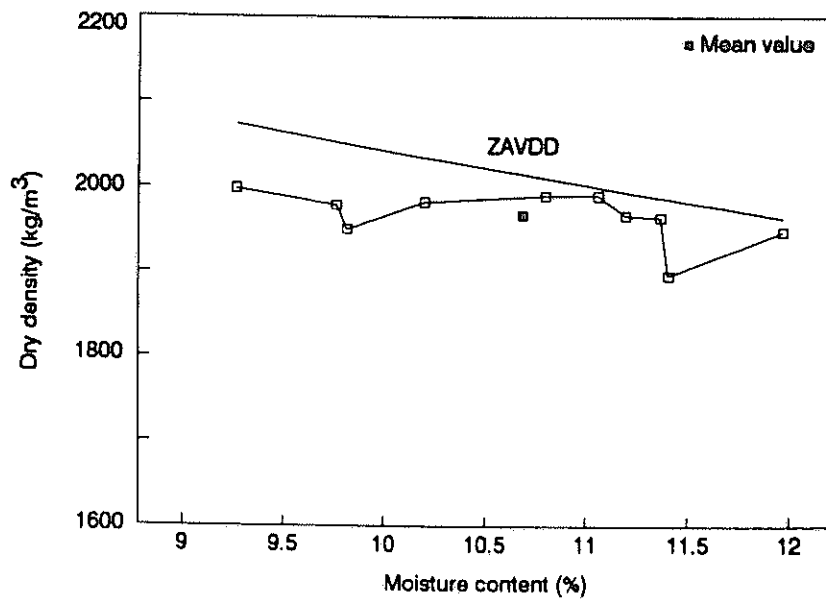


Figure 2.93: Measured dry densities against measured moisture contents on lower selected subgrade layer after one and a half passes with vibratory roller on Section 4

2.8.3 Upper selected subgrade

The material used for the upper selected subgrade was a red shale material (G5-G6) for Sections 1 and 3, and a dark brown loamy material (G5) for Sections 2 and 4 respectively. The measured dry densities against the measured moisture contents after the different activities of the compaction cycle on this layer for Section 2 are shown in Figures 2.94 to 2.99 and the compaction growth curve in Figure 2.100. The compaction growth curves for the other three sections are shown in Figures 2.101 to 2.103 respectively.

Figure 2.100 shows the results of a slight difference in moisture content. It seems that where the material is slightly above optimum at 10,4 % and an extra half pass with the vibratory roller had no influence on dry densities, the dry densities increased substantially when the moisture content dropped to 9,8%. Figure 2.100 shows that the grid roller has a very limited influence on the dry densities compared to half a pass of the vibratory roller. The sudden flattening of the compaction growth curve for next half pass of the vibratory roller is due to the material being too dry, because with a slight increase in the moisture content there is a substantial increase in the dry density level. Figures 2.102 and 2.103 indicate that the materials were probably too wet to compact optimally. Figure 2.104, showing the measured dry densities against the measured moisture contents for Section 4 after one pass with the vibratory roller, confirm this conclusion. Applying more compactive effort would have been pointless until there was a substantial decrease in the moisture content of the layer.

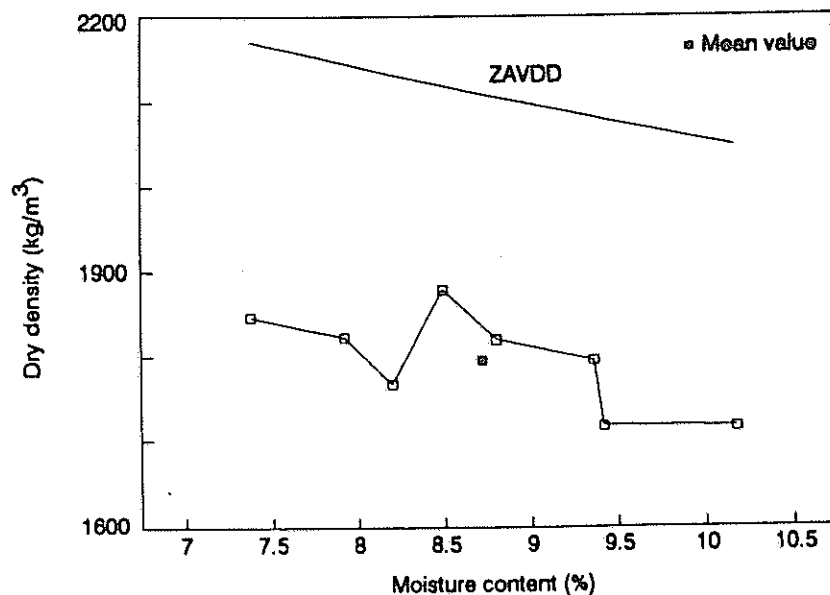


Figure 2.94: Measured dry densities against measured moisture contents on upper selected subgrade layer after half a pass with grid roller following mixing and levelling

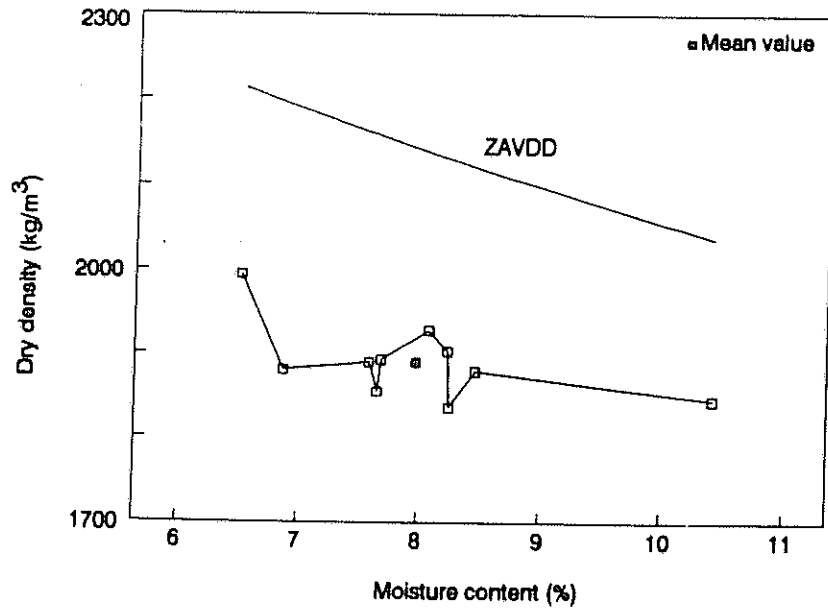


Figure 2.95: Measured dry densities against measured moisture contents on upper selected subgrade layer after one pass with grid roller

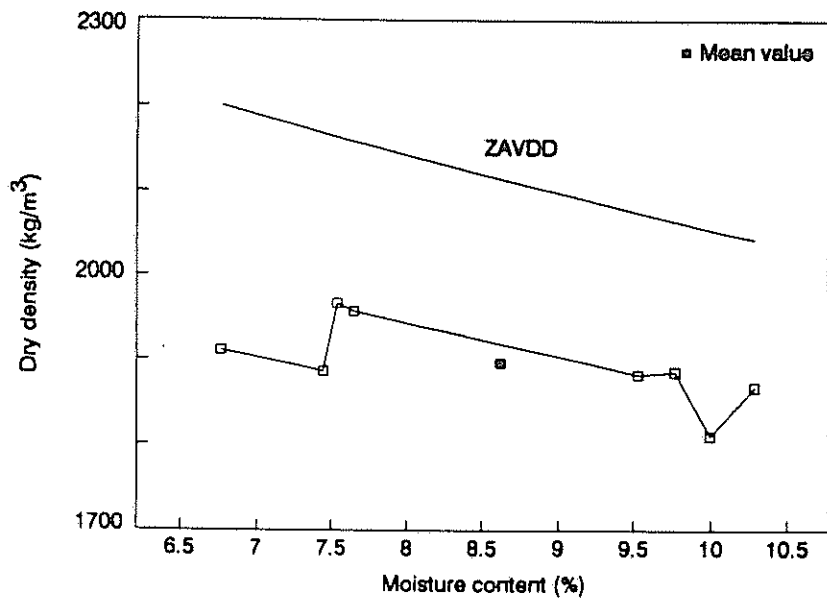


Figure 2.96: Measured dry densities against measured moisture contents on upper selected subgrade layer after two passes with grid roller

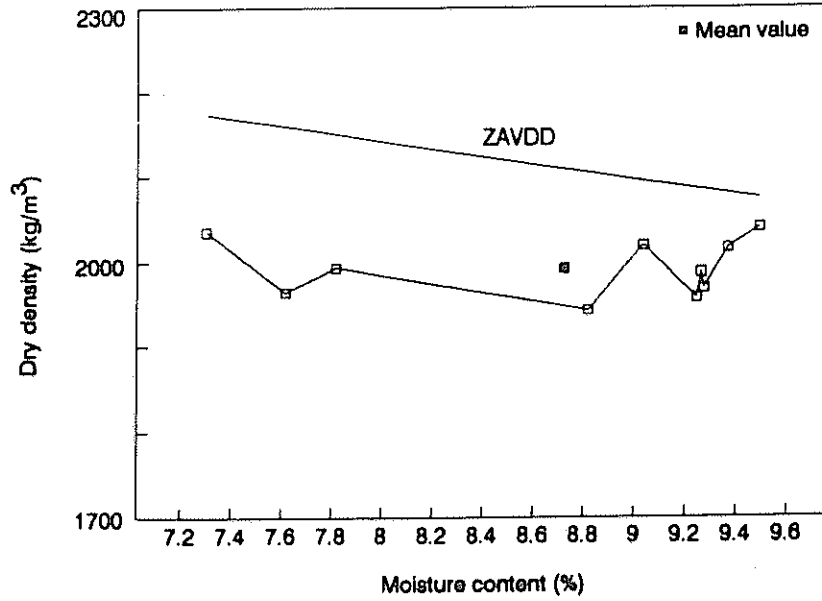


Figure 2.97: Measured dry densities against measured moisture contents on upper selected subgrade layer after half a pass with vibratory roller following on grid roller

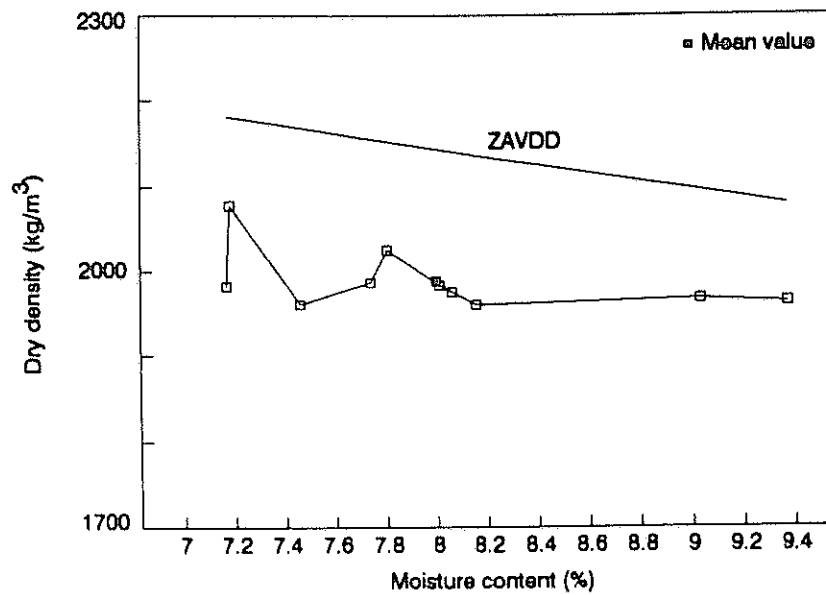


Figure 2.98: Measured dry densities against measured moisture contents on upper selected subgrade layer after one pass with vibratory roller

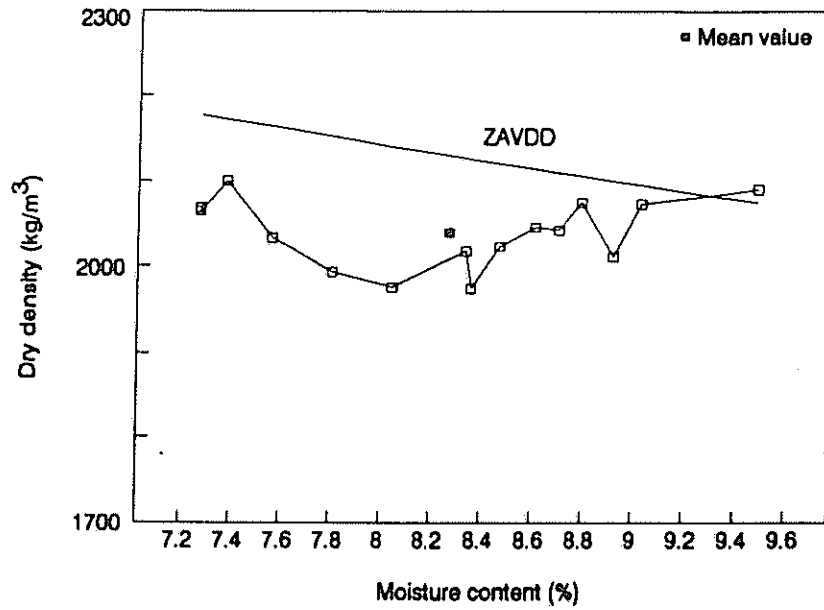


Figure 2.99: Measured dry densities against measured moisture contents on upper selected subgrade layer after one and half passes with vibratory roller

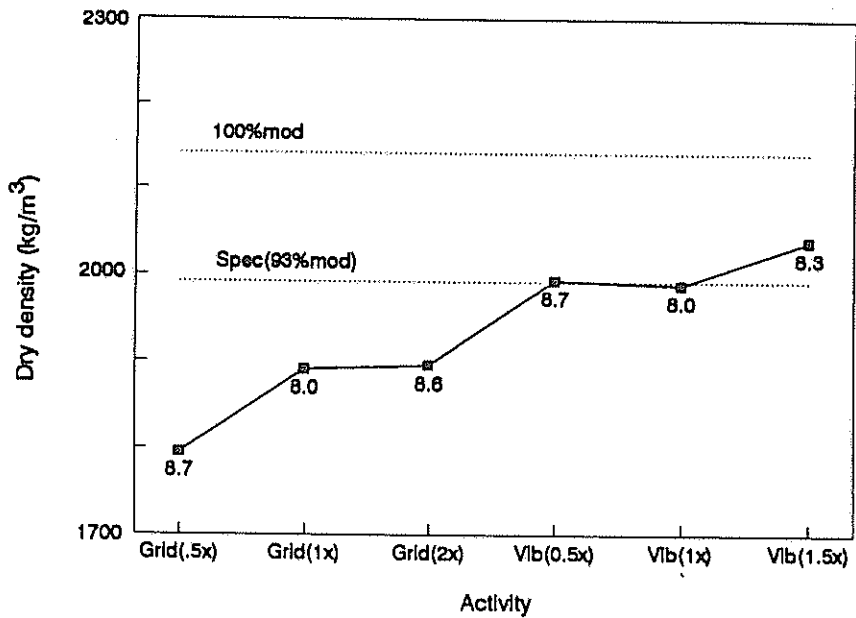


Figure 2.100: The compaction growth curve of the upper selected subgrade layer on Section 2 showing the average measured dry density against the activity prior to taking the moisture/density measurements (average moisture content value is printed below data point)

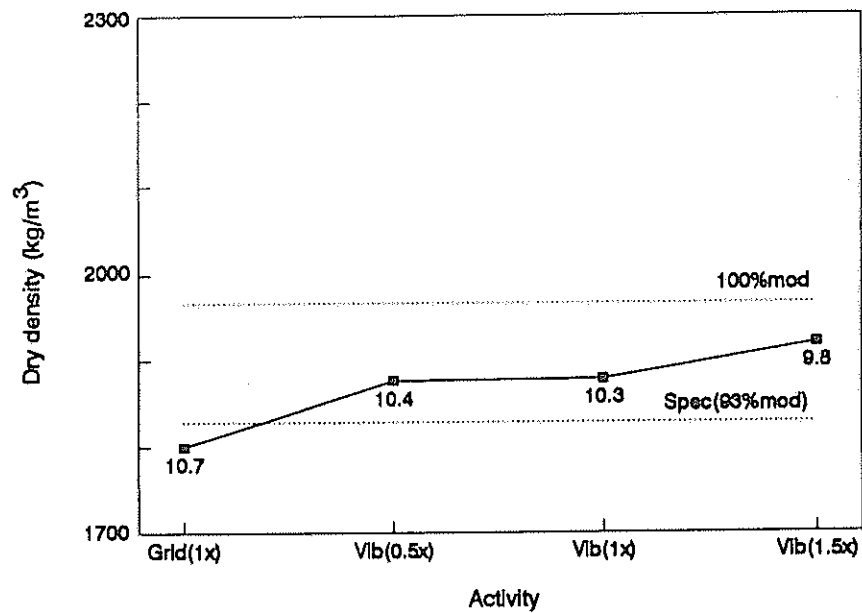


Figure 2.101: The compaction growth curve of the upper selected subgrade layer on Section 1 showing the average measured dry density against the activity prior to taking the moisture/density measurements (average moisture content value is printed below data point)

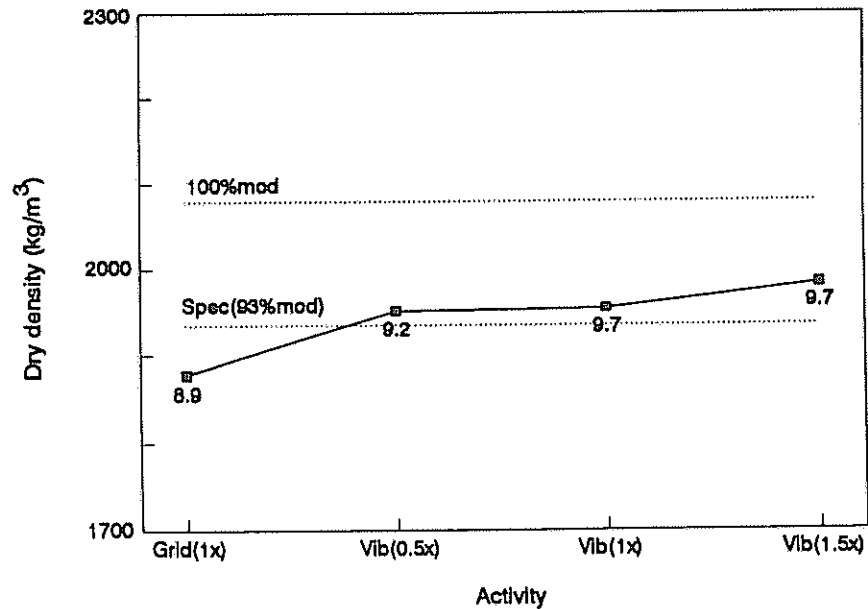


Figure 2.102: The compaction growth curve of the upper selected subgrade layer on Section 3 showing the average measured dry density against the activity prior to taking the moisture/density measurements (average moisture content value is printed below data point)

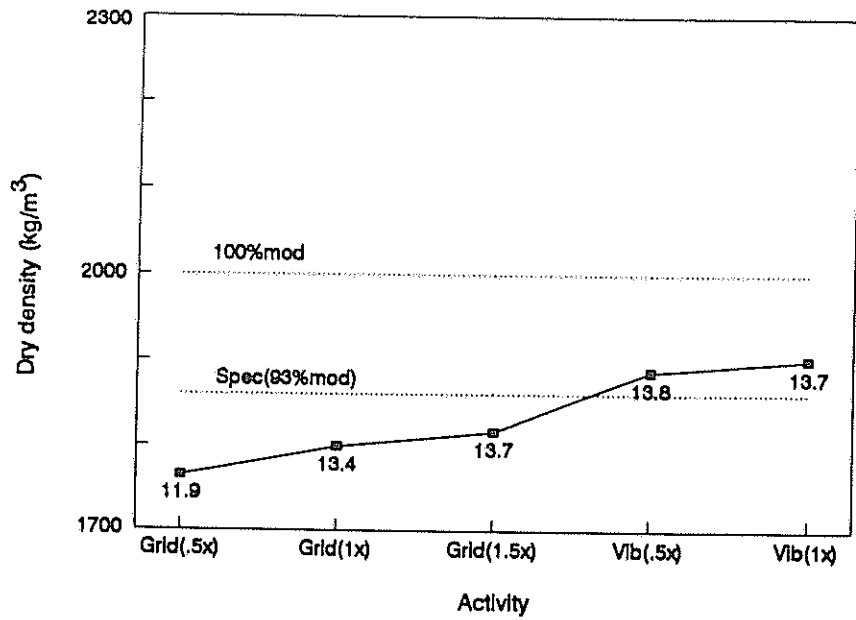


Figure 2.103: The compaction growth curve of the upper selected subgrade layer on Section 4 showing the average measured dry density against the activity prior to taking the moisture/density measurements (average moisture content value is printed below data point)

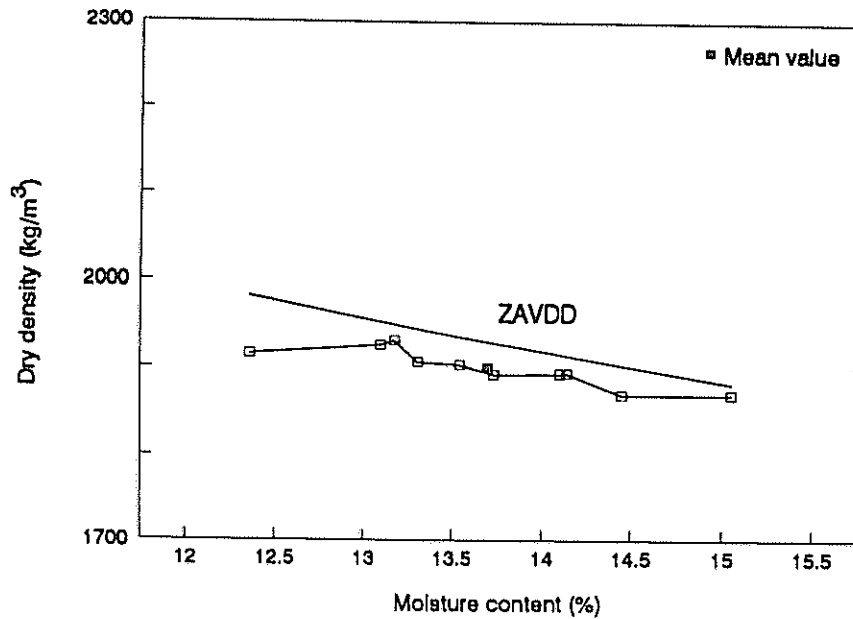


Figure 2.104: Measured dry densities against measured moisture contents on upper selected subgrade layer after one pass with vibratory roller on Section 4

2.8.4 Lower stabilized subbase

The lower stabilized subbase was constructed of weathered sandstone material (G5-G6) in the case of Section 1, from a greyish shale in the case of Sections 2 and 3, and from a reddish shale in the case of Section 4. The mod.AASHTO densities, as determined by the site laboratory, were 2125, 2125, 2100 and 2042 kg/m³ respectively. The measured dry densities against the measured moisture contents after the different compaction activities for Section 2, are shown in sequential order in Figures 2.105 to 2.109 and the compaction growth curve in Figure 2.110. The compaction growth curves for the other three sections are shown in Figures 2.111 to 2.113 respectively.

Figure 2.110 shows an immediate drop in the dry density levels during grid rolling when the moisture content is too high. As soon as the moisture content was lowered, there was a substantial increase in the dry density levels as shown by the mean result after half a pass with the vibratory roller. Note, however, that the increase in density dropped off tremendously during the next half pass of the vibratory roller, owing to an increase in moisture content. The results in Figure 2.109 also indicate that the material was too wet, because the results are more or less parallel to and near to the ZAVDD line. The flat slope of the growth curve of Figure 2.111 indicates that the material on Section 1 was too dry. This is confirmed by the results in Figure 2.114 showing that the measured dry densities after one pass with the vibratory roller on this section were far from the ZAVDD line. The flat slope of the growth curve in Figure 2.112 indicates that the material in Section 3 was too wet (also see Figure 2.115 which shows that the dry density results plot parallel to and near to the ZAVDD line). Figure 2.113 shows that this was also the case with Section 4 (also see Figure 2.116).

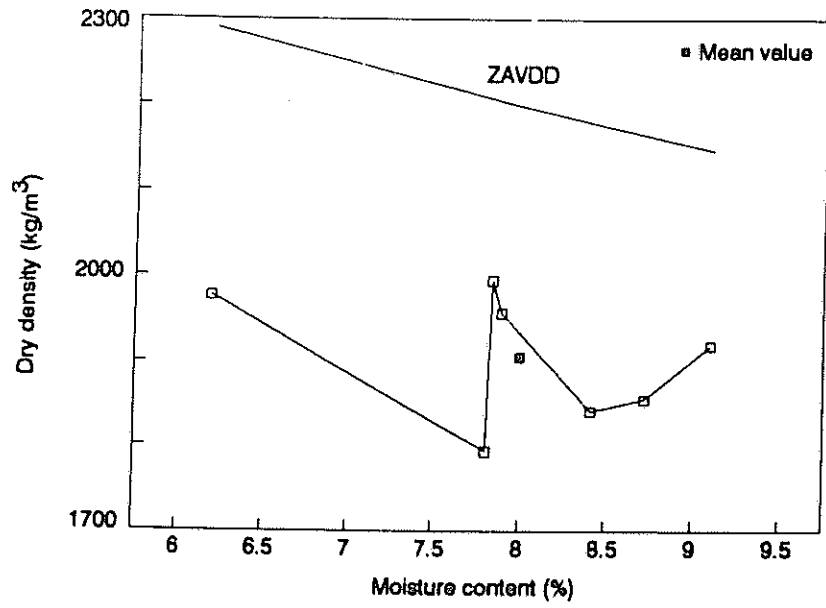


Figure 2.105: Measured dry densities against measured moisture contents on lower stabilized subbase layer after half a pass with grid roller following mixing and levelling

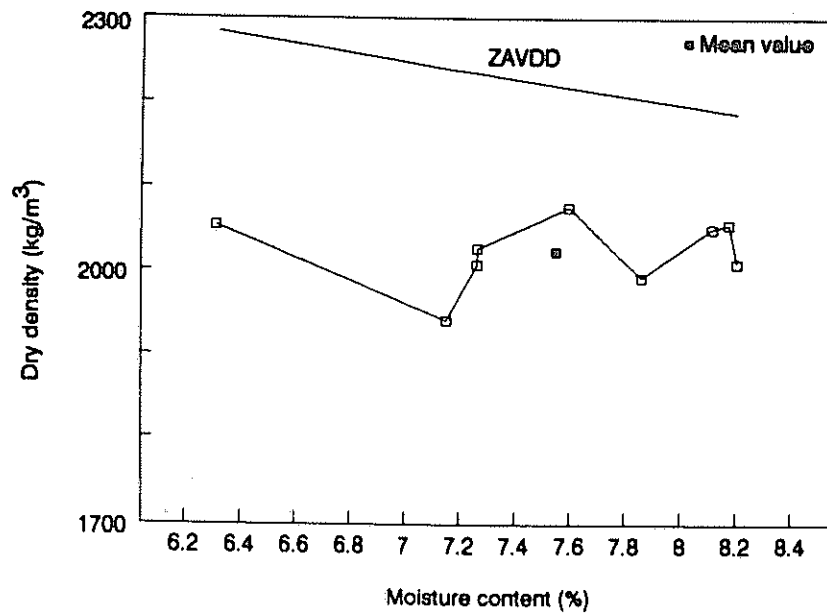


Figure 2.106: Measured dry densities against measured moisture contents on lower stabilized subbase layer after one pass with grid roller

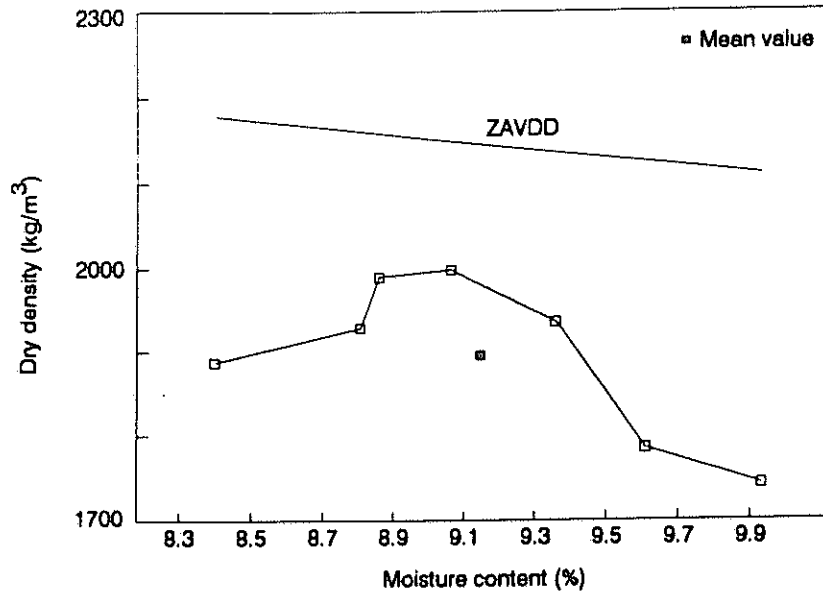


Figure 2.107: Measured dry densities against measured moisture contents on lower stabilized subbase layer after two passes with grid roller

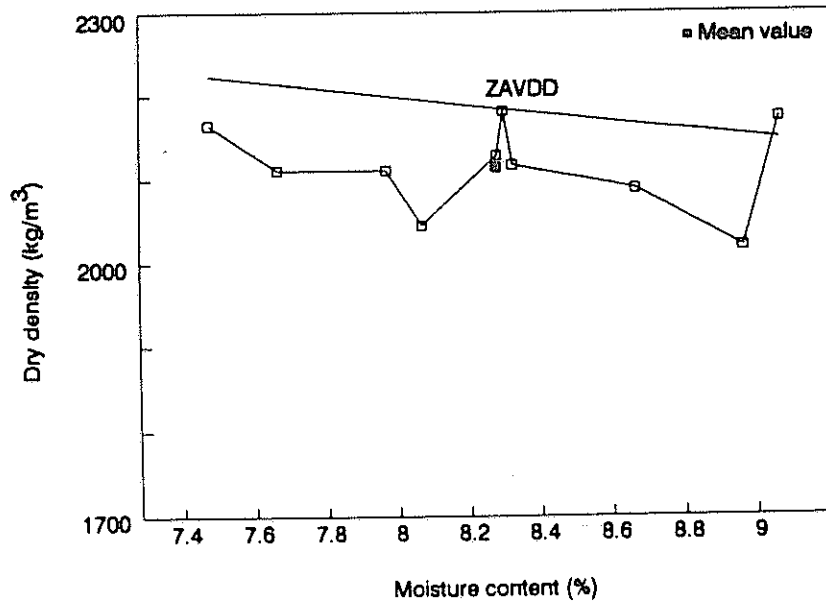


Figure 2.108: Measured dry densities against measured moisture contents on lower stabilized subbase layer after half a pass with vibratory roller following on grid roller

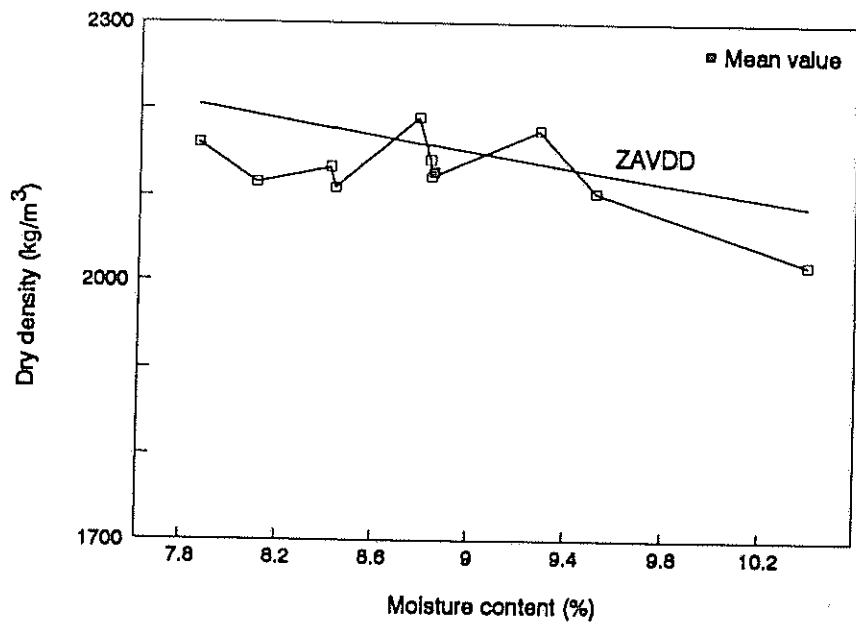


Figure 2.109: Measured dry densities against measured moisture contents on lower stabilized subbase layer after one pass with vibratory roller

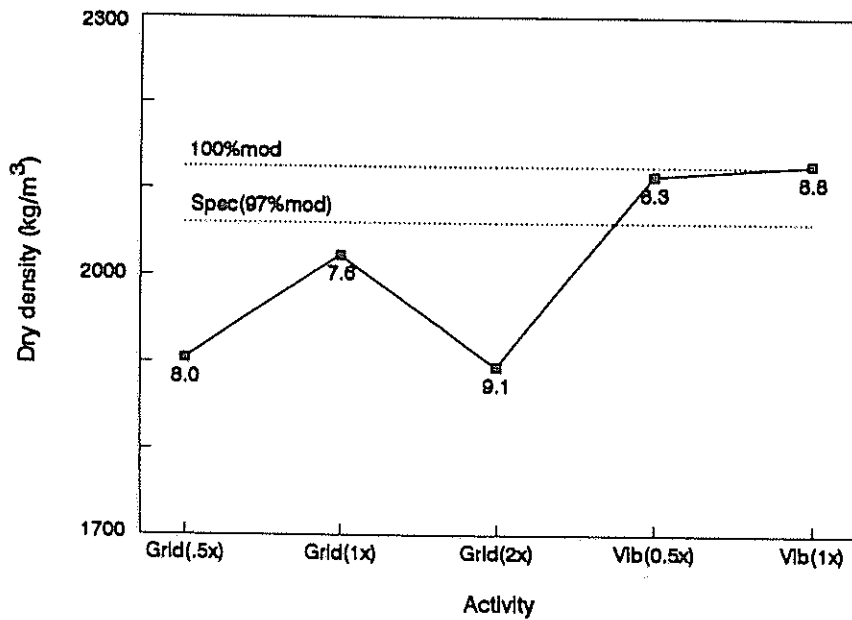


Figure 2.110: The compaction growth curve of the lower stabilized subbase layer on Section 2 showing the average measured dry density against the activity prior to taking the moisture/density measurements (average moisture content value is printed below data point)

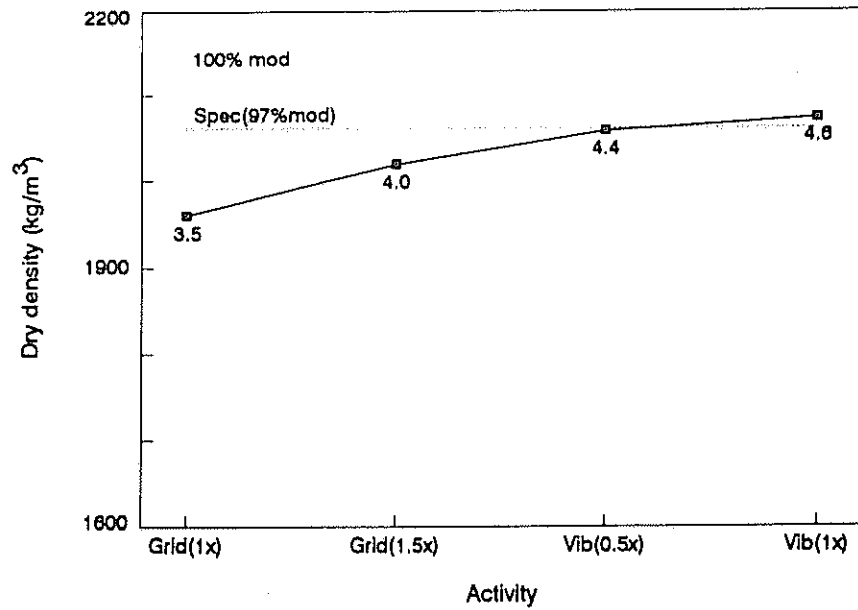


Figure 2.111: The compaction growth curve of the lower stabilized subbase layer on Section 1 showing the average measured dry density against the activity prior to taking the moisture/density measurements (average moisture content value is printed below data point)

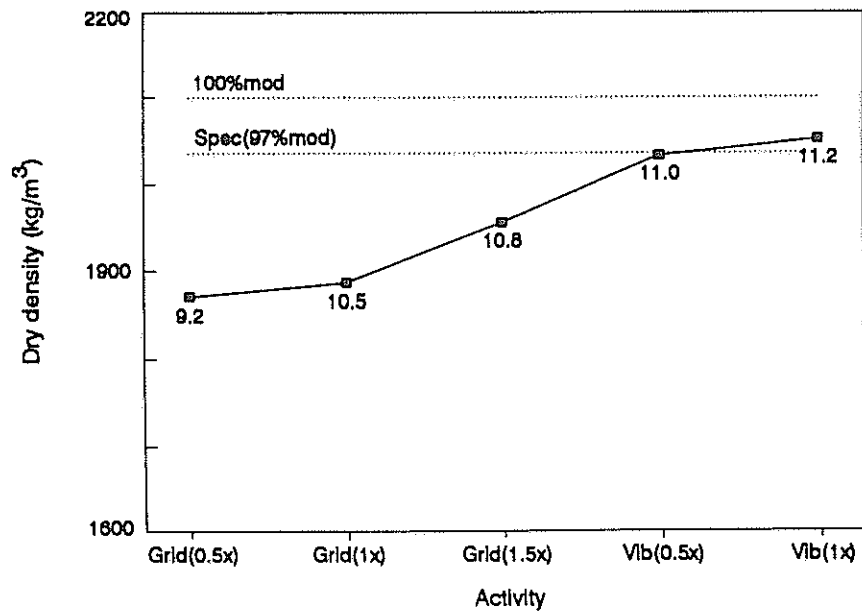


Figure 2.112: The compaction growth curve of the lower stabilized subbase layer on Section 3 showing the average measured dry density against the activity prior to taking the moisture/density measurements (average moisture content value is printed below data point)

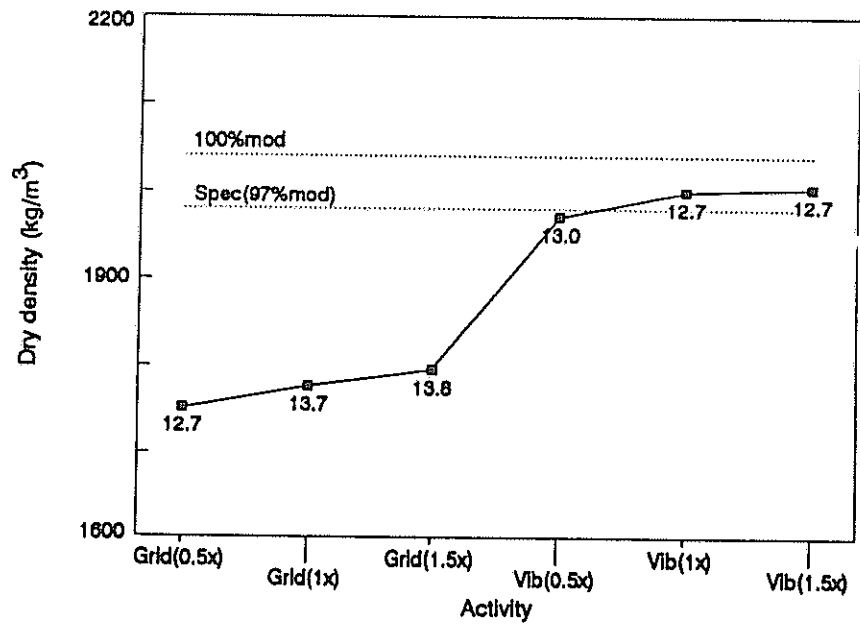


Figure 2.113: The compaction growth curve of the lower stabilized subbase layer on Section 4 showing the average measured dry density against the activity prior to taking the moisture/density measurements (average moisture content value is printed below data point)

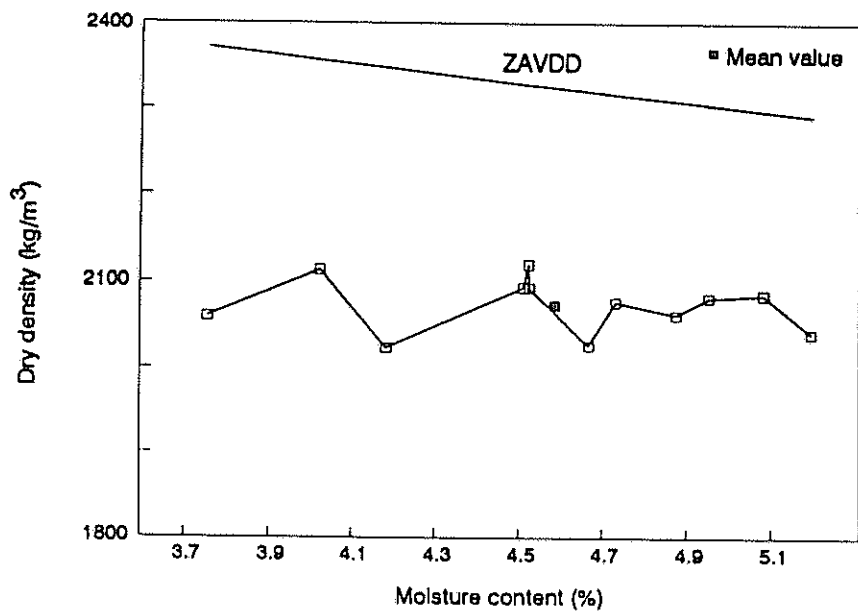


Figure 2.114: Measured dry densities against measured moisture contents on lower stabilized subbase layer of Section 1 after one pass with vibratory roller at the end of the compaction cycle

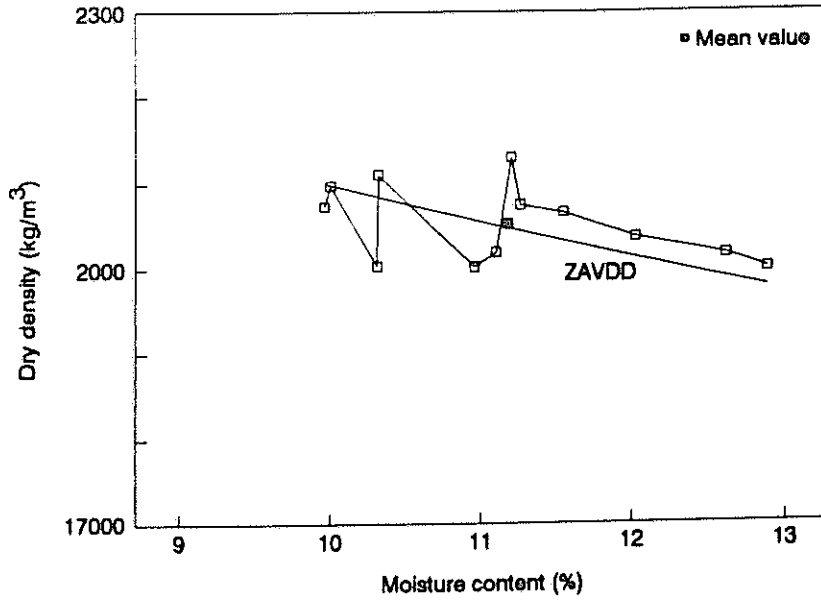


Figure 2.115: Measured dry densities against measured moisture contents on lower stabilized subbase layer of Section 3 after one pass with vibratory roller at the end of the compaction cycle

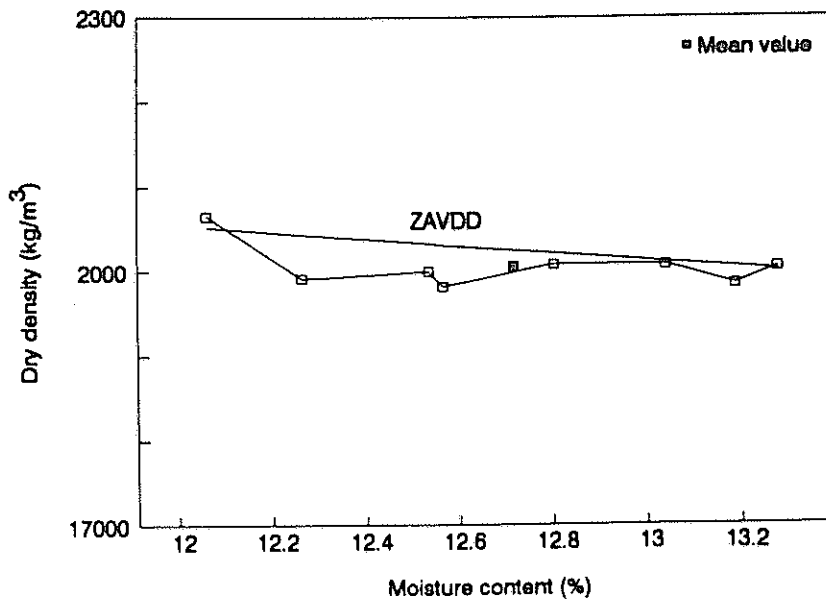


Figure 2.116: Measured dry densities against measured moisture contents on lower stabilized subbase layer of Section 4 after one and a half passes with vibratory roller at the end of the compaction cycle

2.8.5 Upper stabilized subbase

The upper stabilized subbase was also constructed from different materials on the different sections. The layer on Section 1 was constructed from material similar to that used for the lower stabilized subbase, namely a weathered sandstone material (G5-G6). However, the mod.AASHTO density value given for this layer by the site laboratory was 2007 kg/m^3 , which is more than 100 kg/m^3 less than the mod.AASHTO density value for the lower stabilized subbase. The mod.AASHTO density was therefore checked with the compactability software as well as by determining a mod.AASHTO density in the laboratory. The layer on the other three section was mainly constructed from a grey shale (G5-G6) with some red shale fines added in the case of Section 2. The mod.AASHTO densities, as determined by the site laboratory, for Sections 2, 3 and 4 were 2100, 2100 and 2123 kg/m^3 respectively. The measured results of the different operations during the construction of this layer on Section 3 are given in sequential order in Figures 2.117 to 2.124 and the compaction growth is shown in Figure 2.125. The compaction growth curves for the other three sections are shown in Figures 2.126 to 2.128 respectively.

The measured results of the compaction sequence of this layer on Section 3, as shown in Figures 2.117 to 2.123, show that the material was too wet. The flat slope of the compaction growth curve in Figure 2.124 also shows that as soon the material is too wet no roller can effectively compact the material owing to the build up of porewater pressure. The much steeper slope for less compactive effort of the compaction growth curve of Section 2 in Figure 2.126 confirms that it is relatively easy to compact roadbuilding materials provided they are at the correct moisture content. Refusal density for this layer had definitely not been reached when compaction was terminated. The reason for this statement is the fact that the growth curve was still increasing. Normally the dry density of a layer will increase by a few percentage points when it is rolled with a pneumatic-tyred roller after vibratory compaction.

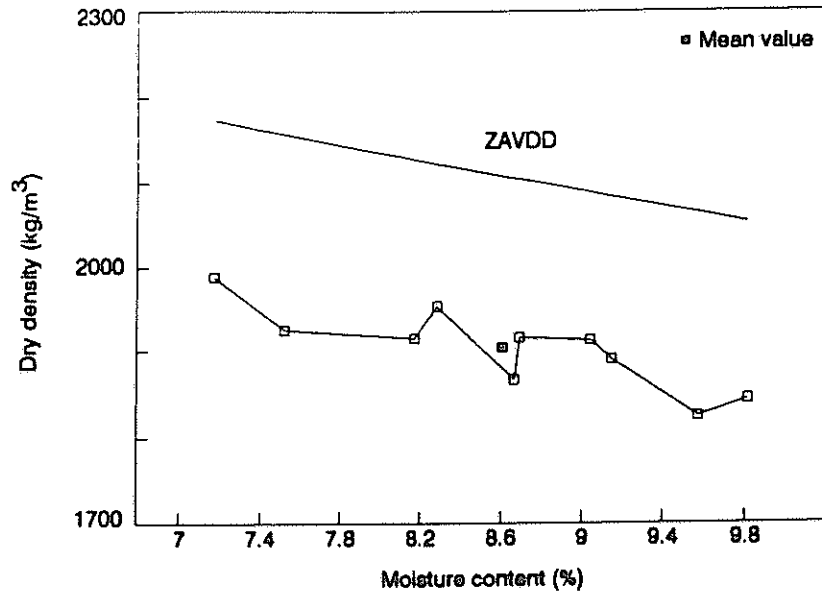


Figure 2.117: Measured dry densities against measured moisture contents on upper stabilized subbase layer after half a pass with grid roller following mixing and levelling

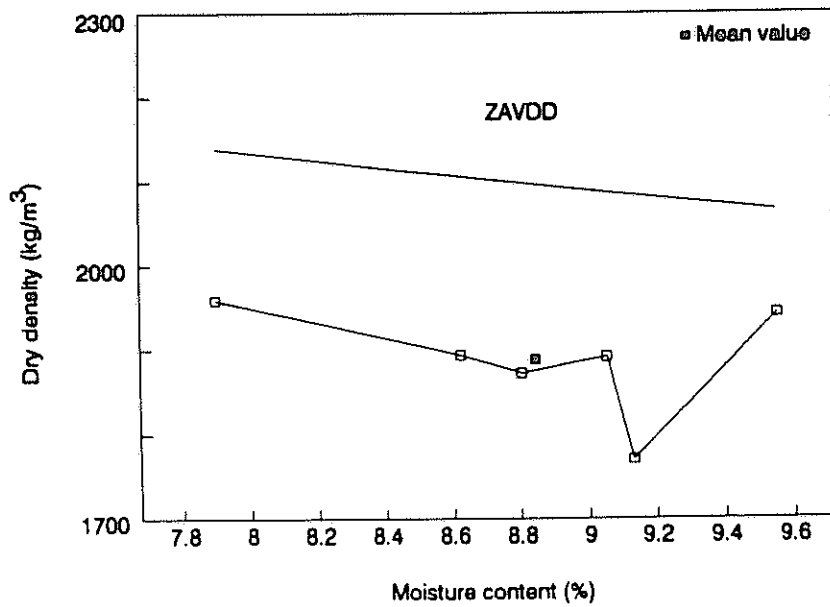


Figure 2.118: Measured dry densities against measured moisture contents on upper stabilized subbase layer after one pass with grid roller

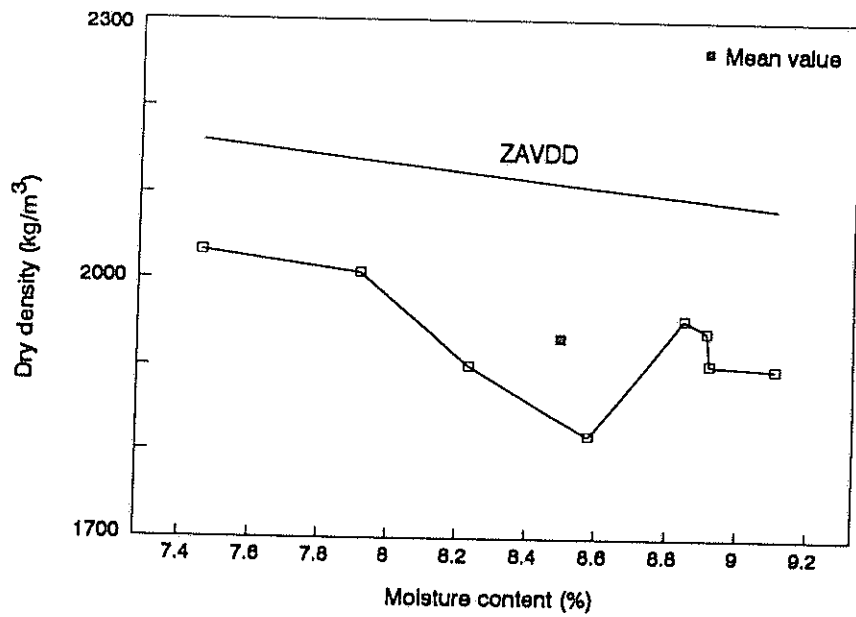


Figure 2.119: Measured dry densities against measured moisture contents on upper stabilized subbase layer after one and a half passes with grid roller

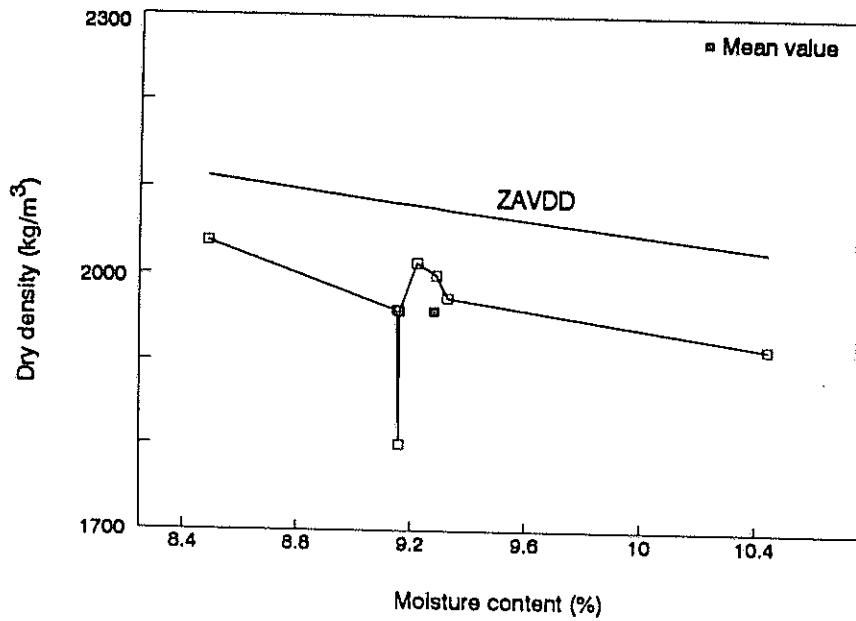


Figure 2.120: Measured dry densities against measured moisture contents on upper stabilized subbase layer after two passes with grid roller

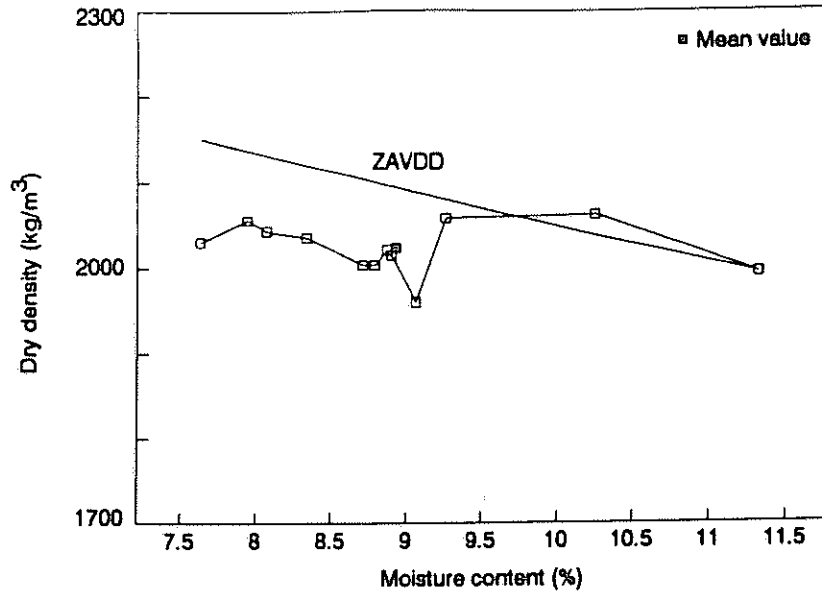


Figure 2.121: Measured dry densities against measured moisture contents on upper stabilized subbase layer after half a pass with vibratory roller following on grid roller

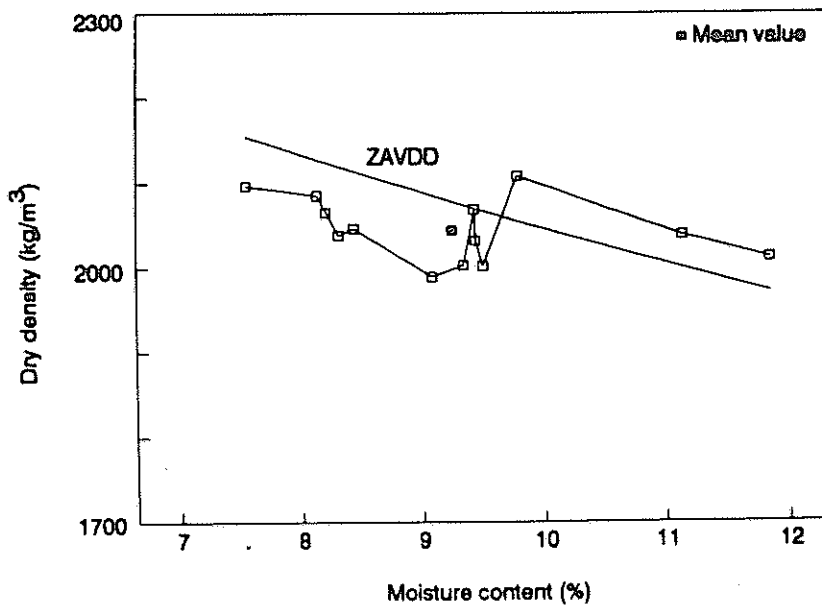


Figure 2.122: Measured dry densities against measured moisture contents on upper stabilized subbase layer after one pass with vibratory roller

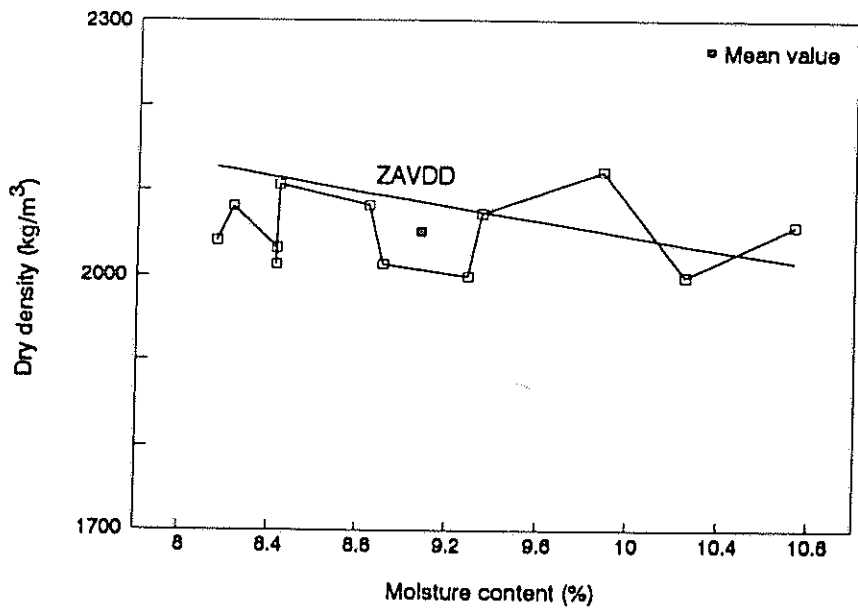


Figure 2.123: Measured dry densities against measured moisture contents on upper stabilized subbase layer after one and a half passes with vibratory roller

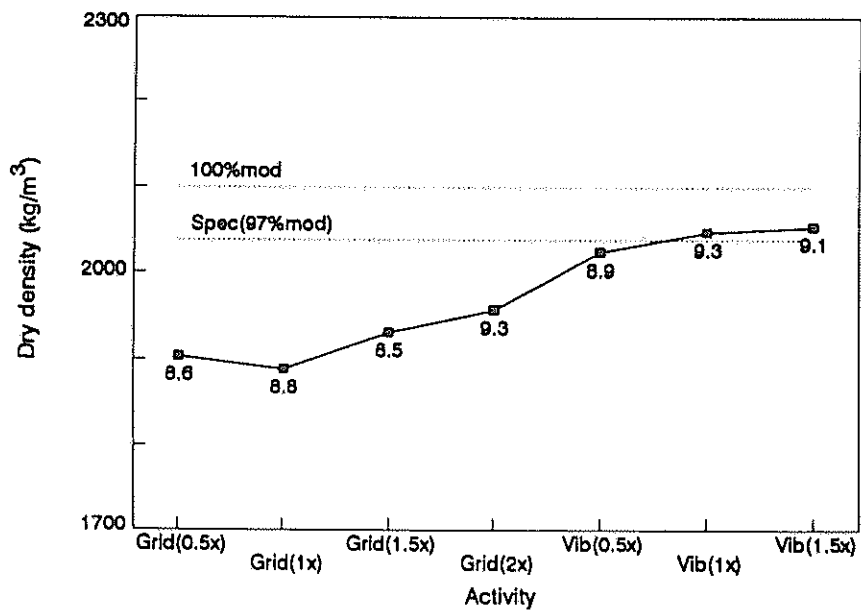


Figure 2.124: The compaction growth curve of the upper stabilized subbase layer on Section 3 showing the average measured dry density against the activity prior to taking the moisture/density measurements (average moisture content value is printed below data point)

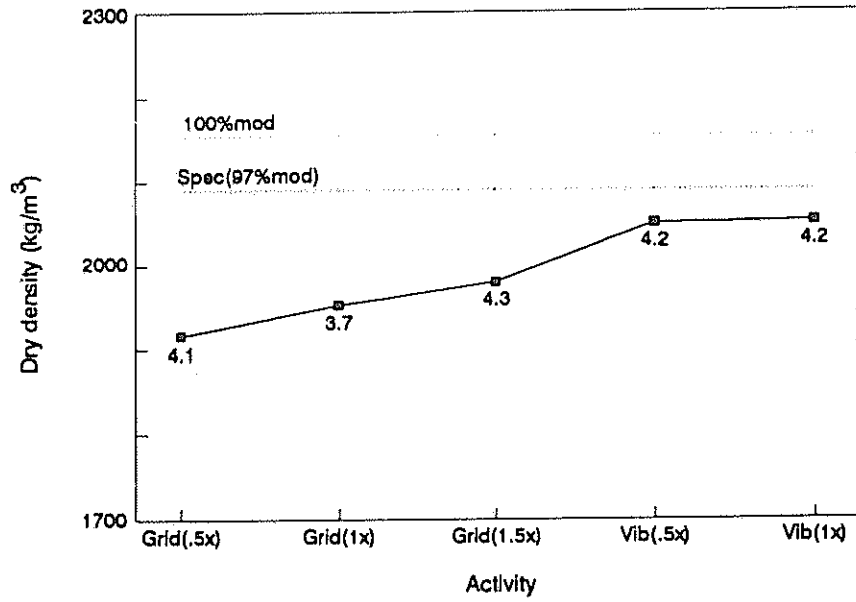


Figure 2.125: The compaction growth curve of the upper stabilized subbase layer on Section 1 showing the average measured dry density against the activity prior to taking the moisture/density measurements (average moisture content value is printed below data point)

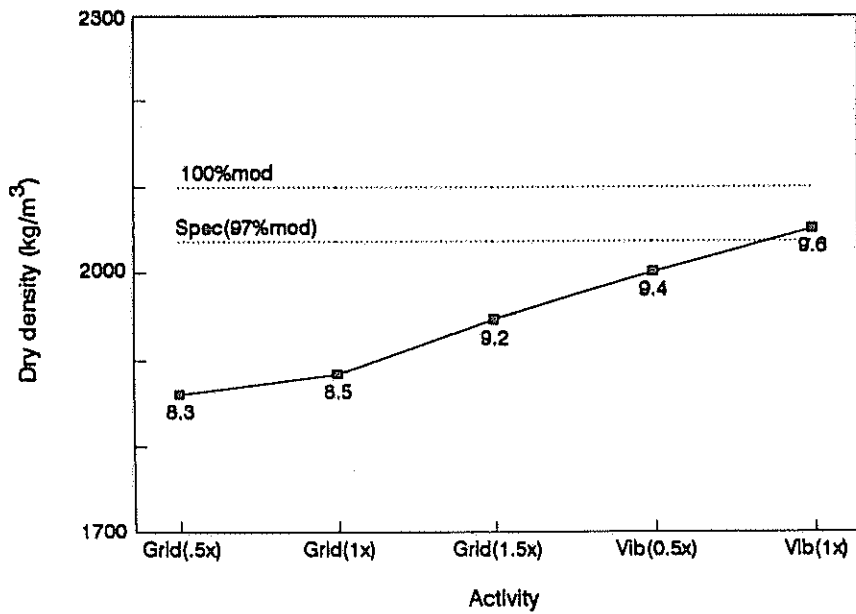


Figure 2.126: The compaction growth curve of the upper stabilized subbase layer on Section 2 showing the average measured dry density against the activity prior to taking the moisture/density measurements (average moisture content value is printed below data point)

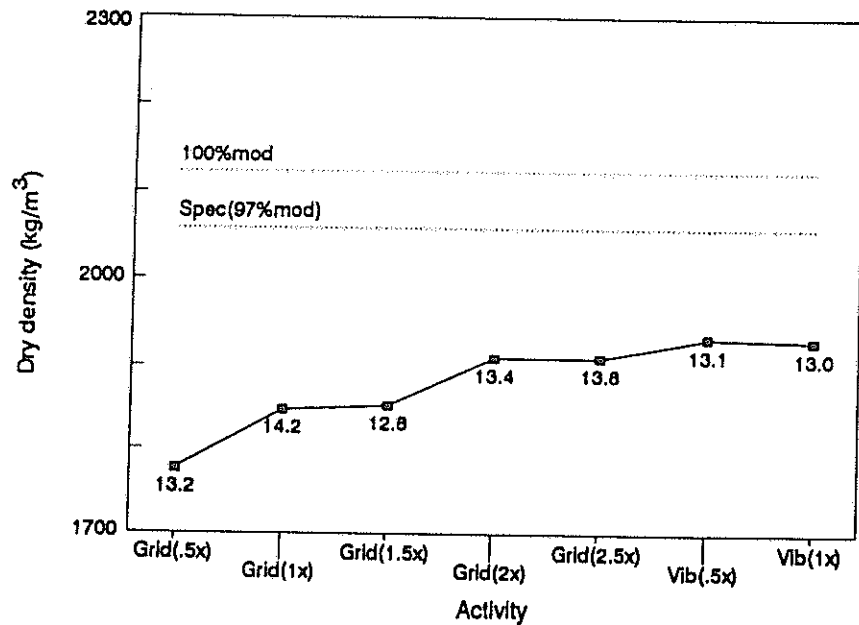


Figure 2.127: The compaction growth curve of the upper stabilized subbase layer on Section 4 showing the average measured dry density against the activity prior to taking the moisture/density measurements (average moisture content value is printed below data point)

2.8.6

Crushed stone base

The base course on Sections 1 to 3 was constructed from crushed quartzite material (G1) obtained from a crushing plant at Bronkhorstspuit. From Section 4 onward towards Bapsfontein the base course was constructed from a quartzite material (G1) obtained from Hippo Quarries in Benoni because this source was closer. The mod.AASHTO densities of the site laboratory for Sections 1, 2, 3, and 4 were 2275, 2200, 2250 and 2200 kg/m³ respectively and the MDDvib densities were 2345, 2340, 2330 and 2320 kg/m³ respectively. The measured results after the different construction activities for this layer on Section 1 are shown in Figures 2.129 to 2.132 respectively and the compaction growth curve is shown in Figure 2.133. The compaction growth curves for the other three sections are shown in Figures 2.134 to 2.136 respectively.

The compaction growth curve of the crushed stone base of Section 1, shown in Figure 2.133, shows once again that even crushed stone materials can be compacted to high densities levels with very little compactive effort provided the moisture content is properly controlled. If the actual compaction sequence had been completed with a pneumatic-tyred roller as recommended, the dry density levels would still have been a few percentage points higher, because the top 50 mm layer of cohesionless material, like crushed stone materials, always shakes slightly loose owing to the vibratory forces acting over a wider area than that just below the drum of the roller. Figure 2.134

shows that the material in Section 2 was too dry and that the material was all but properly compacted when the initial compaction cycle was terminated after one and half cycles of the vibratory roller. The difference in the dry density in this case will therefore require far more compactive effort during the slush rolling cycle, which normally only effects the dry density of the upper 50 mm of the layer. If slush rolling does not bring the dry density requirement to the specified dry density level of 88 %SD, the section may have to be ripped and recompacted. The same applies to the base layer of Section 3 (see Figure 2.135), which was also too dry and received far too little compactive effort.

The crushed stone for Section 4 was supplied by Hippo Quarries in Benoni because this source was closer to the section than the previous source. From this point onward the new source was used on this site. The compaction growth curve (see Figure 2.136) shows that the moisture content of this material was below OMC. However, the growth curve shows that it is possible to achieve dry densities in excess of 85 %SD within the scope of 2 to 3 passes with each roller type. To reach 88 %SD slush-rolling of the layer will be required. This was also the only section on which a pneumatic-tyred roller (PTR) was available. The PTR results on the growth curve show that the pneumatic-tyred roller does increase the density of the layer and should, therefore, form part of the standard compaction team.

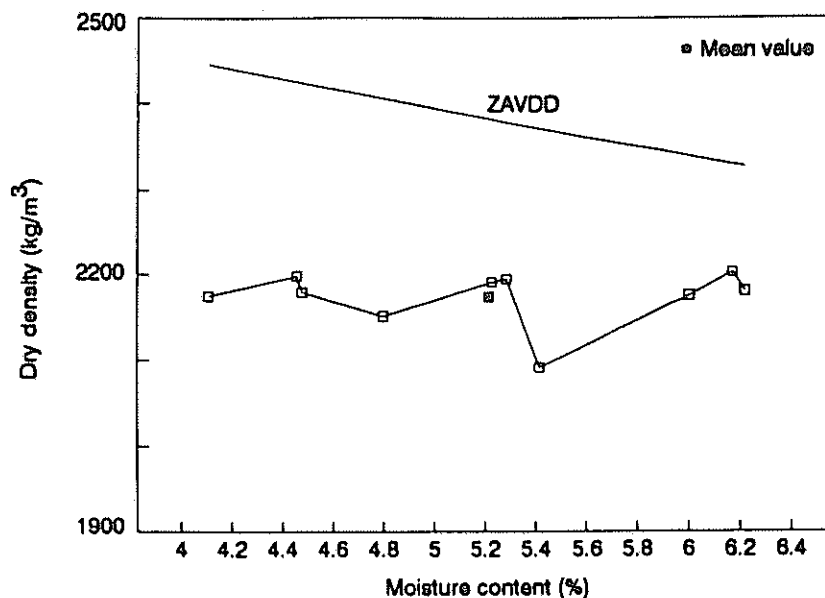


Figure 2.128: Measured dry densities against measured moisture contents on crushed stone base layer after half a pass with vibratory roller following mixing and levelling

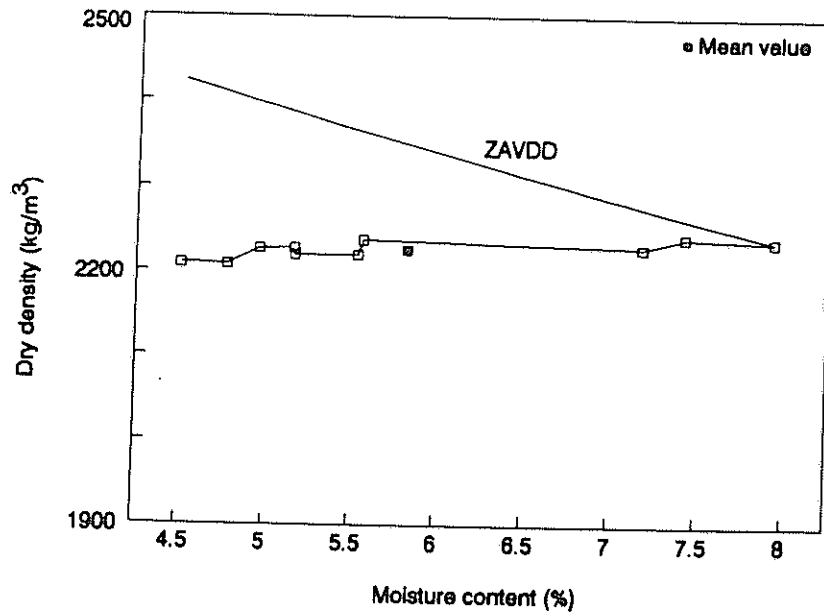


Figure 2.129: Measured dry densities against measured moisture contents on crushed stone base layer after one pass with vibratory roller

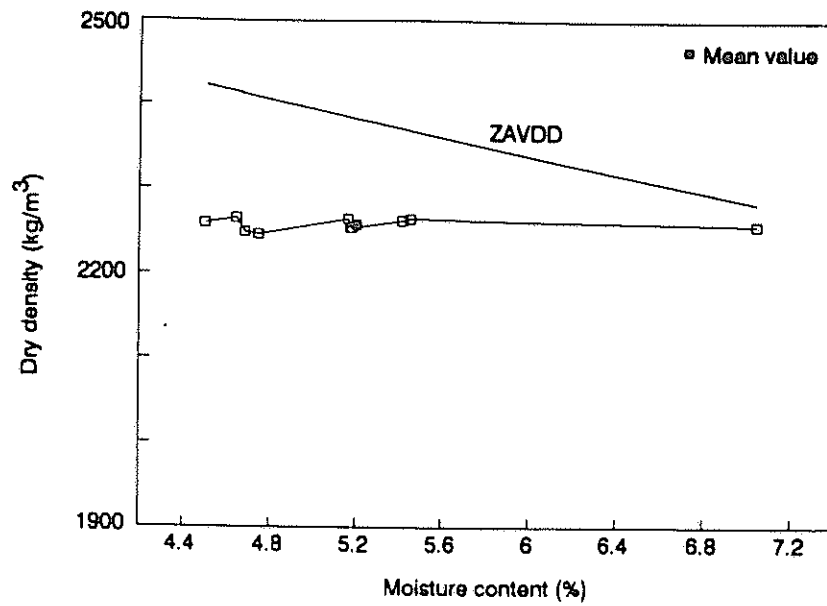


Figure 2.130: Measured dry densities against measured moisture contents on crushed stone base layer after one and a half passes with vibratory roller

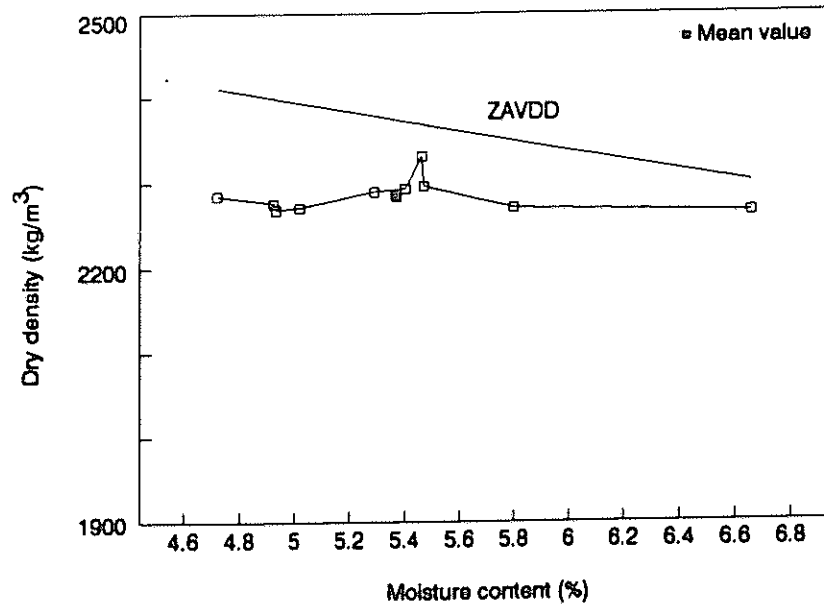


Figure 2.131: Measured dry densities against measured moisture contents on crushed stone base layer after two passes with vibratory roller

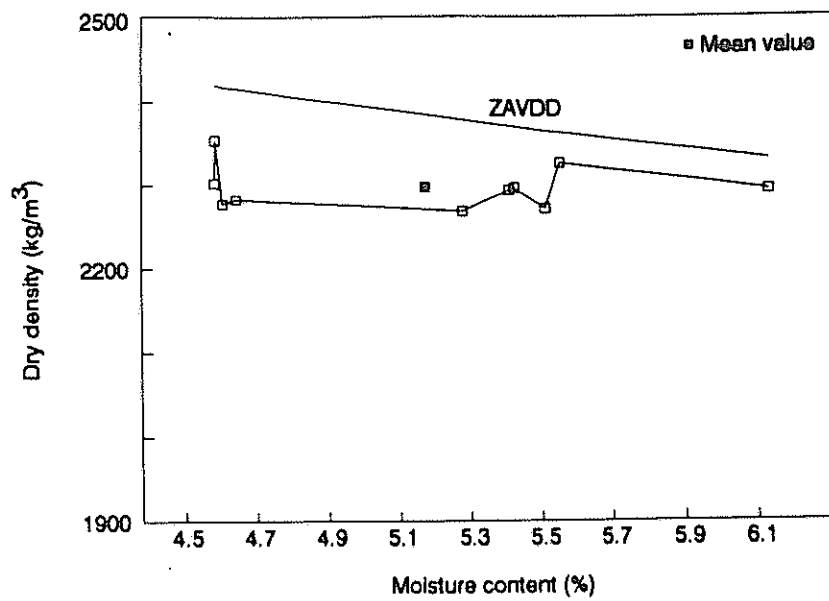


Figure 2.132: Measured dry densities against measured moisture contents on crushed stone base layer after two and half passes with vibratory roller

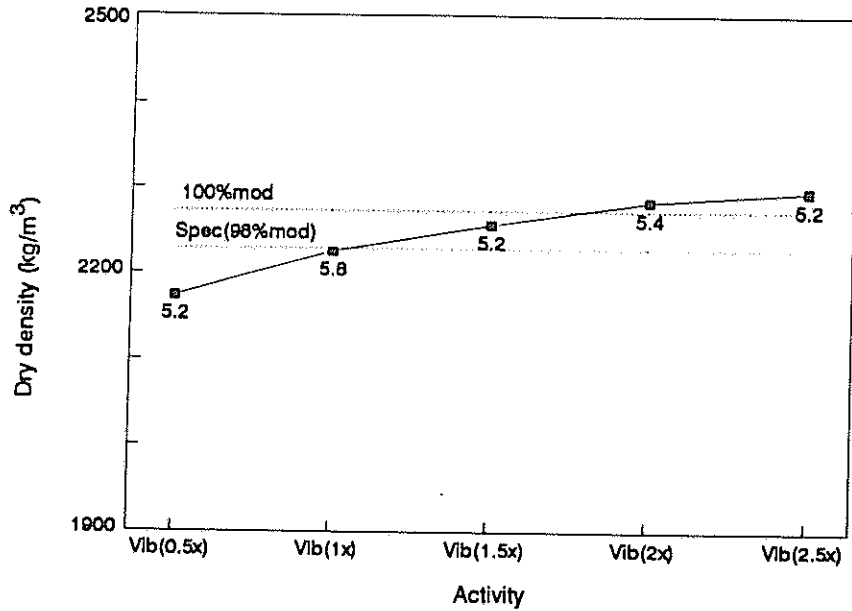


Figure 2.133: The compaction growth curve of the crushed stone base layer on Section 1 showing the average measured dry density against the activity prior to taking the moisture/density measurements (average moisture content value is printed below data point)

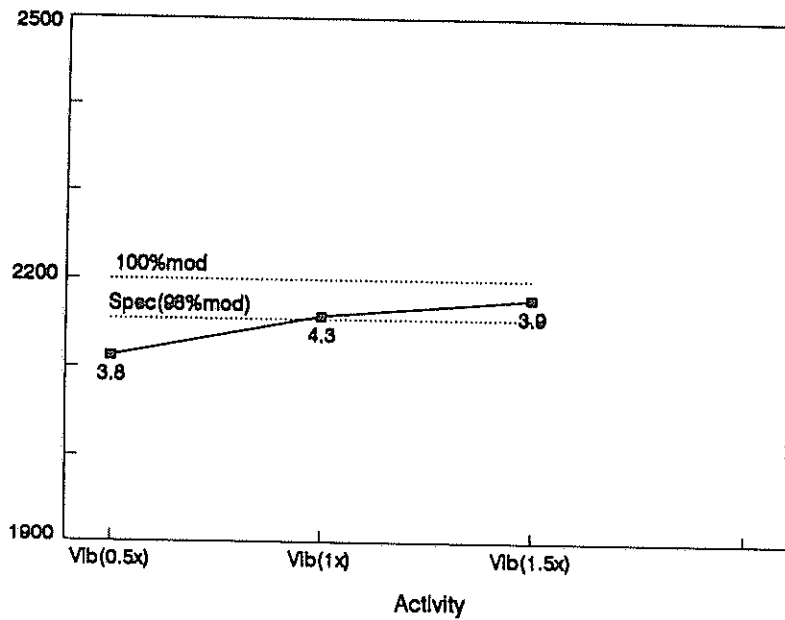


Figure 2.134: The compaction growth curve of the crushed stone base layer on Section 2 showing the average measured dry density against the activity prior to taking the moisture/density measurements (average moisture content value is printed below data point)

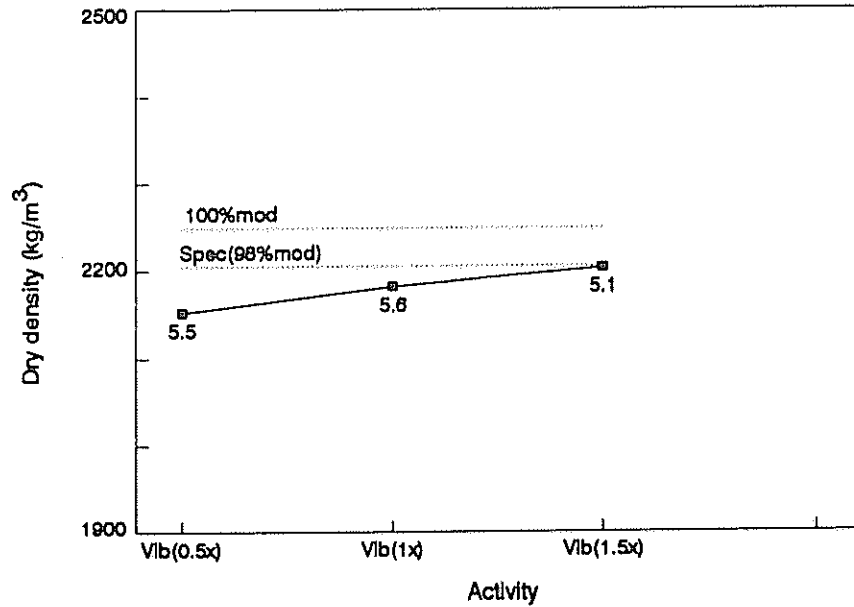


Figure 2.135: The compaction growth curve of the crushed stone base layer on Section 3 showing the average measured dry density against the activity prior to taking the moisture/density measurements (average moisture content value is printed below data point)

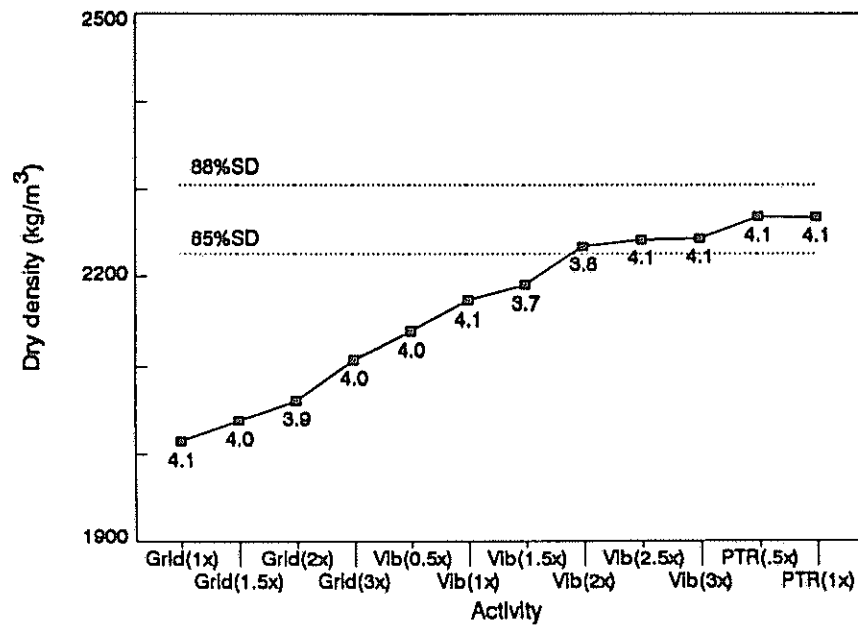


Figure 2.136: The compaction growth curve of the crushed stone base layer on Section 4 showing the average measured dry density against the activity prior to taking the moisture/density measurements (average moisture content value is printed below data point)

RESULTS OF THE VIBRATORY COMPACTION TABLE

Material samples from most of the layers on the test sections were taken for laboratory evaluation. In the laboratory the full grading curve, Atterberg limits and Linear Shrinkage of the -0,425mm material, the ARD and BRD of the +4,75 mm and the ARD of the -4,75 mm fractions of the materials were firstly determined for use with the Compactability Software Package to predict both the MDDs and OMCs of the different layers (see Appendix B for the prediction results). The materials were also compacted in a single layer on the vibratory compaction table for a range of moisture contents to determine the vibratory compaction MDDs and OMCs (see the graphs in Appendix B). Tables 2.1 and 2.2 summarize the predicted and measured MDDs, OMCs and ZAVMCs.

The tables show that, in general, reasonable predictions of the MDDs and OMCs of untreated roadbuilding materials can be made from the indicator test results and ARDs of the +4,75 mm and -4,75 mm fractions and the BRD of the +4,75 mm fraction. Although the measured and predicted MDD(vib) values sometimes differ somewhat, the measured OMC(vib) and the predicted ZAVMC(vib) agree remarkably well with each other. Where this investigation has shown that the critical factor in optimal compaction is the compaction moisture content, the prediction of this moisture content seems feasible by means of the Compactability Software Package provided that the grading is not too coarse and the particle shape and texture is reasonable. Poorly shaped particles have a negative influence on the compactability of material (see Report PR92/471³).

Table 2.1: Predicted and measured Maximum Dry Density and Optimum Moisture Content values using the Compactability Software Package and the vibratory compaction table

Section	Layer	MDDvib measured (kg/m ³)	OMCvib measured (%)	MDDvib predicted (kg/m ³)	OMCvib predicted (%)	MDDmod predicted (kg/m ³)	OMCmod predicted (%)
1	Fill	2030	11,50	2094	10,58	2055	10,52
1	Select1	1800	13,50	2083	10,99	1990	12,56
1	Select2	1870	13,00	2093	10,98	2014	11,92
1	Subbase1	2020	5,70	2253	5,80	2151	7,28
1	Subbase2			2260	5,75	2164	7,13
1	Base	2345	5,75	2415	4,65	2246	5,82
2	Select1	2050	10,50	2083	10,00	2026	10,50
2	Select2	2170	8,90	2281	6,37	2158	8,00
2	Subbase1	2010	7,40	2380	5,26	2234	6,91
2	Subbase2	1950	4,80	2324	6,12	2202	7,50
2	Base	2340	6,20	2425	4,46	2256	5,64
3	Select1	2040	7,80	****	****	****	****
3	Select2	2160	10,40	2263	8,52	2162	9,20
3	Subbase1	2080	8,70	****	****	****	****
3	Subbase2	1930	8,40	2218	7,70	2105	8,58
3	Base1	2330	6,20	2425	4,46	2256	5,64
4	Select1	1950	9,60	2193	8,01	2109	9,62
4	Select2	2140	9,80	2155	8,53	2078	9,50
4	Subbase1	2080	11,60	2140	11,84	2102	11,53
4	Subbase2	2120	11,5	2168	11,17	2118	11,13
4	Base	2320	6,00	2396	4,38	2231	5,55

**** Grading too coarse to predict properties

Table 2.2: Predicted and measured Maximum Dry Density, Optimum Moisture Content and Zero Air Voids Moisture Content values using the Compactability Software Package and the vibratory compaction table

Section	Layer	MDDvib measured (kg/m ³)	OMCvib measured (%)	MDDvib predicted (kg/m ³)	ZAVMC vib predicted (%)	MDDmod predicted (kg/m ³)	ZAVMC mod predicted (%)
1	Fill	2030	11.50	2094	11,62	2055	12,53
1	Select1	1800	13.50	2083	12,66	1990	14,92
1	Select2	1870	13,00	2093	12,48	2014	14,37
1	Subbase1	2020	5,70	2253	7,09	2151	9,20
1	Subbase2			2260	6,99	2164	8,96
1	Base	2345	5,75	2415	5,40	2246	8,51
2	Select1	2050	10,50	2083	11,53	2026	12,88
2	Select2	2170	8,90	2281	7,57	2158	10,07
2	Subbase1	2010	7,40	2380	6,22	2234	8,98
2	Subbase2	1950	4,80	2324	7,01	2202	9,40
2	Base	2340	6,20	2425	5,20	2256	8,31
3	Select1	2040	7,80	****	****	****	****
3	Select2	2160	10,40	2263	9,37	2162	11,43
3	Subbase1	2080	8,70	****	****	****	****
3	Subbase2	1930	8,40	2218	8,53	2105	10,97
3	Base1	2330	6,20	2425	5,20	2256	8,31
4	Select1	1950	9,60	2193	9,43	2109	11,25
4	Select2	2140	9,80	2155	10,09	2078	11,80
4	Subbase1	2080	11,60	2140	12,46	2102	13,29
4	Subbase2	2120	11,5	2168	11,86	2118	12,94
4	Base	2320	6,00	2396	5,14	2231	8,22

**** Grading too coarse to predict properties

3. CONCLUSIONS

The results obtained from the test sections show that the moisture content of the material at the time of compaction as well as the manner in which the material is compacted play a very important part in the in situ dry density that will be achieved with a particular roadbuilding material. Apart from this the actual preparation of the layer like the watering, mixing and levelling of the layer also have an effect on the results. These factors are discussed in more detail below.

3.1 **MOISTURE CONTENT : ITS EFFECT AND THE IMPORTANCE OF CONTROL**

It is an accepted fact that the moisture content of the material plays an extremely important role in ensuring optimum compaction.

Maximum dry density is normally achieved when the material is nearly saturated, as observed with the material reaction on the vibratory compaction table. Present compaction practice often recommends that roadbuilding materials should be compacted at a moisture content of one to two per cent lower than OMC (mod.AASHTO) for two reasons, namely:

- (a) To prevent the build-up of porewater pressure the moisture content should always be lower than total saturation.
- (b) The grading of the coarse-graded material on site and the grading of the coarse-graded material in the mod.AASHTO density test differ significantly from each other. The material in the laboratory test is substantially finer because all coarse fractions are crushed to pass the 19 mm sieve. This leads to an increase in voids which, in turn, leads to a lower dry density (see Figure 1.1) and an increase in void content, requiring a greater amount of water to saturate the material (i.e. too high a OMC for the coarser grading on site).

It is, however, clear that without the proper control of the moisture content of all roadbuilding materials which use water as lubricant, it would be impossible to achieve optimal compaction. Presently, the compaction teams have to guess the moisture content by "feel" or "look" as there is no formal process control for moisture content during construction. Although it is possible to establish the "optimum moisture content" fairly accurately through visual observation, a **substantial improvement in construction dry density levels can be achieved if the moisture added to the material is controlled more accurately during the construction process.** The compaction results of the crushed stone base course layer on Site 1 show that an excessive amount of compaction

effort cannot rectify the adverse conditions created by an excessive amount of moisture (see Section 2 of report).

Too dry material also causes lower densities because of higher shear forces. In many cases more compaction effort in terms of more roller passes will be totally ineffective as these shear forces are too great to be overcome by the "compactive effort" of the roller. For example, in a number of cases on Site 1 (92/93) it was found that even the vibratory roller had no effect on the compaction of the layer (i.e. no increase in density). However, immediately after wetting the layer with an additional spray, the measured dry densities after the next half pass of the vibratory roller showed a substantial increase (also see Figure 3.1).

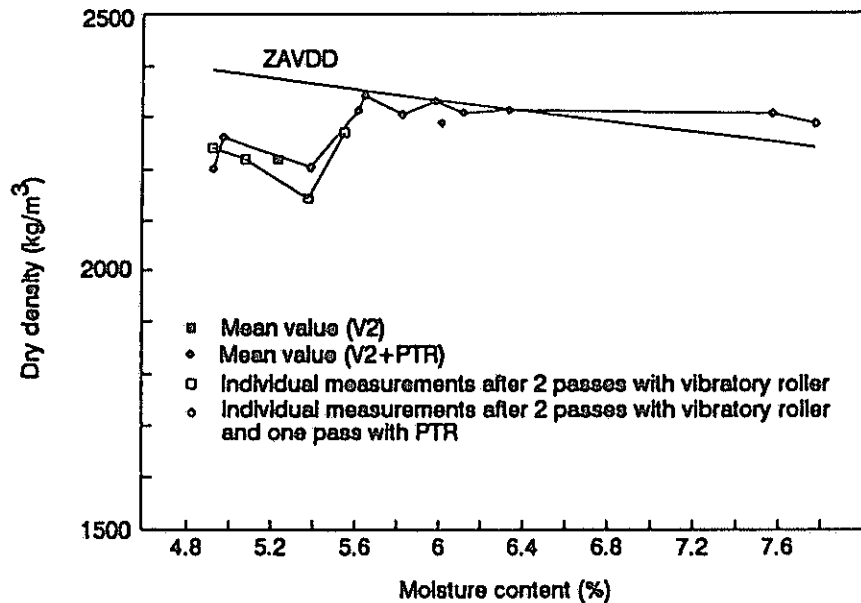


Figure 3.1: Measured dry densities against measured moisture contents for crushed stone base course on Section 1 (Site 2)(92/93) showing the effect of the moisture content on the dry density that can be achieved at the end of the compaction sequence

It has been proved in practice that unnecessary (excessive) rolling can actually lead to the unnecessary degradation of the material which, in turn, leads to a finer grading, higher void content, lower dry density and a higher required "optimum moisture content".

3.2 THE COMPACTIVE EFFORT APPLIED

It is gratifying to note that if the moisture content is correct, approximately the same amount of compactive effort is generally required to compact different roadbuilding materials optimally. This accords with the observation of the compactability study¹ where it was found that most materials were compacted optimally for the same amount of compactive effort on the vibratory compaction table.

In general the optimum amount of compactive effort is the following:

- (a) One half to one full pass with the vibratory roller (high amplitude/low frequency)
- (b) One half to one full pass with the vibratory roller (low amplitude/high frequency)
- (c) One to two full passes with pneumatic-tyred roller.

If the amount of compactive effort required is substantially greater, the moisture content is most probably either too high or too low.

The current practice of excessive use of the grid roller as well as the use of random rolling patterns do not serve any useful purpose either. Rather, this investigation showed that unnecessary rolling with the grid roller does not increase the in situ density at all. By determining the optimum moisture content (OMC) from the expected after-compaction grading, the Atterberg limits, linear shrinkage and the water absorption of the aggregate and controlling the OMC more accurately by means of a properly calibrated nuclear gauge or microwave oven, it is envisaged that most roadbuilding materials can be compacted to densities greater than the present specification requirements. The benefits include the following:

- Compaction production rate improves owing to effective control.
- Higher densities reduce the amount of "plastic" deformation (rutting) and increase the strength of the material, leading to improved pavement performance.

The only exception to the compaction procedure in normal layer work is probably the crushed stone base course layers (G1 and G2 at least) which still need to be slush-rolled to reach the required density level of 86 % SD (i.e. AD or DBD depending on the material) to 88 % SD. This should be done by static three-wheel rollers and pneumatic-tyred rollers.

3.3 THE LEVELLING OF THE LAYER

Although not conclusive, the compaction growth curves, particularly on Site 1, show that unnecessary re-levelling of the layer very often disturbs the layer to such an extent that the dry density after re-levelling virtually reverts to where it was after being levelled initially. Wherever possible the layer should therefore only be mixed and levelled once, as all unnecessary handling of materials leads to a substantial increase in the compactive effort without improving the quality of the layer.

3.4 THE DRY DENSITIES THAT CAN BE ACHIEVED

The investigation confirmed the finding of the earlier laboratory investigation that it is possible to compact most roadbuilding materials to greater dry densities than are specified by the present specifications. However, the increases are not necessarily the same for all classes of materials. The increase in the maximum dry density is also critically dependent on the scientific control of the moisture content for compaction purposes. Up till now this aspect has received very little attention and is ignored in most cases because of the general approach of Acceptance Control rather than Process Control. None of the sites used in this investigation controlled the moisture application in a scientific manner. The reason for this is twofold, namely:

- nuclear density/moisture gauges are generally not available for process control
- the oven drying test used for the determination of moisture content is not practical for process control because it can take up to 24 hours to dry the sample.

Although most contractors do their utmost to cut costs, in many cases the optimal rolling pattern is not determined by means of a test strip, as recommended. In general, the rolling continues until the layer is perceived to be dense or until the roller operators are instructed to stop which, in many cases, is at the end of the day.

3.5 PREDICTION OF REQUIRED MOISTURE CONTENT BY MEANS OF COMPACTABILITY SOFTWARE PACKAGE

Comparison of the results from the laboratory compaction of samples on the vibratory compaction table and the predicted MDD, OMC and ZAVMC values using the Compactability Software Package (see Section 2.9 of Report), show that very good predictions of the required moisture content can be made from the grading, Atterberg Limits, Linear Shrinkage and the ARD and BRD of +4.75 mm fraction and the ARD of the -4.75 mm fraction of the material. The fact that the

OMC does not have to be guesstimated but can be predicted reasonably accurately, should also assist in improving the compaction process in general and change the approach of compaction of untreated roadbuilding materials from an art to a science. This is extremely important, because many problems presently being experienced in this field can be directly related to the lack of understanding of the factors that influence the compactability of untreated roadbuilding materials. For example, in a recent case a contractor was required to achieve 88% AD with crushed stone irrespective of where the grading of the material fell within the present grading envelope. On site the contractor was only able to achieve 84.59 %AD on average. The Compactability Software Package predicted an average of 85.16 %AD for the material. No amount of extra compactive effort is going to improve the in situ density of this material to the required 88% AD. On the contrary, extra rolling will lead to a reduction in density owing to breakdown of the material under the rollers in this case. At the other end of the scale the mod.AASHTO test does not give the correct OMC (higher) or MDD (lower) for coarse granular materials for reasons given under 3.1. The lower MDD values will lead to lower compaction requirements and indirectly to reduced pavement performance because the material will compact further under traffic until it reaches the densest packing arrangement the grading of the material will allow.

Although this may entail an initial expenditure on the part of most contractors and consulting engineers as well as the road authorities the Compactability Software Package is user-friendly and is marketed at a very reasonable price. The cost of the investment is probably less than the cost of reworking of one section. Not only will unnecessary reworking be eliminated, but it can also assist in identifying the causes of compaction problems and therefore lead better decisions in overcoming the experienced problems. For example, in the previously mentioned example it could have been predicted from the start that the locally available crushed stone source does not produce material with which it is possible to achieve the generally specified 88 %AD. Alternative provisions should therefore have been made in the contract.

3.6

POSSIBLE RAPID METHODS FOR THE DETERMINATION OF THE OMC

At the request of one of the reviewers for a simple method to determine the OMC, the information of the original compactability investigation was re-evaluated. The information showed that $OMC(vib)$ was equal to 0.923 times $ZAVMC(vib)$ ($r^2 = 0.978$) for the 21 materials ranging from well-graded crushed stone to a black clay. Where the amount of voids in a well-compacted material is actually determined by the grading after compaction, which should then be filled with water at ZAVMC, the following two proposals are made:

(a) A sample of the material is saturated in a bowl or bucket, after the use of the grid roller (if required for adjusting the grading), whereafter the wet sample is sieved through a 4,75 mm sieve to get rid of the of the larger particles. Use is now made of a moisture saturation meter which is set to 100 % saturation in the fine portion of this sample. The moisture content on site can now be controlled by aiming for 92 % to 94 % saturation of the -4,75 mm fraction of the material in the section. Although this method has not been tried by the research team, independent work on a limited scale by Mr. B. Dumas of CPA Roads Department showed that the correct moisture content was between 93 % and 94 % of the saturation moisture content.

(b) The problem with the first method, however, is that the moisture content as a percentage by mass is not known. To enable the use of normal nuclear density/moisture content gauges for control purposes, a sample of the material is once again saturated in a bowl or bucket for a few minutes after which the sample is put on reasonably fine sieve (e.g 0,425 mm) to drain of the excess water. Once the excess water has been drained off the whole sample is rapidly dried to determine the ZAVMC as a percentage of the dry mass of the sample. The moisture content on site should then be in the order of 93 % to 94 % of this value.

As both methods have not yet been tried extensively the research team would preferably do further work on this for verification purposes as a new project.

4. RECOMMENDATIONS

Before adjusting the present compaction requirements it is necessary that an improved approach to compaction of roadbuilding materials in practice be established as a matter of urgency. It is extremely important that all road construction teams should approach the compaction of roadbuilding materials in the correct manner. This may require a shift away from acceptance control with greater emphasis being placed on process control. This would mean that the results of measured moisture contents on the material prior to compaction may have to be submitted in future as well. The specification should possibly read as follows:

" As the moisture content of the material has a critical influence on the compactability and bearing strength of the material, the compaction of roadbuilding materials using water as lubricant may only commence when the average value of 4 randomly measured moisture contents of the in-place material is within the range of $\pm 1,0$ % of the optimum moisture content (OMC) of the particular material, and all 4 the measured moisture contents fall in the range of $\pm 2,5$ % of OMC."

Although the amount of compactive effort required to compact roadbuilding materials optimally is fairly uniform, it is recommended that the practice of constructing a test strip form part of the standard specification. It should possibly be worded as follows:

"The optimal rolling pattern for each material, differing in quality or supply source, used on this project shall be determined by the construction of a test strip on the first section using the particular material source. The compaction of the test strip may only commence once the measured moisture content satisfies the criteria set out above. During the compaction of the test strip at least 4 half-minute density/moisture content readings for the full depth of the layer shall be taken on the layer with a nuclear density/moisture gauge after each half pass of each roller. The use of a particular roller type shall be discontinued as soon as the average of the measured results shows that there is little or no increase in the dry density after this roller half pass. Only one roller at a time will be allowed on the test strip and the specified roller sequence is as follows:

- grid roller for breakdown purposes only (try to get a well-graded material wherever possible)
- vibratory roller (high amplitude/low frequency)
- vibratory roller (low amplitude/high frequency)
- pneumatic-tyred roller
- pneumatic-tyred roller and three-wheel static roller for slush-rolling of crushed stone only

All the roller types listed shall be used in the recommended sequence and each roller shall be withdrawn as soon as the in situ measured dry densities do not increase any more or drop off slightly with a subsequent half-pass of the particular roller. This half-pass shall also be left out of the recommended compaction sequence. This is done to prevent unnecessary over-rolling which can lead to dedensification. The measured compaction growth curve shall be submitted to the Resident Engineer for record purposes. The final average measured dry density shall in no case be less than the present specification requirements. For all sections constructed from the same material the optimal rolling pattern shall be applied once the measured moisture contents are within the specified moisture content range. The measured moisture contents of each subsequent section shall also be submitted as proof of proper control of the moisture content for record purposes. After compaction the in situ dry density of each section completed shall still be determined for Acceptance Control and compared with the specification requirement. For layers compacted to the mod.AASHTO standard, the present mod.AASHTO standard shall be the required minimum standard acceptable."

This approach should then be followed in practice for at least two years to enable the collection of a wider amount of information on properly compacted layerwork. The measured dry densities and moisture contents of the acceptance control results, as well as the measured compaction growth curves and measured moisture contents of subsequent sections should be collected together with the indicator test results of each material (i.e. the full grading, Atterberg limits, Linear Shrinkage, ARD and BRD of the +4,75 mm fraction, and the ARD of the -4,75 mm fraction). The indicator test results can be used to predict the MDDs (vibratory and mod.AASHTO) and OMCs (vibratory and mod.AASHTO). These predicted values can be compared with the measured values. A comparison of the measured and predicted MDD and OMC results for the materials on a vast range of contracts will assist in confirming the material behaviour patterns as observed from the observations the compactability research in the laboratory on a limited number of materials and on site during this project. It can also be used to determine the probable cause of compaction problems, where experienced, and possibly even be used to quantify the expected amount of rutting. This can be compared later with the measured amount of rutting.

After the initial evaluation period of 2 years, a decision can be taken whether higher fixed density standards should be specified, or the approach in which the moisture content and compactive effort is properly controlled during construction should be followed or even a combination of the two approaches be used. It should be emphasized that specified standards should be practically achievable. For this reason it is also recommended that the BRD of the +4,75 mm material and the ARD of the -4,75 mm material be used to determine the Solid Density (SD) of crushed stone materials. It would be a great step forward if all compaction standards could be expressed in terms

of %SD, as it is not the dry density in kg/m^3 which determines the layers performance, but the percentage compaction in terms of %SD. As this information is already available from the indicator tests, the solid density of different materials can readily be calculated from the percentage passing the 4,75 mm sieve and the $\text{BRD}_{+4,75}$ and the $\text{ARD}_{.4,75}$ values. The higher the degree of compaction in terms of %SD the greater the strength of the layer. Higher density specifications are already being applied by some of the provincial road authorities in some layers, such as 97 % mod.AASHTO for granular subbase and 95 % mod.AASHTO for top of selected subgrade by the CPA.

Apart from this, it is recommended that serious consideration be given to the acceptance of a policy of proof-rolling of the roadbed, preferably with an impact roller. This will ensure that weak spots in the roadbed are picked up and rectified prior to the construction of the rest of the road structure. This is already done on DOT contracts.

Where many roads are presently being reconstructed, using the old pavement structure as part of the new structure, the policy of ripping and recompacting existing layers should seriously be reconsidered. Many of these layers have been optimally compacted by road traffic through years of service. In many cases the dry densities achieved after ripping and recompacting will be lower than in situ dry densities. Apart from a possible reduction in dry density any unnecessary handling of the material will usually cause a certain amount of degradation of the material, which in turn reduces the MDD that can be achieved. Lower MDDs, in turn, cause lower bearing capacities. Therefore, instead of improving the quality of the road by ripping and recompacting, the quality is actually reduced. The policy of ripping and recompacting should only be used in cases where definite weakness in the in situ structure have been identified.

Where the laboratory investigation into the compactability of untreated roadbuilding materials showed that the moisture regime is totally dependent on the grading of the material, the homogeneity of the material composition in each layer on each section is important. Because the investigation also showed the critical importance of the correct moisture content, the length of each construction section should be determined by the ability of the water application system to get the material to the correct moisture content in a reasonable time rather than on a standard length. This will avoid situations occurring where the OMC is never reached because of evaporation as well as having to compact lime- or cement-stabilized layers below OMC.

Because of the critical influence of the material grading on both the MDD and moisture regime, serious consideration should also be given to the replacement of the mod.AASHTO compaction test

with a test where the material is compacted in a single layer without disturbing the grading (e.g. the vibratory compaction table).

5. **REFERENCES**

1. Semmelink, C J. An index for describing the compactability of untreated roadbuilding materials. DPVT-141, CSIR, April 1990.
2. Shackleton, M C. Permanent deformation in pavements with granular bases and subbases. Draft Contract Report DPVT/C 164.1, CSIR, July 1990.
3. Semmelink, C J. The fine aggregate characteristics of crushed stone bases. Department of Transport, Pretoria, Project Report PR92/471, October 1993.

APPENDIX A

**ORIGINAL PROPOSED TECHNIQUE FOR THE CONSTRUCTION OF THE TEST STRIP FOR
THE OPTIMIZATION OF DENSITY STANDARDS
AND
COMPACTION TECHNIQUES
AND
ADDITIONAL RECOMMENDATIONS FOR DUAL-AMPLITUDE VIBRATORY ROLLERS**

PROPOSED TECHNIQUE FOR THE CONSTRUCTION OF THE TEST STRIP FOR THE OPTIMIZATION OF DENSITY STANDARDS

1. The test strip must preferably be at least 50 m long. The aim is that each layer from the roadbed to the base should be compacted to "refusal density", that is to a point where the density does not want to go higher with the correct application of the normal compaction effort. This density may never be less than the specified density requirement.
2. Before any roller is brought onto the test strip, it must be assured that the material is uniform in quality, with a uniform moisture content and with a uniform layer thickness. The cutting and shaping of the layer should therefore be completed beforehand.

It should be noted that the OMC is very dependent on the compactive effort used and will vary from roller type to roller type. It should normally be determined by means of a test strip for every new material source and roller type used for initial compaction (i.e. low frequency/high amplitude, high frequency/low amplitude, or static).

3. Use only one roller at a time on the test strip and apply the compactive effort in a uniform manner (i.e. keep frequency, amplitude (for vibratory rollers) and rolling speed as constant as possible). The overlap of adjacent roller tracks should be kept to a minimum. (See document "Compactions Techniques").
4. In the case of vibratory rollers always make sure that the drum turns in the same direction as the eccentric moment of vibratory force.
5. The following sequence of roller application is recommended for the test strip (if the equipment is available or necessary):
 - (a) Grid roller in the shaping stage to crush oversize material if required.
 - (b) Vibratory roller: low frequency/high amplitude (until the density growth curve flattens off); or
vibratory roller: high frequency/low amplitude (until the density growth curve flattens off);
or
static three point roller (until the density growth curve flattens off).

- (c) Pneumatic-tyred roller (until the density growth curve flattens off again). Ensure that the tyre pressure is correct and that roller is properly ballasted.

For general layer work compaction, the low frequency/high amplitude vibratory roller is recommended for the initial compaction. The only exception is the compaction of crushed stone bases where the use of the low frequency/high amplitude combination is recommended for the breakdown pass. Follow up using the high frequency/low amplitude combination. The static three point roller is not generally used for initial compaction any more; it may be used, but is less effective. It is very useful for the slushing process of crushed stone bases. Tamping-foot rollers should be used for layers of cohesive materials and smooth drum rollers for layers of non-cohesive materials, as well as the final pavement layers.

6. To plot the density growth curve, the density must be measured at the same spot (in the same probe hole) after each half or full roller pass. The dry density should be plotted against roller pass to get the compaction growth curve. As soon as two subsequent readings with the same roller application shows no increase in density or the density is even slightly reduced, the next roller type recommended under point (5) should be brought on.
7. Preferably the density should be measured at four to five randomly selected sampling positions. The density and moisture counts need not be longer than half a minute.
8. When the density growth curve shows that refusal density has been reached, the rolling should be stopped. The density can now be determined more accurately at four other randomly selected sampling positions. Take one minute counts.
9. Take a small sample for the determination of the moisture content by means of oven drying at each of these points as well as a larger sample of at least two kg at one of these positions to determine the grading after compaction. Send the results only.
10. A bag of ± 50 kg of material from each layer should also be sent to TRANSPORTEK for evaluation of the compactability on the vibratory table. The MDD(vib), OMC(vib), BRD and ARD will be determined.
11. If static three point rollers are used, the layer thickness should be adjusted for this roller type (i.e. thinner layers).

12. Apply the recommendations for the correct application of different rollers listed in the document "Compaction Techniques".
13. Note the roller type for each roller pass on the density growth curve.
14. Density results from a number of sections which were constructed according to the normal specification, must also be included for comparative purposes. It would be appreciated if the normal rolling pattern is also mentioned to assist with the comparison of the compaction effort and cost.

The values of the indicator tests for each layer should also be supplied (i.e. the grading, Atterberg Limits, and linear shrinkage).

15. Please send the results to:

TRANSPORTEK (Attention: C J Semmelink)

CSIR

P O Box 395

PRETORIA

0001

COMPACTION TECHNIQUES

For most of the compaction of roadbuilding materials (especially the actual pavement structure) vibratory rollers, grid rollers or pneumatic-tyred rollers are used. For the proper densification of every layer, it is absolutely essential to ensure that each of these rollers are applied for the right purpose, at the right time and in the right manner. It is, therefore, essential that the engineer, foreman, roller operators, laboratory technician and mechanic should all know the important aspects of compaction and to what to give attention.

The work should always be done scrupulously according to fixed rules. Most problems with compaction are the result of arbitrary and uncontrolled action. It should be emphasized that success with compaction will not be achieved unless the approach to the building of the layer is purposeful right from the beginning when the material is brought in: the material should be uniform in composition and the moisture content at the correct value and uniformly mixed over the whole width and depth of the layer, prior to the rolling of the layer.

To ensure that the material used is as uniform as possible, the material should preferably come from one source only. Even when one source is used, checks should be run continuously to ensure that the material composition basically remains the same. Any noteworthy changes of any of the indicator test values (i.e. grading, Atterberg limits, or linear shrinkage) point to the fact that the material has changed. As soon as this happens, new values for the MDD and OMC have to be determined, and a test strip must be built with the material to determine the optimum rolling pattern for the densification of the material. This rolling pattern is then used as long as the material basically remains the same. This approach ensures that compaction is done systematically and leads to greater efficiency and productivity.

APPLICATION OF ROLLERS

As far the application of rollers is concerned, attention should be paid to the following aspects:

- (1) Only one roller should be used at a particular time to ensure that the same amount of compaction effort is applied at each point. If, for some reason, it is essential to speed up the work, only an exactly identical roller, which has been similarly adjusted, may be used. (It must also be applied in an identical manner.)
- (2) The rollers must travel at a constant speed over the whole section to ensure that the same amount of compaction effort is applied everywhere. Speed should therefore be positively controlled.
- (3) The sequence in which rollers are used must also be the same everywhere as this pattern also affects the final result.

- (4) Each rollers track must be covered by a "forward and backward" pass of the roller. (This is regarded as a single roller pass.) If rollers cover tracks continuously in one direction only, cracks and fissures may form in the layer. This phenomenon is particularly noticeable with vibratory rollers and impact rollers.
- (5) The overlap of adjacent roller tracks should be limited to an absolute minimum, preferably 100 mm or less. The old rule of 50 % overlap only applies to the old three point rollers of which only the large back wheels really compact, while the smaller wheel at the front is essentially there for steering purposes.
- (6) In the case of vibratory rollers, the direction of rotation of the eccentric moment also plays a very important part. For effective compaction the direction of rotation of the roll should the same as that of the eccentric moment. If the direction of rotation of the roll is opposite to the direction of rotation of the eccentric moment, the layer may actually dedensify (the density of layer is lowered). With the "breakdown pass" this aspect is less critical, because the roller sinks a fair distance into the layer. But for all consecutive passes this phenomenon has a tremendous effect on the densification of material. If this aspect is ignored, it could even mean that double the number of roller passes could be required to achieve the required result. This aspect is particularly critical with non-drum-drive rollers. In the case of drum-drive rollers this is less critical, but even in their case they are still less effective in this mode than when the roller is applied correctly.
- (7) Where vibratory rollers are used, one should always start with the high amplitude/low frequency combination to achieve "in-depth" compaction. If the low amplitude/high frequency combination is used first, a crust is formed on the surface which impedes "in-depth" compaction. For the same reason it is essential that only one amplitude/frequency combination be used at one time. Where dual amplitude rollers are used, the difference in amplitude is usually obtained by changing the direction of rotation of the eccentric moment. In the light of what has been stated in point (6) about the effect of the direction of application, some contractors use the high amplitude/low frequency combination in the one direction and the low amplitude/high frequency combination in the opposite direction. This approach is detrimental for effective compaction because of the formation of a crust. If the direction of rotation of the eccentric moment changes automatically with the direction of travel of the roller, one should make sure that the amplitude and frequency are the same in both directions.
- (8) The effective frequency range of all vibratory rollers falls in a very narrow frequency range which is dependent on the size of the eccentric moment and the sprung and unsprung mass on the roll. To determine the effective frequency range it is essential to have the correct values of the eccentric

moment and the sprung and unsprung mass on the roll. With dual-amplitude rollers it is essential to have the correct values for both eccentric moments, as there will be an effective frequency range for each of these amplitudes at which the roller will perform optimally.

The highest efficiency of a vibratory roller is achieved when the centrifugal or dynamic force is equal to 3,1 to 3,2 times the static load on the drum.

$$\text{Centrifugal or dynamic force} = (m.r).4\pi^2.f^2$$

where $m.r$ = eccentric moment (kg-m)
 f = vibration frequency (Hz)

$$\text{Maximum effective dynamic force} = k.M_1.g$$

where k = constant (= 3,2 to 3,2)
 M_1 = static load on drum (spring and unsprung mass) (kg)
 g = speed of gravity (= 9,81 m/s²)

$$\therefore f = \sqrt{(k.M_1.g)/(m.r.4.\Pi^2)}$$

As the radius of the eccentric moment changes between high and low amplitude, the effective frequency range of the roller also changes. Because the efficiency of the roller is severely influenced by the correct frequency, it is absolutely essential that a frequency meter or a revolution meter be fitted to every vibratory roller to ensure optimal performance. Apart from the disadvantages of varying amplitude during one roller pass mentioned in point (7), a further disadvantage is added to the list in that the roller operator must keep track of the correct frequency for the particular amplitude being used. It should be abundantly clear that all these variables are open to human error, for example the wrong frequency at the wrong time, which will detrimentally affect the density results. Therefore, it is strongly recommended that only one amplitude/frequency combination be used at a time during a roller pass on a section.

- (9) It is regularly found in practice that vibratory rollers are not properly balanced. The result of this is that the amplitudes on the two sides of the roll differ. This leads to varying densities (greater variability). To ensure more uniform results it is essential that the roll of every vibratory roller be checked to see that they are properly balanced. To do this the following procedure is recommended (for both drum-drive and non-drum-drive rollers):

- (a) Determine the number isolation mountings on each side of the roll.

- (b) If there is a difference in the number of isolation mountings, extra mountings should be added to the side with the least number of mountings, until both sides have an equal number of isolation mountings. This may require that the mounting plates be modified. The isolation mountings should also be checked regularly to ensure that they are not stretched.
- (c) Determine the static contact load with the soil on both sides of the roll on a level surface. The difference may amount to several hundred kilograms.
- (d) If there is a difference in load, an extra mass should be added to the lighter side of the drum to equalise the loads. This extra mass is uniformly distributed on the side of the drum in the circle segments of the plate which are welded in position.
- (e) Determine the optimum frequency range for the new contact load of the roll, and set the engine, vibration pump, and motor to deliver that frequency.
- (f) In the event of the vibrator eccentric housings having been off-set in the drum, i.e. the one eccentric housing mounting plate having been positioned deeper in the drum than the other (to accommodate the drum drive transmission and hydraulic motor), additional balancing will be required. The greater the eccentrics are off-set, the greater the amplitude difference across the width of the drum.

By systematically welding additional steel segments to that side of the drum which is recording the higher amplitude (i.e. the side which has the eccentric housing closer to the drum end) the amplitude can be equalised.

Additional weight should be added, until the compactor can be driven straight on a flat, firm surface without having to use the steering to counter drum side drift, a condition that is created by unequal amplitude over the width of the drum module.

During the equalising exercise, all testing must be carried out with the eccentrics operating at optimum frequency.

ADDITIONAL RECOMMENDATIONS FOR DUAL-AMPLITUDE VIBRATORY ROLLERS

- (1) Under no circumstances should a dual-amplitude roller be operated by personnel who have not received special training in the correct functions and application of these rollers.
- (2) The maximum recommended speed for dual-amplitude rollers of 10 to 15 tonne is 5 km/h.
- (3) All rolling must be performed with the engine at full throttle and the vibration system at optimum frequency.
- (4) All rolling must be performed with drive system in the working range (low gear). If the rolling speed is too high, it causes a corrugated surface. When the rolling speed is too low, it reduces productivity.
- (5) All rolling should be done at a constant speed; this prevents unnecessary variation in density. To ensure this, an accurate speedometer should be standard instrumentation on all rollers. As an alternative; the speed control quadrant should be marked at the positions where desired and forward and reverse speed is achieved.
- (6) Because irregular densities are caused by variation in the rolling speed, under no circumstances should the vibratory system be activated until the desired or pre-determined rolling speed has been achieved. At the beginning of each section provision should therefore be made for an overlapping area with the previous section as well as an over-run area at the end of the section. These sections should be long enough for the roller to reach the correct rolling speed, so that the vibration mechanism can be activated at the right moment (at the beginning and the end). As soon as the roller reaches the "end" (the end of half a roller pass) or the "beginning" (at the end of a full roller pass), the vibration mechanism should be switched off so that very little extra energy is transferred to these overlap areas.
- (7) When compacting base course layers of well-graded non-cohesive material at optimum moisture content, it is recommended that the use of high amplitude be restricted to a single roller pass (forward and backward). The high total applied forces generated by these compactors in the high amplitude mode can have a damaging effect on the subbase layer, particularly if it is stabilized.
- (8) Dependent on conditions and the type of material to be compacted, the use of low amplitude will normally result in uniform density through to within approximately 40 mm of the layer surface. Static rolling is required to consolidate and densify this surface layer.

- (9) Do not operate the compactor in the high amplitude setting when in close proximity to tall building structures. It is advisable to do a proper "crack survey" of adjacent structures before actual rolling starts to prevent wrongful claims for damage.
- (10) Do not operate the compactor in the high amplitude setting when compacting soil or aggregate that has been thinly placed on a solid rock subbase. This situation is frequently encountered in cut and fill operations.
- (11) Do not use a "pad-foot" compactor on non-cohesive material. Do not attempt the compaction of deep lifts of high PI material with a smooth drum compactor.
- (12) Never leave the compactor without the park and emergency brake applied. This also applies to other roller types.
- (13) Never attempt to start the roller engine without checking to ensure that the park and emergency brakes are applied. This also applies to other roller types.
- (14) Make a thorough study of the contents of the service manual and maintain the machine in accordance with recommendations.
- (15) Do not attempt to compact badly placed fill, containing large stones or boulders.
- (16) When rockfill has to be compacted with a vibratory roller, a carpet of fine material should first be placed over the top of the rockfill prior to commencing compaction. Point loadings at high total applied force have a detrimental effect on both drum and machine. Compactors of less than 14 tonne are not recommended for use on the compaction of shot or dump rock. Heavy rollers with thicker drum shells (50 mm +) are recommended for this type of work, the compactor should be operated at rolling speeds below 2 km/h. The maximum particle size of the rock must not exceed 66 % of the minimum layer thickness. The life expectancy of vibratory compactors, used on this type of work, is considerably less than that of machines used on graded or low shear strength materials. Preventative and scheduled maintenance services must be increased when operating under these conditions.
- (17) When checks or adjustments are to be made to the vibratory system, two large tyres should be placed under the drum. By supporting the drum in this manner, the forces generated by the vibratory system are largely neutralised.

- (18) Regularly check the density of the layer with a nuclear gauge to prevent dedensification owing to over-rolling.

GRID ROLLERS

The main function of grid rollers is to break down the larger particles; because of its small contact area, it is not very efficient for the compaction of thick layers. Where thin layers are cut across, a grid roller may be used for part of this operation. In such a situation the roller must be applied consistently (fixed rolling speed and minimum overlap). To ensure optimal performance one should check that the roller is properly ballasted. As for other roller types, a roller pass is defined as a "forward and backward" pass in the same roller track.

PNEUMATIC-TYRED ROLLERS

Pneumatic-tyred rollers are mainly used to compact the thin loose surface layer at the top of a layer. To ensure that it works effectively, one should check that the roller is properly ballasted and that the tyre pressure is correct and uniform. Apart from this the roller must be applied consistently (fixed rolling speed and minimum overlap).

As for other roller types, a roller pass is defined as a "forward and backward" pass in the same roller track.

IF YOU DON'T KNOW, FIND OUT - DON'T GUESS OR TAKE A CHANCE.

APPENDIX B

**PREDICTION RESULTS OF COMPACTABILITY SOFTWARE PACKAGE
AND DRY DENSITY - MOISTURE CONTENT CURVES OF
VIBRATORY COMPACTION**

SAMPLE No. : S1FILL

DATE : 93-09-27

DESCRIPTION : Fill (Section 1 CH21600-22200)

REMARK :

INPUT INFORMATION

MATERIAL TYPE 2

GRADING Metric Units		ATTEBERG LIMITS (Casagrande Apparatus)		
SIEVE (mm)	% PASSING	L.L.	P.I.	L.S.
75	100,00	25,97	5,48	3,98
63	100,00	DENSITY AND SHAPE INFORMATION		
53	100,00			
37,5	100,00	ARD (+4,75)	ARD (-4,75)	S B D
26,5	97,03	2,739	2,766	0,00
19,0	96,51	BRD (+4,75)	BRD (-4,75)	W F D
13,2	94,27	2,439	2,766	0,00
4,75	82,41			
2,00	68,15			
0,425	52,95			
0,075	24,98			

OUTPUT PREDICTIONS

MDD in kg/cub. metre

M D D (VIB)	O M C (VIB)	ZAVMC (VIB)	WA	C M C
2094,21	10,58	11,00 - 11,62	0,790	8,405
MDD Mod AASHTO	OMC Mod AASHTO	ZAVMC Mod.	WA	R S D
2054,86	10,52	12,63 - 12,53	0,790	2,708

C B R NOT PREDICTED WITHOUT "SBD" AND "WFD"

SAMPLE No. : S1SL1

DATE : 93-09-27

DESCRIPTION : Selected layer 1 (lower) (Section 1 CH21600-22200)

REMARK :

INPUT INFORMATION

MATERIAL TYPE 2

GRADING Metric Units		ATTERBERG LIMITS (Casagrande Apparatus)		
SIEVE (mm)	% PASSING	L.L.	P.I.	L.S.
75	100,00	28,37	4,11	4,71
63	100,00	DENSITY AND SHAPE INFORMATION		
53	100,00			
37,5	93,17	ARD (+4,75)	ARD (-4,75)	S B D
26,5	80,14	2,772	2,789	0,00
19,0	65,03	BRD (+4,75)	BRD (-4,75)	W F D
13,2	54,30	2,160	2,789	0,00
4,75	38,72			
2,00	31,20			
0,425	24,64			
0,075	18,93			

OUTPUT PREDICTIONS

MDD in kg/cub. metre

M D D (VIB)	O M C (VIB)	ZAVMC (VIB)	WA	C M C
2083,28	10,99	11,27 - 12,66	6,264	10,468
MDD Mod AASHTO	OMC Mod AASHTO	ZAVMC Mod.	WA	R S D
1989,55	12,56	13,37 - 14,92	6,264	2,404

C B R NOT PREDICTED WITHOUT "SBD" AND "WFD"

SAMPLE No. : S1SL2

DATE : 93-09-27

DESCRIPTION : Selected layer 2 (upper) (Section 1 CH21600-22200)

REMARK :

INPUT INFORMATION

MATERIAL TYPE 2

GRADING Metric Units		ATTERBERG LIMITS (Casagrande Apparatus)		
SIEVE (mm)	% PASSING	L.L.	P.I.	L.S.
75	100,00	26,13	5,19	4,01
63	100,00	DENSITY AND SHAPE INFORMATION		
53	100,00			
37,5	90,60	ARD (+4,75)	ARD (-4,75)	S B D
26,5	84,65	2,795	2,778	0,00
19,0	73,10	BRD (+4,75)	BRD (-4,75)	W F D
13,2	67,71	2,179	2,778	0,00
4,75	51,29			
2,00	40,29			
0,425	30,53			
0,075	19,00			

OUTPUT PREDICTIONS

MDD in kg/cub. metre

M D D (VIB)	O M C (VIB)	ZAVMC (VIB)	WA	C M C
2092,94	10,98	11,24 - 12,48	4,927	10,058
MDD Mod AASHTO	OMC Mod AASHTO	ZAVMC Mod.	WA	R S D
2013,69	11,92	13,24 - 14,37	4,927	2,486

C B R NOT PREDICTED WITHOUT "SBD" AND "WFD"

SAMPLE No. : S1SB1

DATE : 93-09-27

DESCRIPTION : Subbase 1 (lower) (Section 1 CH21600-22200)

REMARK :

INPUT INFORMATION

MATERIAL TYPE 2

GRADING Metric Units		ATTEBERG LIMITS (Casagrande Apparatus)		
SIEVE (mm)	% PASSING	L.L.	P.I.	L.S.
75	100,00	22,84	0,00	3,05
63	100,00	DENSITY AND SHAPE INFORMATION		
53	100,00			
37,5	84,84	ARD (+4,75)	ARD (-4,75)	S B D
26,5	80,69	2,680	2,681	0,00
19,0	67,53	BRD (+4,75)	BRD (-4,75)	W F D
13,2	57,93	2,550	2,681	0,00
4,75	43,55			
2,00	36,92			
0,425	27,38			
0,075	8,94			

OUTPUT PREDICTIONS

MDD in kg/cub. metre

M D D (VIB)	O M C (VIB)	ZAVMC (VIB)	WA	C M C
2253,69	5,80	6,20 - 7,09	1,074	5,392
MDD Mod AASHTO	OMC Mod AASHTO	ZAVMC Mod.	WA	R S D
2151,13	7,28	8,32 - 9,20	1,074	2,607

C B R NOT PREDICTED WITHOUT "SBD" AND "WFD"

SAMPLE No. : S1SB2

DATE : 93-09-27

DESCRIPTION : Subbase 2 (upper) (Section 1 CH21600-22200)

REMARK :

INPUT INFORMATION

MATERIAL TYPE 2

GRADING Metric Units		ATTERBERG LIMITS (Casagrande Apparatus)		
SIEVE (mm)	% PASSING	L.L.	P.I.	L.S.
75	100,00	16,58	0,00	1,52
63	100,00	DENSITY AND SHAPE INFORMATION		
53	100,00			
37,5	86,97	ARD (+4,75)	ARD (-4,75)	S B D
26,5	76,74	2,687	2,681	0,00
19,0	71,69	BRD (+4,75)	BRD (-4,75)	W F D
13,2	63,82	2,579	2,681	0,00
4,75	52,84			
2,00	48,55			
0,425	40,97			
0,075	13,41			

OUTPUT PREDICTIONS

MDD in kg/cub. metre

M D D (VIB)	O M C (VIB)	ZAVMC (VIB)	WA	C M C
2260,38	5,75	6,05 - 6,99	0,735	5,449
MDD Mod AASHTO	OMC Mod AASHTO	ZAVMC Mod.	WA	R S D
2164,08	7,13	8,10 - 8,96	0,735	2,633

C B R NOT PREDICTED WITHOUT "SBD" AND "WFD"

SAMPLE No. : S1Base

DATE : 93-09-27

DESCRIPTION : Base (Section 1 CH21600-22200)

REMARK :

INPUT INFORMATION

MATERIAL TYPE 2

GRADING Metric Units		ATTERBERG LIMITS (Casagrande Apparatus)		
SIEVE (mm)	% PASSING	L.L.	P.I.	L.S.
75	100,00	0,00	0,00	0,00
63	100,00	DENSITY AND SHAPE INFORMATION		
53	100,00			
37,5	100,00	ARD (+4,75)	ARD (-4,75)	S B D
26,5	91,68	2,775	2,778	0,00
19,0	66,57	BRD (+4,75)	BRD (-4,75)	W F D
13,2	54,69	2,687	2,778	0,00
4,75	36,34			
2,00	24,34			
0,425	16,69			
0,075	7,96			

OUTPUT PREDICTIONS

MDD in kg/cub. metre

M D D (VIB)	O M C (VIB)	ZAVMC (VIB)	WA	C M C
2414,67	4,65	5,68 - 5,40	0,751	3,614
MDD Mod AASHTO	OMC Mod AASHTO	ZAVMC Mod.	WA	R S D
2245,86	5,82	8,03 - 8,51	0,751	2,720

C B R NOT PREDICTED WITHOUT "SBD" AND "WFD"

SAMPLE No. : S2SL1

DATE : 93-09-27

DESCRIPTION : Selected layer 1 (lower) (Section 2 CH27900-28500)

REMARK :

INPUT INFORMATION

MATERIAL TYPE 2

GRADING Metric Units		ATTERBERG LIMITS (Casagrande Apparatus)		
SIEVE (mm)	% PASSING	L.L.	P.I.	L.S.
75	100,00	26,67	6,13	2,58
63	100,00	DENSITY AND SHAPE INFORMATION		
53	100,00			
37,5	100,00	ARD (+4,75)	ARD (-4,75)	S B D
26,5	97,29	2,752	2,717	0,00
19,0	95,61	BRD (+4,75)	BRD (-4,75)	W F D
13,2	92,14	2,236	2,717	0,00
4,75	79,60			
2,00	64,49			
0,425	46,66			
0,075	30,00			

OUTPUT PREDICTIONS

MDD in kg/cub. metre

M D D (VIB)	O M C (VIB)	ZAVMC (VIB)	WA	C M C
2083,07	10,00	10,64 - 11,53	1,711	8,562
MDD Mod AASHTO	OMC Mod AASHTO	ZAVMC Mod.	WA	R S D
2026,34	10,50	12,45 - 12,88	1,711	2,619

C B R NOT PREDICTED WITHOUT "SBD" AND "WFD"

SAMPLE No. : S2SL2

DATE : 93-09-27

DESCRIPTION : Selected layer 2 (upper) (Section 2 CH27900-28500)

REMARK :

INPUT INFORMATION

MATERIAL TYPE 2

GRADING Metric Units		ATTERBERG LIMITS (Casagrande Apparatus)		
SIEVE (mm)	% PASSING	L.L.	P.I.	L.S.
75	100,00	28,78	6,05	4,15
63	100,00	DENSITY AND SHAPE INFORMATION		
53	100,00			
37,5	84,65	ARD (+4,75)	ARD (-4,75)	S B D
26,5	75,24	2,758	2,740	0,00
19,0	66,90	BRD (+4,75)	BRD (-4,75)	W F D
13,2	54,63	2,499	2,740	0,00
4,75	35,10			
2,00	26,84			
0,425	17,18			
0,075	11,25			

OUTPUT PREDICTIONS

MDD in kg/cub. metre

M D D (VIB)	O M C (VIB)	ZAVMC (VIB)	WA	C M C
2281,21	6,37	6,81 - 7,57	2,439	5,933
MDD Mod AASHTO	OMC Mod AASHTO	ZAVMC Mod.	WA	R S D
2157,90	8,00	9,02 - 10,07	2,439	2,584

C B R NOT PREDICTED WITHOUT "SBD" AND "WFD"

SAMPLE No. : S2SB1

DATE : 93-09-27

DESCRIPTION : Subbase 1 (lower) (Section 2 CH27900-28500)

REMARK :

INPUT INFORMATION

MATERIAL TYPE 2

GRADING Metric Units		ATTERBERG LIMITS (Casagrande Apparatus)		
SIEVE (mm)	% PASSING	L.L.	P.I.	L.S.
75	100,00	36,78	0,00	7,44
63	100,00			
53	100,00	DENSITY AND SHAPE INFORMATION		
37,5	92,93	ARD (+4,75)	ARD (-4,75)	S B D
26,5	81,05	2,766	2,849	0,00
19,0	69,32	BRD (+4,75)	BRD (-4,75)	W F D
13,2	52,75	2,585	2,849	0,00
4,75	27,80			
2,00	18,81			
0,425	8,64			
0,075	5,12			

OUTPUT PREDICTIONS

MDD in kg/cub. metre

M D D (VIB)	O M C (VIB)	ZAVMC (VIB)	WA	C M C
2380,23	5,26	5,82 - 6,22	1,828	4,700
MDD Mod AASHTO	OMC Mod AASHTO	ZAVMC Mod.	WA	R S D
2233,81	6,91	8,10 - 8,98	1,828	2,658

C B R NOT PREDICTED WITHOUT "SBD" AND "WFD"

SAMPLE No. : S2SB2

DATE : 93-09-27

DESCRIPTION : Subbase 2 (upper) (Section 2 CH27900-28500)

REMARK :

INPUT INFORMATION

MATERIAL TYPE 2

GRADING Metric Units		ATTERBERG LIMITS (Casagrande Apparatus)		
SIEVE (mm)	% PASSING	L.L.	P.I.	L.S.
75	100,00	36,82	0,00	7,44
63	100,00	DENSITY AND SHAPE INFORMATION		
53	100,00			
37,5	89,73	ARD (+4,75)	ARD (-4,75)	S B D
26,5	69,32	2,727	2,853	0,00
19,0	60,57	BRD (+4,75)	BRD (-4,75)	W F D
13,2	51,44	2,554	2,853	0,00
4,75	33,96			
2,00	26,16			
0,425	14,00			
0,075	7,52			

OUTPUT PREDICTIONS

MDD in kg/cub. metre

M D D (VIB)	O M C (VIB)	ZAVMC (VIB)	WA	C M C
2324,16	6,12	6,52 - 7,01	1,640	5,321
MDD Mod AASHTO	OMC Mod AASHTO	ZAVMC Mod.	WA	R S D
2201,81	7,50	8,70 - 9,40	1,640	2,656

C B R NOT PREDICTED WITHOUT "SBD" AND "WFD"

SAMPLE No. : S2BASE

DATE : 93-09-27

DESCRIPTION : Base (Section 2 CH 27900-28500)

REMARK :

INPUT INFORMATION

MATERIAL TYPE 2

GRADING Metric Units		ATTERBERG LIMITS (Casagrande Apparatus)		
SIEVE (mm)	% PASSING	L.L.	P.I.	L.S.
75	100,00	0,00	0,00	0,00
63	100,00	DENSITY AND SHAPE INFORMATION		
53	100,00			
37,5	100,00	ARD (+4,75)	ARD (-4,75)	S B D
26,5	90,88	2,794	2,740	0,00
19,0	74,85	BRD (+4,75)	BRD (-4,75)	W F D
13,2	55,38	2,725	2,740	0,00
4,75	33,55			
2,00	24,20			
0,425	16,87			
0,075	6,36			

OUTPUT PREDICTIONS

MDD in kg/cub. metre

M D D (VIB)	O M C (VIB)	ZAVMC (VIB)	WA	C M C
2425,43	4,46	5,49 - 5,20	0,602	3,442
MDD Mod AASHTO	OMC Mod AASHTO	ZAVMC Mod.	WA	R S D
2255,63	5,64	7,85 - 8,31	0,602	2,730

C B R NOT PREDICTED WITHOUT "SBD" AND "WFD"

SAMPLE No. : S3SL2

DATE : 93-09-27

DESCRIPTION : Selected layer 2 (upper) (Section 3 CH29300-29900)

REMARK :

INPUT INFORMATION

MATERIAL TYPE 2

GRADING Metric Units		ATTERBERG LIMITS (Casagrande Apparatus)		
SIEVE (mm)	% PASSING	L.L.	P.I.	L.S.
75	100,00	24,80	4,45	3,70
63	100,00	DENSITY AND SHAPE INFORMATION		
53	100,00			
37,5	91,92	ARD (+4,75)	ARD (-4,75)	S B D
26,5	85,67	2,811	2,894	0,00
19,0	75,71	BRD (+4,75)	BRD (-4,75)	W F D
13,2	66,87	2,468	2,894	0,00
4,75	51,38			
2,00	40,74			
0,425	21,42			
0,075	13,47			

OUTPUT PREDICTIONS

MDD in kg/cub. metre

M D D (VIB)	O M C (VIB)	ZAVMC (VIB)	WA	C M C
2263,02	8,52	9,00 - 9,37	2,404	7,317
MDD Mod AASHTO	OMC Mod AASHTO	ZAVMC Mod.	WA	R S D
2162,36	9,20	11,09 - 11,43	2,404	2,687

C B R NOT PREDICTED WITHOUT "SBD" AND "WFD"

SAMPLE No. : S3SB2

DATE : 93-09-27

DESCRIPTION : Subbase 2 (upper) (Section 3 CH29300-29900)

REMARK :

INPUT INFORMATION

MATERIAL TYPE 2

GRADING Metric Units		ATTERBERG LIMITS (Casagrande Apparatus)		
SIEVE (mm)	% PASSING	L.L.	P.I.	L.S.
75	100,00	49,75	0,00	11,34
63	100,00	DENSITY AND SHAPE INFORMATION		
53	100,00			
37,5	92,97	ARD (+4,75)	ARD (-4,75)	S B D
26,5	83,05	2,759	2,685	0,00
19,0	65,52	BRD (+4,75)	BRD (-4,75)	W F D
13,2	52,83	2,504	2,685	0,00
4,75	34,75			
2,00	25,29			
0,425	11,03			
0,075	5,76			

OUTPUT PREDICTIONS

MDD in kg/cub. metre

M D D (VIB)	O M C (VIB)	ZAVMC (VIB)	WA	C M C
2218,44	7,70	8,01 - 8,53	2,408	6,379
MDD Mod AASHTO	OMC Mod AASHTO	ZAVMC Mod.	WA	R S D
2104,51	8,58	10,15 - 10,97	2,408	2,567

C B R NOT PREDICTED WITHOUT "SBD" AND "WFD"

SAMPLE No. : S3Base

DATE : 93-09-27

DESCRIPTION : Base (Section 3 CH29300-29900)

REMARK :

INPUT INFORMATION

MATERIAL TYPE 2

GRADING Metric Units		ATTERBERG LIMITS (Casagrande Apparatus)		
SIEVE (mm)	% PASSING	L.L.	P.I.	L.S.
75	100,00	0,00	0,00	0,00
63	100,00	DENSITY AND SHAPE INFORMATION		
53	100,00			
37,5	100,00	ARD (+4,75)	ARD (-4,75)	S B D
26,5	90,88	2,794	2,740	0,00
19,0	74,85	BRD (+4,75)	BRD (-4,75)	W F D
13,2	55,38	2,725	2,740	0,00
4,75	33,55			
2,00	24,20			
0,425	16,87			
0,075	6,36			

OUTPUT PREDICTIONS

MDD in kg/cub. metre

M D D (VIB)	O M C (VIB)	ZAVMC (VIB)	WA	C M C
2425,43	4,46	5,49 - 5,20	0,602	3,442
MDD Mod AASHTO	OMC Mod AASHTO	ZAVMC Mod.	WA	R S D
2255,63	5,64	7,85 - 8,31	0,602	2,730

C B R NOT PREDICTED WITHOUT "SBD" AND "WFD"

SAMPLE No. : S4SL1

DATE : 93-09-27

DESCRIPTION : Selected layer 1 (lower) (Section 4 CH17300-17600)

REMARK :

INPUT INFORMATION

MATERIAL TYPE 2

GRADING Metric Units		ATTERBERG LIMITS (Casagrande Apparatus)		
SIEVE (mm)	% PASSING	L.L.	P.I.	L.S.
75	100,00	27,68	5,16	3,77
63	100,00	DENSITY AND SHAPE INFORMATION		
53	100,00			
37,5	81,76	ARD (+4,75)	ARD (-4,75)	S B D
26,5	66,36	2,743	2,759	0,00
19,0	61,69	BRD (+4,75)	BRD (-4,75)	W F D
13,2	56,69	2,393	2,759	0,00
4,75	47,60			
2,00	41,22			
0,425	35,20			
0,075	24,89			

OUTPUT PREDICTIONS

MDD in kg/cub. metre

M D D (VIB)	O M C (VIB)	ZAVMC (VIB)	WA	C M C
2193,40	8,01	8,27 - 9,43	2,794	7,603
MDD Mod AASHTO	OMC Mod AASHTO	ZAVMC Mod.	WA	R S D
2109,31	9,62	10,28 - 11,25	2,794	2,567

C B R NOT PREDICTED WITHOUT "SBD" AND "WFD"

SAMPLE No. : S4SL2

DATE : 93-09-27

DESCRIPTION : Selected layer 2 (upper) (Section 4 CH17300-17600)

REMARK :

INPUT INFORMATION

MATERIAL TYPE 2

GRADING Metric Units		ATTERBERG LIMITS (Casagrande Apparatus)		
SIEVE (mm)	% PASSING	L.L.	P.I.	L.S.
75	100,00	17,31	1,64	1,35
63	100,00	DENSITY AND SHAPE INFORMATION		
53	100,00			
37,5	96,28	ARD (+4,75)	ARD (-4,75)	S B D
26,5	92,15	2,940	2,692	0,00
19,0	91,19	BRD (+4,75)	BRD (-4,75)	W F D
13,2	87,82	2,423	2,692	0,00
4,75	75,70			
2,00	59,56			
0,425	45,77			
0,075	21,73			

OUTPUT PREDICTIONS

MDD in kg/cub. metre

M D D (VIB)	O M C (VIB)	ZAVMC (VIB)	WA	C M C
2155,05	8,53	9,30 - 10,09	1,764	7,766
MDD Mod AASHTO	OMC Mod AASHTO	ZAVMC Mod.	WA	R S D
2078,54	9,50	11,23 - 11,80	1,764	2,627

C B R NOT PREDICTED WITHOUT "SBD" AND "WFD"

SAMPLE No. : S4SB1

DATE : 93-09-27

DESCRIPTION : Subbase 1 (lower) (Section 4 CH17300-17600)

REMARK :

INPUT INFORMATION

MATERIAL TYPE 2

GRADING Metric Units		ATTERBERG LIMITS (Casagrande Apparatus)		
SIEVE (mm)	% PASSING	L.L.	P.I.	L.S.
75	100,00	30,18	4,50	5,28
63	100,00	DENSITY AND SHAPE INFORMATION		
53	100,00			
37,5	92,92	ARD (+4,75)	ARD (-4,75)	S B D
26,5	91,60	2,886	2,894	0,00
19,0	85,40	BRD (+4,75)	BRD (-4,75)	W F D
13,2	79,77	2,381	2,894	0,00
4,75	67,24			
2,00	57,95			
0,425	45,01			
0,075	32,79			

OUTPUT PREDICTIONS

MDD in kg/cub. metre

M D D (VIB)	O M C (VIB)	ZAVMC (VIB)	WA	C M C
2139,74	11,84	11,76 - 12,46	2,408	9,615
MDD Mod AASHTO	OMC Mod AASHTO	ZAVMC Mod.	WA	R S D
2102,37	11,53	13,44 - 13,29	2,408	2,726

C B R NOT PREDICTED WITHOUT "SBD" AND "WFD"

SAMPLE No. : S4SB2

DATE : 93-09-27

DESCRIPTION : Subbase 2 (upper) (Section 4 CH17300-17600)

REMARK :

INPUT INFORMATION

MATERIAL TYPE 2

GRADING Metric Units		ATTERBERG LIMITS (Casagrande Apparatus)		
SIEVE (mm)	% PASSING	L.L.	P.I.	L.S.
75	100,00	26,45	0,00	4,13
63	100,00	DENSITY AND SHAPE INFORMATION		
53	100,00			
37,5	100,00	ARD (+4,75)	ARD (-4,75)	S B D
26,5	97,83	3,103	2,833	0,00
19,0	94,88	BRD (+4,75)	BRD (-4,75)	W F D
13,2	87,87	2,543	2,833	0,00
4,75	69,49			
2,00	57,83			
0,425	39,66			
0,075	17,14			

OUTPUT PREDICTIONS

MDD in kg/cub. metre

M D D (VIB)	O M C (VIB)	ZAVMC (VIB)	WA	C M C
2167,91	11,17	11,33 - 11,86	2,165	9,135
MDD Mod AASHTO	OMC Mod AASHTO	ZAVMC Mod.	WA	R S D
2118,26	11,13	13,12 - 12,94	2,165	2,745

C B R NOT PREDICTED WITHOUT "SBD" AND "WFD"

SAMPLE No. : S4SB2

DATE : 93-09-27

DESCRIPTION : Subbase 2 (upper) (Section 4 CH17300-17600)

REMARK :

INPUT INFORMATION

MATERIAL TYPE 2

GRADING Metric Units		ATTERBERG LIMITS (Casagrande Apparatus)		
SIEVE (mm)	% PASSING	L.L.	P.I.	L.S.
75	100,00	26,45	0,00	4,13
63	100,00	DENSITY AND SHAPE INFORMATION		
53	100,00			
37,5	100,00	ARD (+4,75)	ARD (-4,75)	S B D
26,5	97,83	3,103	2,833	0,00
19,0	94,88	BRD (+4,75)	BRD (-4,75)	W F D
13,2	87,87	2,543	2,833	0,00
4,75	69,49			
2,00	57,83			
0,425	39,66			
0,075	17,14			

OUTPUT PREDICTIONS

MDD in kg/cub. metre

M D D (VIB)	O M C (VIB)	ZAVMC (VIB)	WA	C M C
2167,91	11,17	11,33 - 11,86	2,165	9,135
MDD Mod AASHTO	OMC Mod AASHTO	ZAVMC Mod.	WA	R S D
2118,26	11,13	13,12 - 12,94	2,165	2,745

C B R NOT PREDICTED WITHOUT "SBD" AND "WFD"

SAMPLE No. : S4Base

DATE : 93-09-27

DESCRIPTION : Base (Section 4 CH17300-17600)

REMARK :

INPUT INFORMATION

MATERIAL TYPE 2

GRADING Metric Units		ATTERBERG LIMITS (Casagrande Apparatus)		
SIEVE (mm)	% PASSING	L.L.	P.I.	L.S.
75	100,00	0,00	0,00	0,00
63	100,00	DENSITY AND SHAPE INFORMATION		
53	100,00			
37,5	100,00	ARD (+4,75)	ARD (-4,75)	S B D
26,5	87,42	2,739	2,721	0,00
19,0	66,36	BRD (+4,75)	BRD (-4,75)	W F D
13,2	58,20	2,727	2,721	0,00
4,75	38,99			
2,00	27,89			
0,425	15,52			
0,075	7,91			

OUTPUT PREDICTIONS

MDD in kg/cub. metre

M D D (VIB)	O M C (VIB)	ZAVMC (VIB)	WA	C M C
2395,63	4,38	5,52 - 5,14	0,098	3,237
MDD Mod AASHTO	OMC Mod AASHTO	ZAVMC Mod.	WA	R S D
2231,08	5,55	7,85 - 8,22	0,098	2,725

C B R NOT PREDICTED WITHOUT "SBD" AND "WFD"

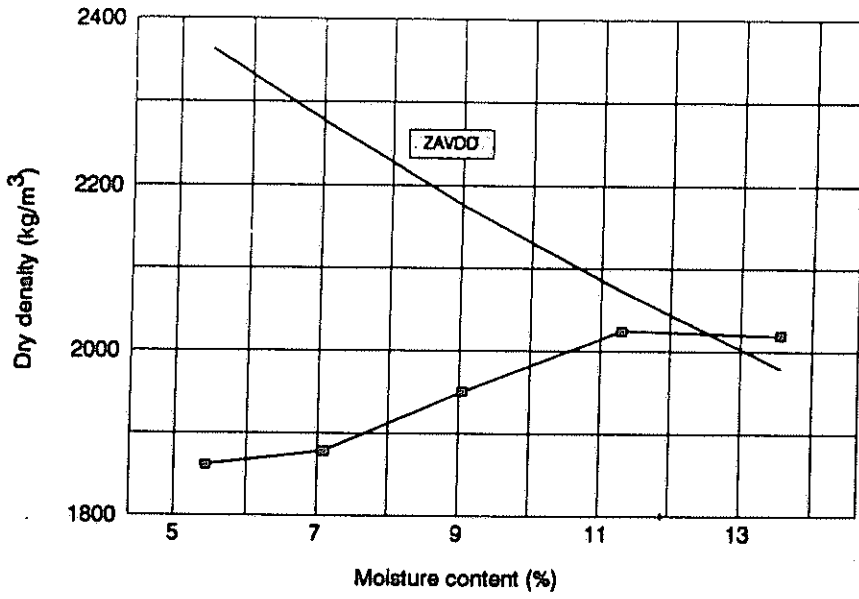


Figure B1: Dry density against moisture content after compaction on the vibratory compaction table for fill on Section 1

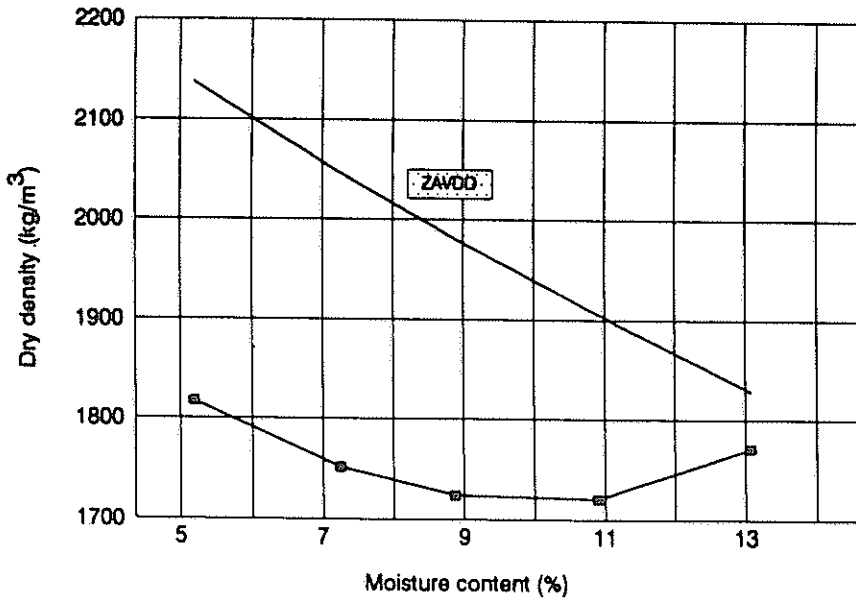


Figure B2: Dry density against moisture content after compaction on the vibratory compaction table for lower selected layer on Section 1

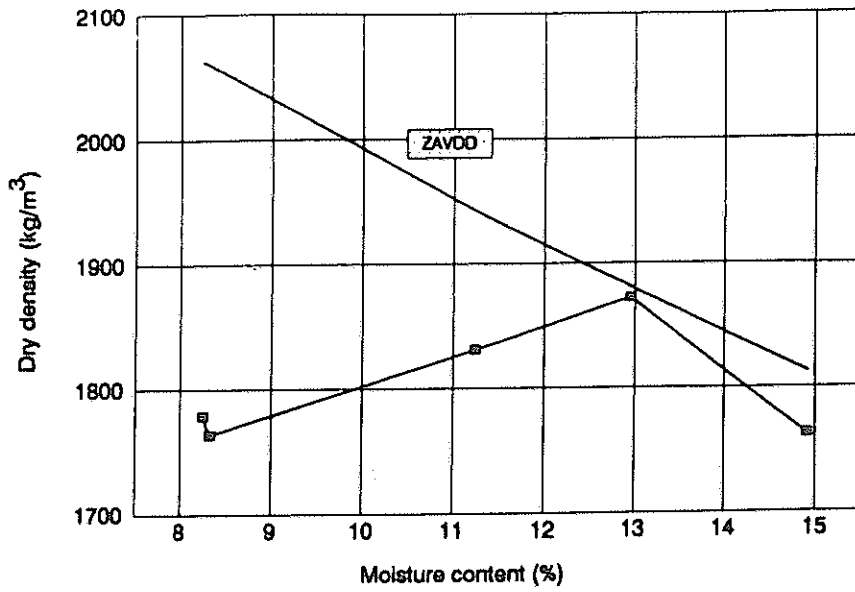


Figure B3: Dry density against moisture content after compaction on the vibratory compaction table for upper selected layer on Section 1

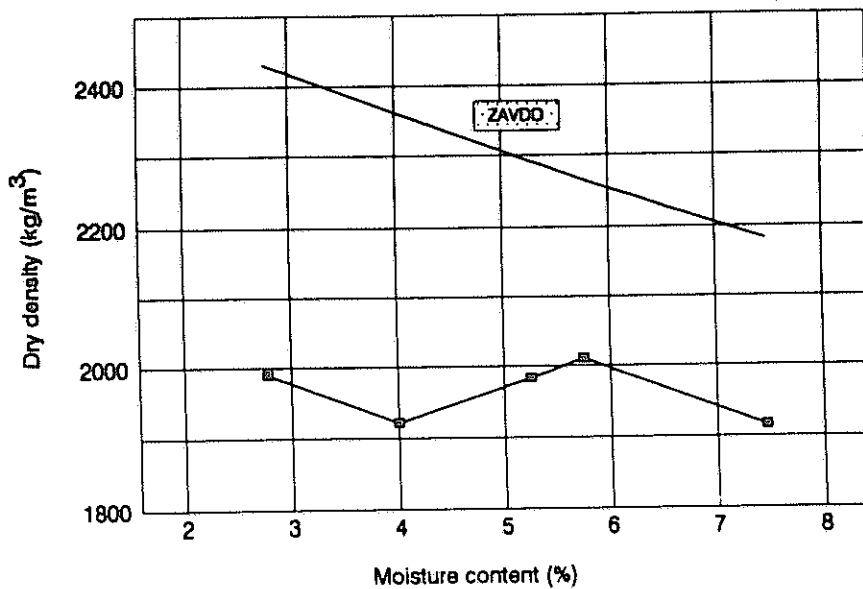


Figure B4: Dry density against moisture content after compaction on the vibratory compaction table for lower subbase on Section 1

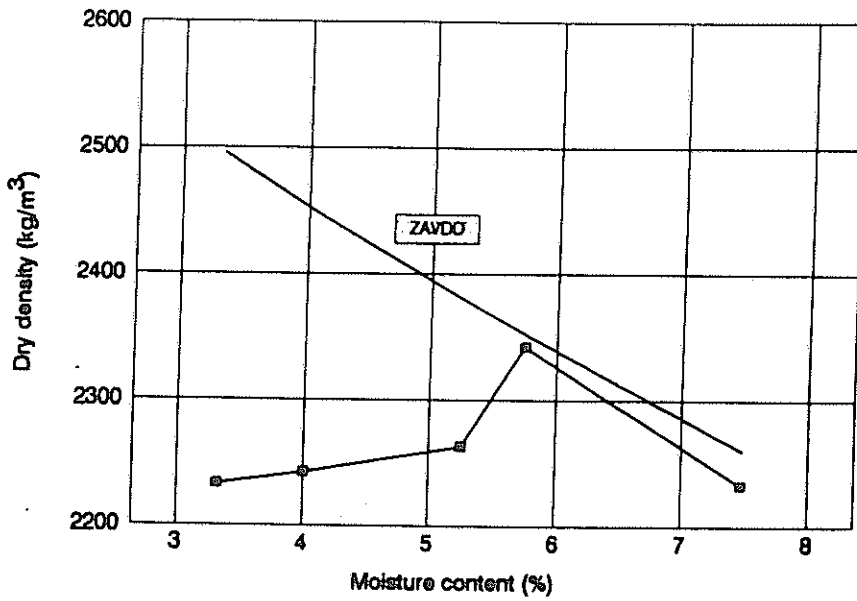


Figure B5: Dry density against moisture content after compaction on the vibratory compaction table for base on Section 1

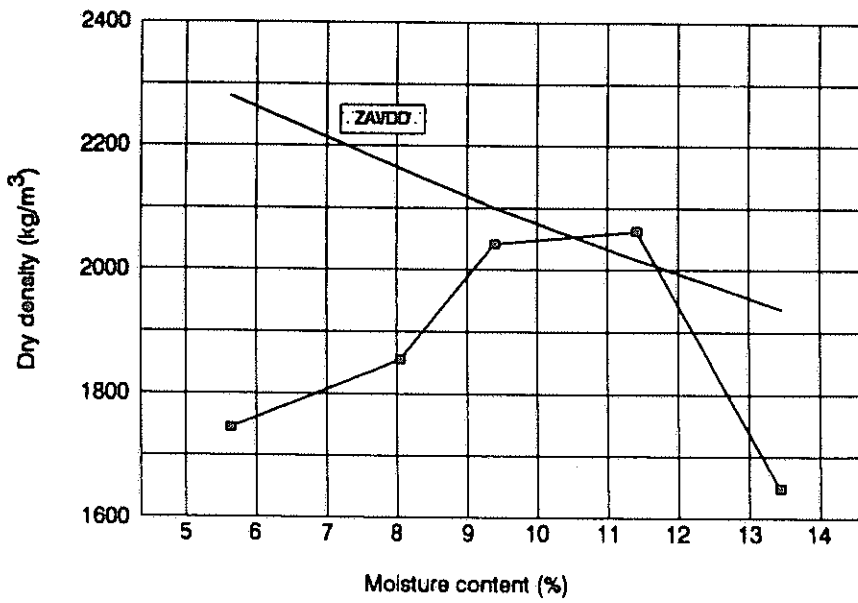


Figure B6: Dry density against moisture content after compaction on the vibratory compaction table for lower selected layer on Section 2

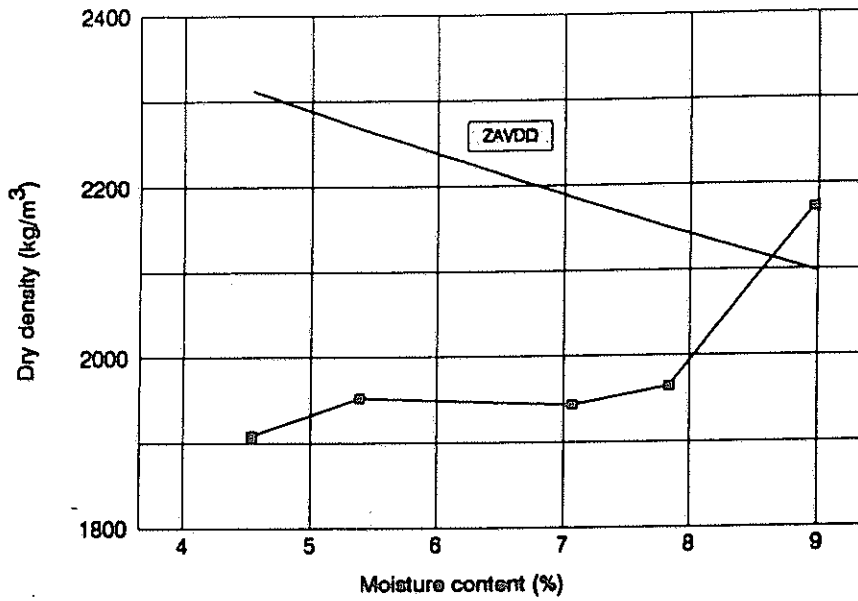


Figure B7: Dry density against moisture content after compaction on the vibratory compaction table for upper selected layer on Section 2

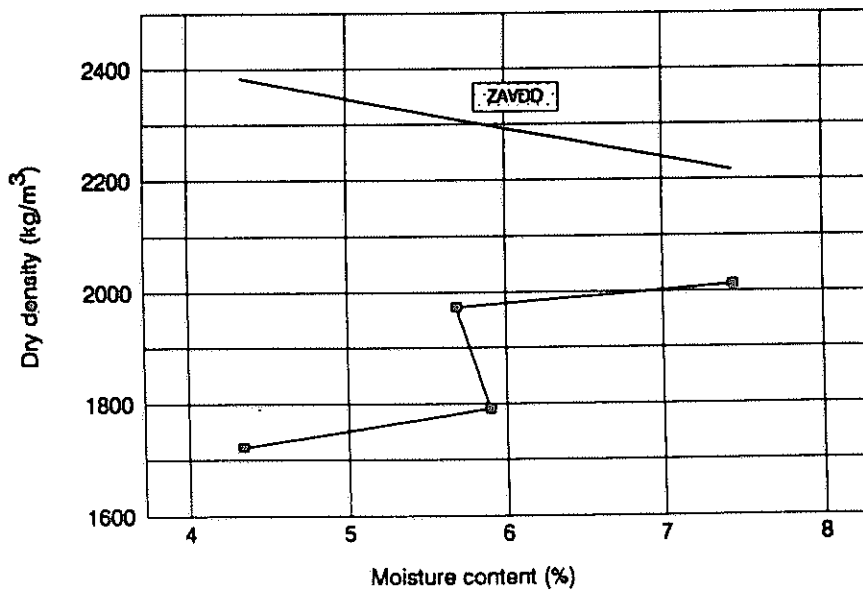


Figure B8: Dry density against moisture content after compaction on the vibratory compaction table for lower subbase on Section 2

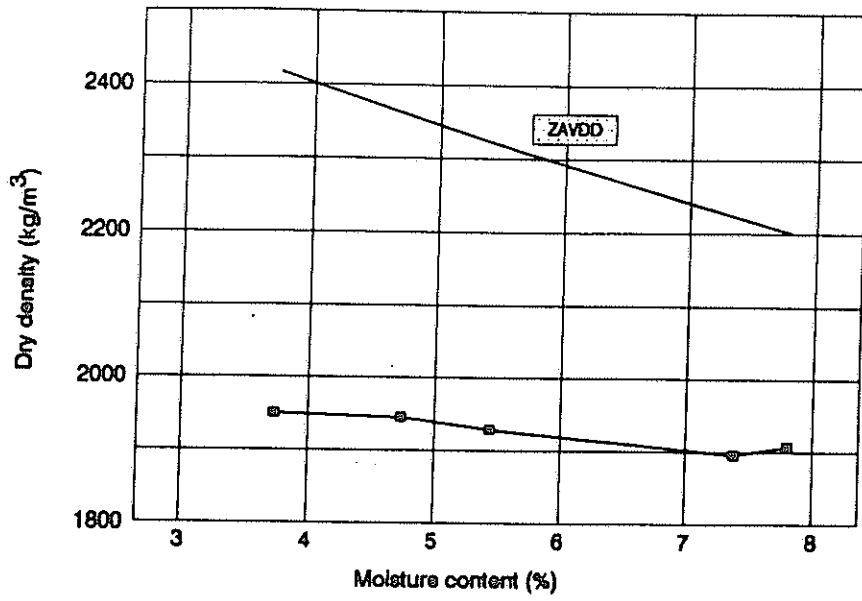


Figure B9: Dry density against moisture content after compaction on the vibratory compaction table for upper subbase on Section 2

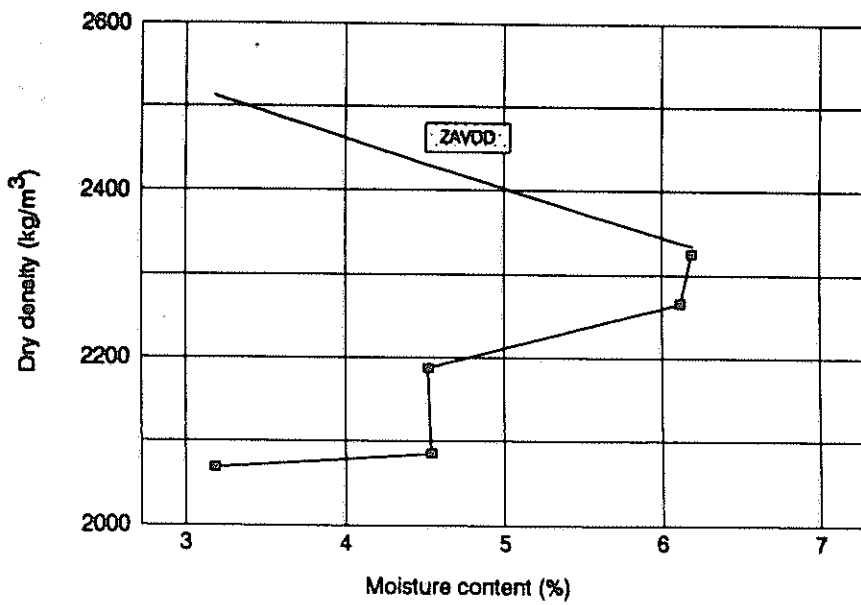


Figure B10: Dry density against moisture content after compaction on the vibratory compaction table for base on Section 2

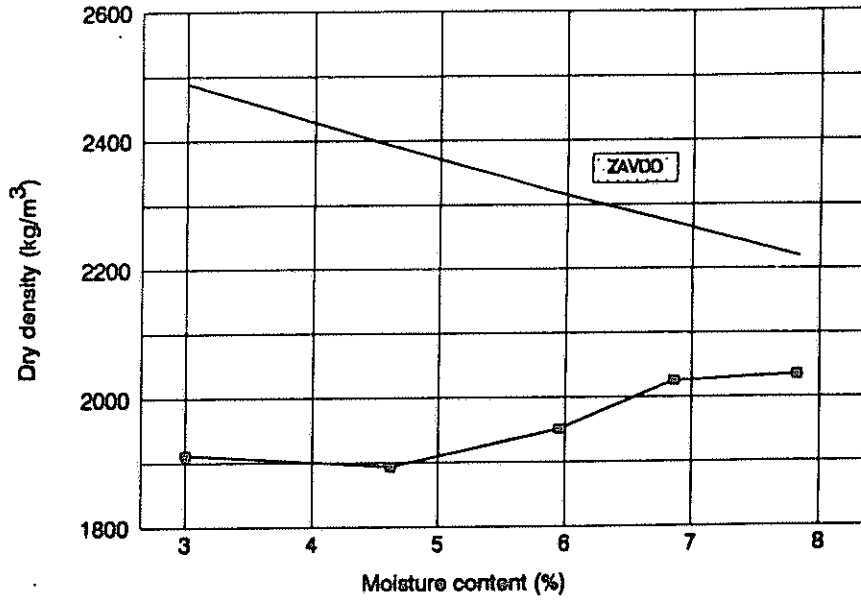


Figure B11: Dry density against moisture content after compaction on the vibratory compaction table for lower selected layer on Section 3

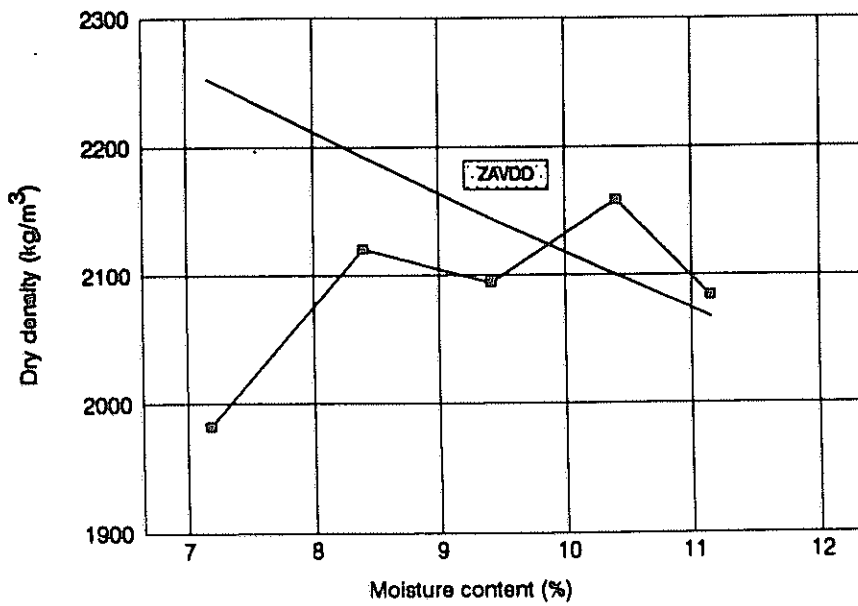


Figure B12: Dry density against moisture content after compaction on the vibratory compaction table for upper selected layer on Section 3

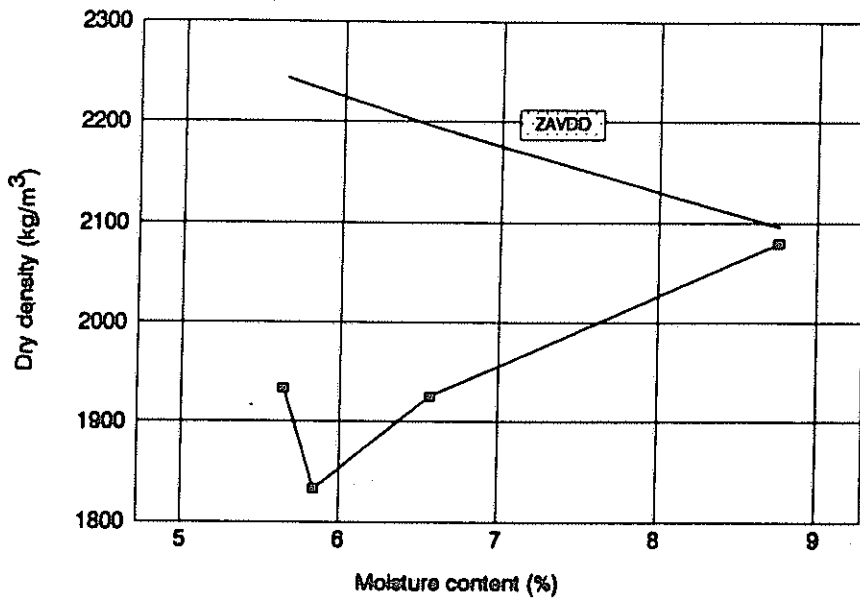


Figure B13: Dry density against moisture content after compaction on the vibratory compaction table for lower subbase on Section 3

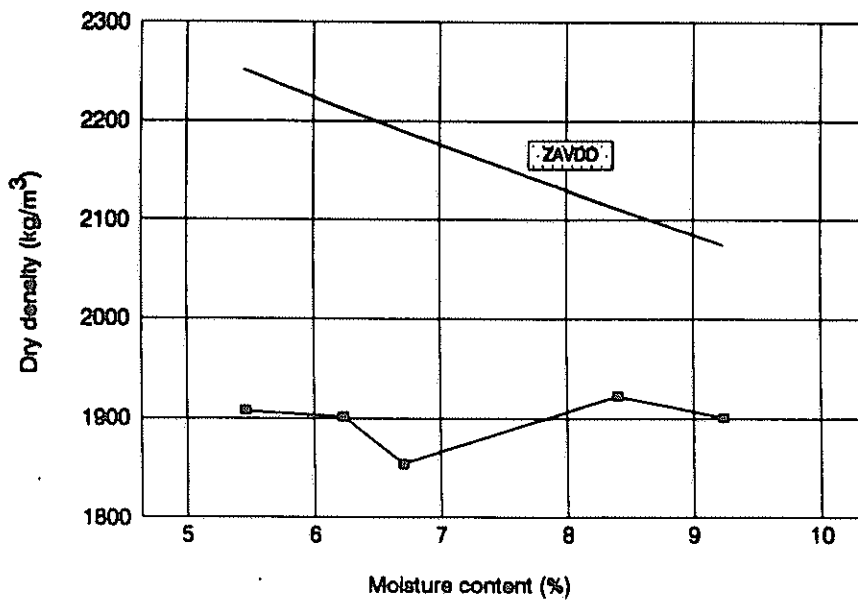


Figure B14: Dry density against moisture content after compaction on the vibratory compaction table for upper subbase on Section 3

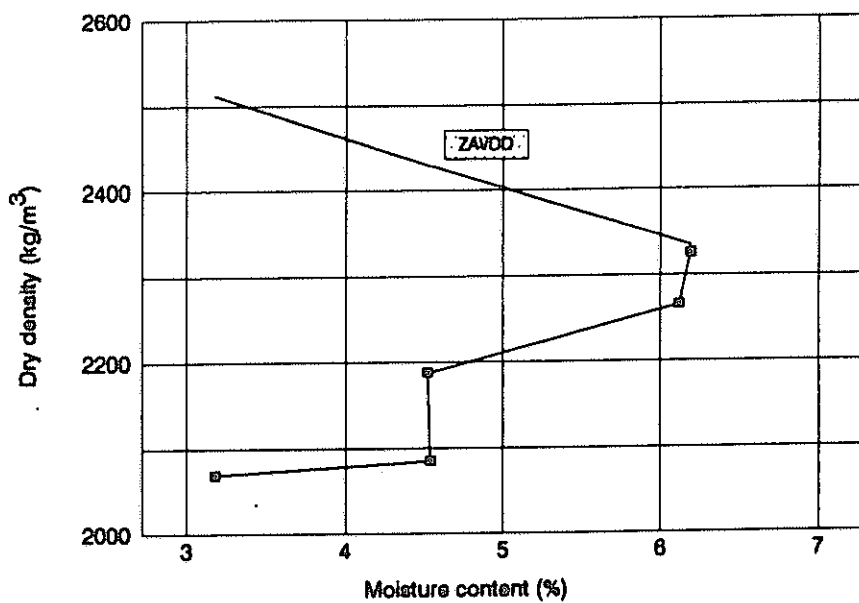


Figure B15: Dry density against moisture content after compaction on the vibratory compaction table for base on Section 3

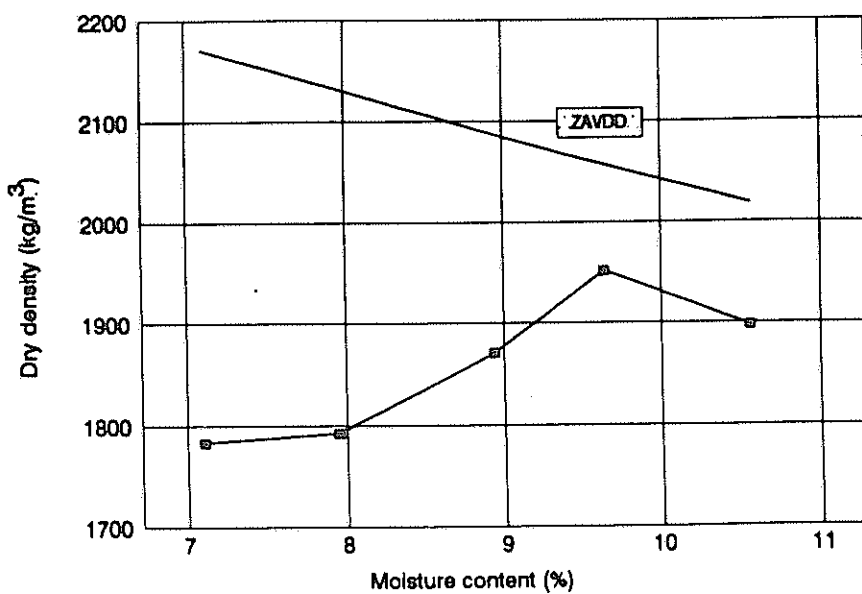


Figure B16: Dry density against moisture content after compaction on the vibratory compaction table for lower selected layer on Section 4

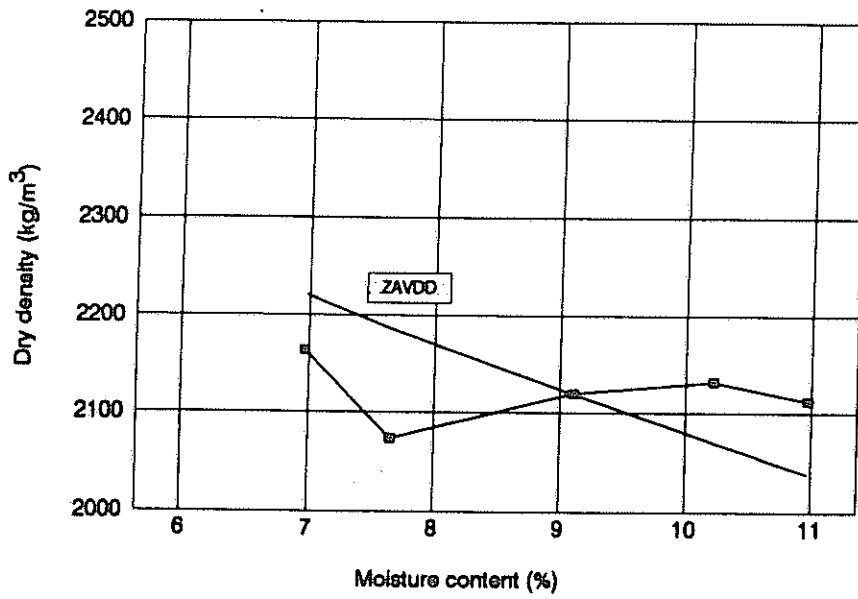


Figure B17: Dry density against moisture content after compaction on the vibratory compaction table for upper selected layer on Section 4

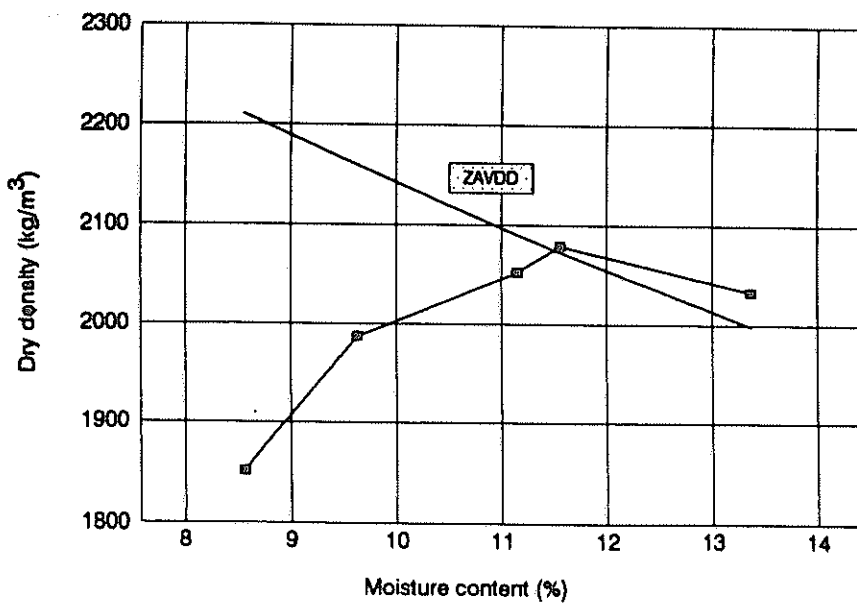


Figure B18: Dry density against moisture content after compaction on the vibratory compaction table for lower subbase on Section 4

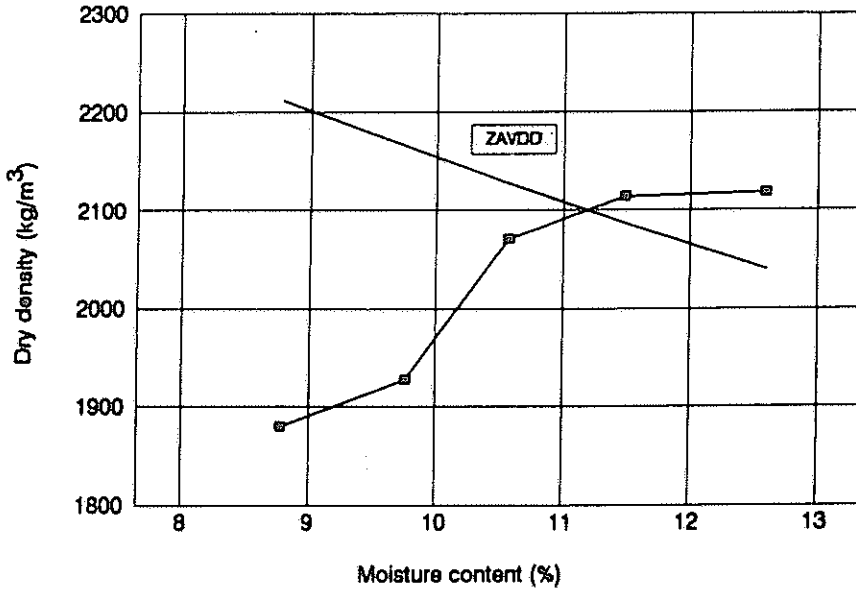


Figure B19: Dry density against moisture content after compaction on the vibratory compaction table for upper subbase on Section 4

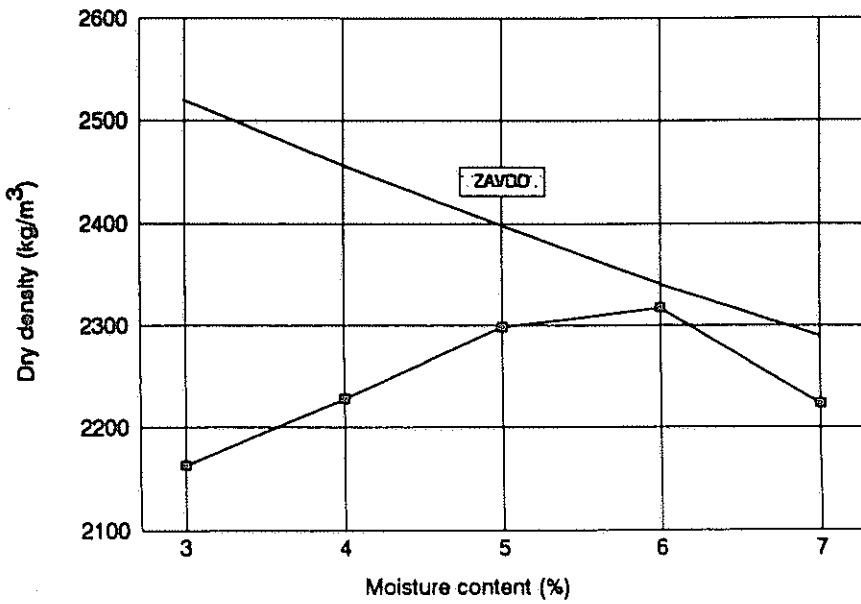


Figure B20: Dry density against moisture content after compaction on the vibratory compaction table for base on Section 4